SYNGAS GENERATION FROM THERMOCHEMICAL CONVERSION OF LOCALLY AVAILABLE BIOMASS WASTE FOR AUTOMOTIVE
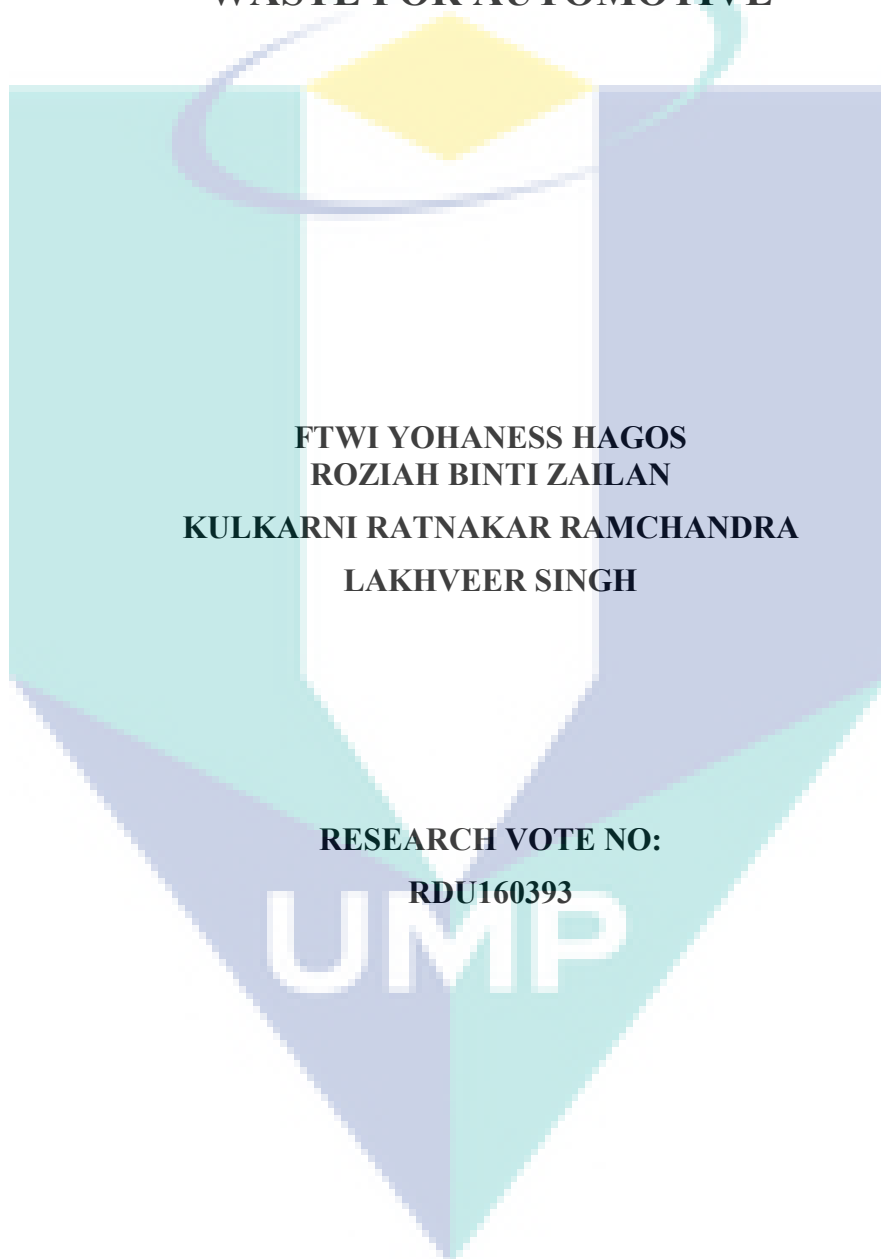
FTWI YOHANESS HAGOS
ROZIAH BINTI ZAILAN

KULKARNI RATNAKAR RAMCHANDRA

LAKHVEER SINGH

RESEARCH VOTE NO:

RDU160393

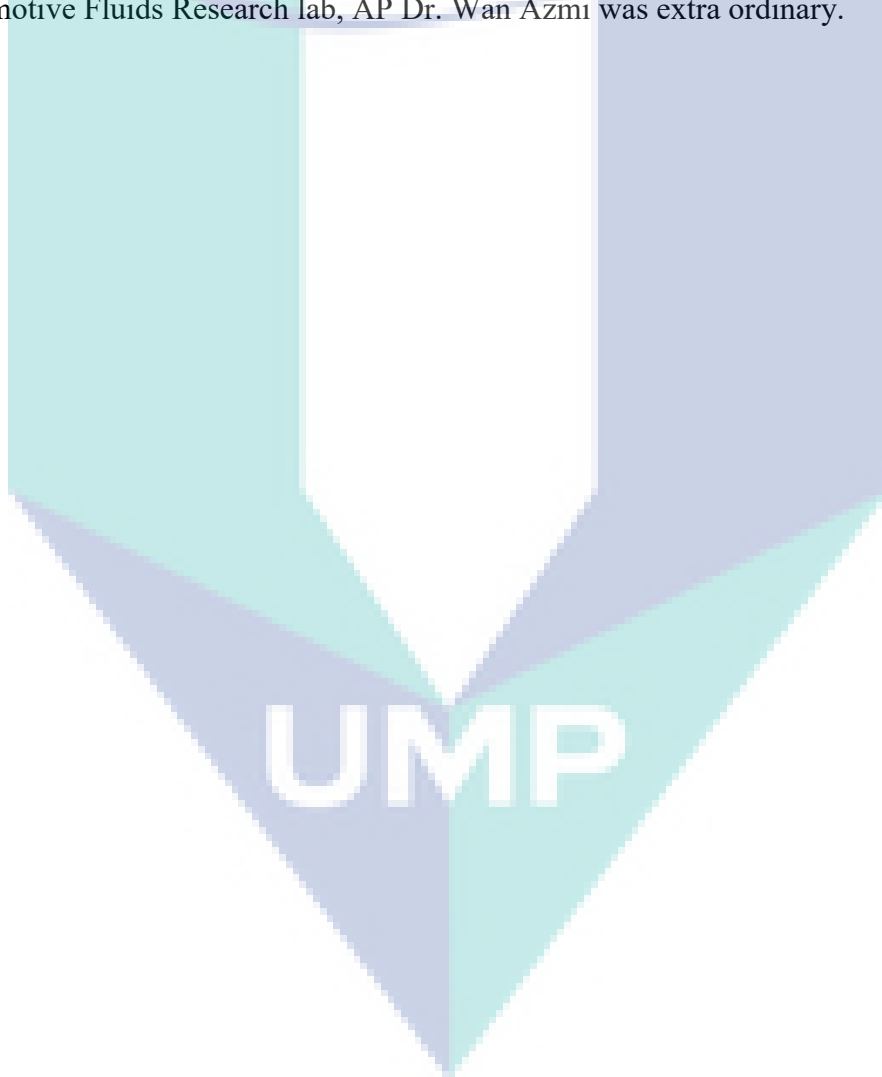**Faculty of Mechanical Engineering**

UNIVERSITI MALAYSIA PAHANG

i

Dedicated to team members in Automotive Engineering Centre (AEC) and Automotive Engineering Research Group (AERG), Faculty of Mechanical Engineering, Universiti Malaysia Pahang

ACKNOWLEDGEMENTS

ABSTRACT

SYNGAS GENERATION FROM THERMOCHEMICAL CONVERSION OF LOCALLY AVAILABLE BIOMASS WASTE FOR AUTOMOTIVE

(Keywords: syngas, thermochemical conversion, biomass, fuel, IC engine)

The growth of the world population as well as the ever-advancing development of the developing countries into industrialized countries leads to an increasing demand for energy and raw materials. As energy production increases, the emissions emitted increase as well. To counteract this pollution, the states adopt measures to reduce air pollution. The car industry is also affected. Lowering both, CO and NOX is the challenge. One possibility for the internal combustion engine is the use of alternative fuels to achieve this goal. These can reduce the emissions incurred. One alternative fuel is synthetic gas which consist primarily of hydrogen, carbon monoxide and often carbon dioxide. Using this gas the unburned hydrocarbons will decrease and an increase in thermal efficiency is to observe. To produce syngas, there are many reforming processes, each with its own benefits and disadvantages. This project has the task of designing an inline reformer for producing syngas in a retrofitted Otto internal combustion engine with natural gas. The fuel supply of the internal combustion engine has to be completely converted to a natural gas - syngas mixture. The engines demand for fuel should inherit a maximum amount of 15% syngas which will be mixed to the prime source, natural gas, after conversion.

ABSTRAK

Pertumbuhan penduduk dunia serta pembangunan yang terus maju dari negara-negara membangun ke negara-negara industri membawa kepada peningkatan permintaan tenaga dan bahan mentah. Apabila pengeluaran tenaga meningkat, pelepasan emisi juga meningkat. Untuk mengatasi pencemaran ini, negeri-negeri mengambil langkah-langkah untuk mengurangkan pencemaran udara. Industri kereta turut terjejas. Menurunkan kedua-duanya, CO dan NOX adalah cabaran. Satu kemungkinan untuk enjin pembakaran dalaman adalah penggunaan bahan api alternatif untuk mencapai matlamat ini. Ini dapat mengurangkan pengeluaran yang dikeluarkan. Satu bahan api alternatif adalah gas sintetik yang terdiri terutamanya daripada hidrogen, karbon monoksida dan sering karbon dioksida. Menggunakan gas ini hidrokarbon yang tidak terbakar akan berkurangan dan peningkatan dalam kecekapan terma adalah untuk diamati. Untuk menghasilkan syngas, terdapat banyak proses pembaharuan, masing-masing dengan faedah dan kelemahannya sendiri. Projek ini mempunyai tugas merancang pembaharu sebaris untuk menghasilkan syngas dalam enjin pembakaran dalaman Otto yang dipasang dengan gas asli. Bekalan bahan bakar enjin pembakaran dalaman perlu ditukar sepenuhnya kepada campuran gas asli - syngas. Enjin permintaan untuk bahan bakar harus mewarisi maksimum syngas 15% yang akan bercampur dengan sumber utama, gas asli, selepas penukaran.

Key Researcher:

Dr. Ftwi Yohaness Hagos, Senior Lecturer, FKM, UMP

Co-Researcher:

Dr. ROZIAH BINTI ZAILAN, FTEK, UMP

Dr. KULKARNI RATNAKAR RAMCHANDRA, FTEK, UMP

Dr. LAKHVEER SINGH, FTEK, UMP

E-mail : ftwi@ump.edu.my

Tel. No. : +6094246367

Vote No. : RDU160393

TABLE OF CONTENT

Title:
Natural Gas Engine Technologies: Challenges and Energy Sustainability Issue
Journal:
Energies ISI Q2 (IF=2.676)
Volume / Page Number:
11/2934

Title:
Application of The Chain Code and Fourier Analysis Techniques for The Investigation of Wrinkles and Distortions on Early Flames
Journal:
International Journal of Automotive and Mechanical Engineering
Volume / Page Number:
15/ 5709-5728

CHAPTER 4   MSC THESIS (FIRST 10 PAGES)   31

Title:
Design of an inline reformer for syngas production in a natural gas vehicle
Student:
VITALI MUELLER (KMM18004)
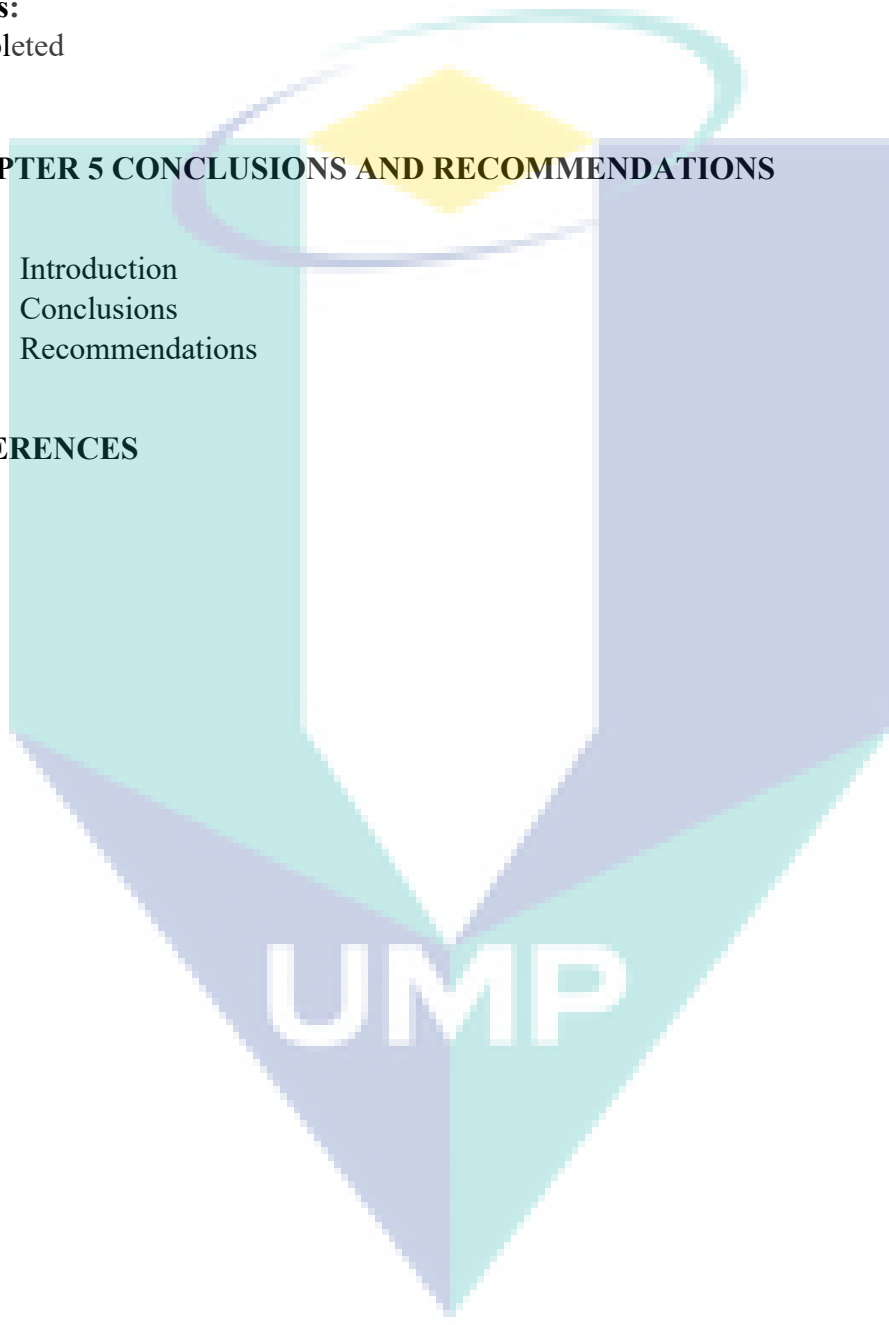**Status:**
Completed

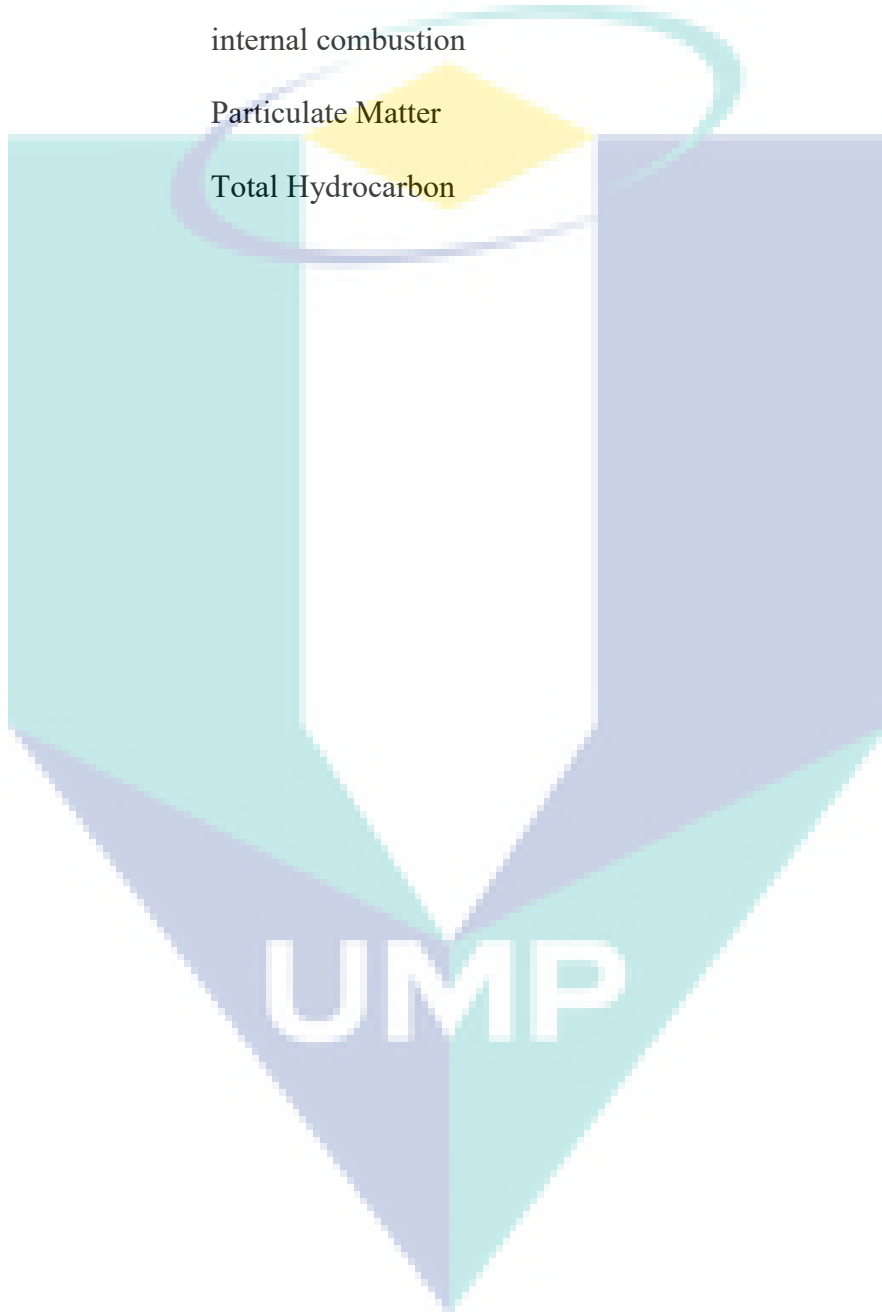
CHAPTER 5 CONCLUSIONS AND RECOMMENDATIONS

LIST OF ABBREVIATIONS

CI   Compression Ignition

IC   internal combustion

PM   Particulate Matter

THC   Total Hydrocarbon

CHAPTER 1

INTRODUCTION

1.1 BACKGROUND OF STUDY

The rise in fossil fuel prices, their finite and non-renewable existence and the need for energy independence create a higher need for renewable and alternative energy sources. Hence, there is a need for renewable and environmentally friendly energy sources, which is sustainable, less costly and not contributing to current environmental problems [1, 2]. Biomass is a major renewable energy source which is environmental friendly with net zero CO_2 emission to the atmosphere, and sustainable with time because of its short term replenishment unlike fossil fuels. Biomass is a highly heterogeneous solid fuel with complex chemical structures and ligno-cellulosic composition. Moreover, key characteristics of different biomass materials vary widely in terms of its chemical and physical properties, ligno-cellulosic composition, morphological characteristics, energy density, ash content, mass/bulk density, ash melting behavior, charring behavior etc. [2, 3]. Because of these great variations of fuels in their characteristics they require specific gasification methods and fuel-based performance studies in order to determine the optimum conditions for gasification of a given biomass fuel. A number of studies had been carried out in literature to study the gasification performance of various solid fuels. Studies conducted in earlier times are found to mainly focus on gasification of coal and woody biomass feedstocks: coal [4-6], woody biomass [7-13], furniture wood [13].

1.2 PROBLEM STATEMENT

One big problem humanity has is global warming, caused by greenhouse gases like CO2. The global warming causes the polar ice caps to melt. One consequence of this is the rise in sea level, which causes many areas of the earth to be flooded and therefore people to flee. A new wave of refugees will occur. By reducing greenhouse gases, we can make an important contribution to the environment and our well-being. CO2 is one of the big influencer on global warming. The automotive sector is producing a big amount of CO2. As this greenhouse gas is produced by fossil fuels at the motor combustion process, measures must be taken to reduce this harmful gas. As hydrogen is one of the possible solutions to reduce the greenhouse gases in a natural gas fired vehicle, on the other hand this technology is in its initial stage and not very common in use. Syngas is believed to take the role of hydrogen in the automotive sector. However, the physical and chemical characteristics and ligno-cellulosic composition of different biomass fuels widely vary resulting in variations on the performance and output from gasification of each biomass. Hence, the gasification performance of a given biomass material need to be studied in order to determine the range of operating conditions suitable for its optimum conversion and to determine its potential as a gasification fuel.

1.3 SIGNIFICANCE OF THE STUDY

Due to an increase in domestic consumption of fossil fuels, Malaysia is declared net importer of crude oil since early 2015. Malaysia has proven reserve of natural gas at its current level 83 trillion cubic feet. Malaysia is placed 2nd and in the top 15 highest natural gas producer in South East Asia and in the world, respectively. Despite the prospect of natural gas, decline in the export of crude oil and the government incentives towards NGV, the market share of the natural gas in the transport sector is still too low with less than 2% share [24]. At macro level, the prototype will have bigger role in promoting the use of natural gas in the transport sector, public transport in particular. Thereby Malaysia can retain annual net crude oil exporter. As a result, the national revenue of the country as well as crude oil market dependence will be improved. At micro level, liquid fuel based public transport vehicles will be encouraged to use NGV thereby improving their income. Besides, the performance improvement on the exiting NGV fueled vehicles will improve the fuel consumption. While this is the case on the energy side, emissions and well-being

of the citizens will be improved with the expansion of NGV vehicles. Therefore, promotion of the technology will have impact both at micro and macro-economic levels.

1.4 OBJECTIVE

The gasification performance of a given biomass material need to be studied in order to determine the range of operating conditions suitable for its optimum conversion and to determine its potential as a gasification fuel. The current research focuses on the performance study of downdraft gasification of OPF and parametric investigation on the influence of various operating conditions on resulting syngas composition and heating value.

1.4.1   Specific Objective:

The Research will have three specific objectives:

Specific Objective 1: For characterization of the biomass feedstock

Specific Objective 2: To investigate variation of gasification performance and output with various operating conditions and feedstock characteristics

Specific Objective 3: To facilitate performance prediction of downdraft gasifiers, over a range of operating conditions and feedstock characteristics, in terms of product gas composition and heating value

1.5 SCOPE OF STUDY

The study is conducted is to investigate the effect of biomass input of the product of syngas through the thermochemical conversion. Three different biomasses are to be characterized through Pre- processing: Pre- processing of feedstock involves chipping

and pulverizing to a size of dimension less than 1 mm diameter and drying. Cutting to size: Biomass chipping machine and proper granulator will be used to pulverize the fuel to proper size. 3. Characterization: Characterization of sample from the different biomass materials will be done using standard proximate analyzer, CHNS analyzer and bomb calorimeter in the lab. The proximate analysis will determine the physical composition volatile matter (VM), fixed carbon (FC), Ash, and moisture content (MC)) and a CHNS machine will be used to measure the elemental composition (carbon, hydrogen, nitrogen, sulfur and oxygen). Whereas the heating value of the solid fuel will be determined using a bomb calorimeter. Further parametric Study: The parametric study to investigate influence of the operating conditions will be done by carrying out experiments for various values of the operating conditions (temperature, air fuel ratio, moisture content and particle size).

CHAPTER 2

ISI JOURNAL

Title:

Natural Gas Engine Technologies: Challenges and Energy Sustainability Issue

Journal:

Energies ISI Q2 (IF=2.676)

Volume / Page Number:
11/2934

Natural Gas Engine Technologies: Challenges and Energy Sustainability Issue

Girma T. Chala [1] [ID], **Abd Rashid Abd Aziz** [2] and **Ftwi Y. Hagos** [3,4,*] [ID]

[1] Mechanical Engineering Department, INTI International University, Persiaran Perdana BBN, Nilai 71800, Negeri Sembilan, Malaysia; girma_tade@yahoo.com

[2] Center for Automotive Research and Electric Mobility (CAREM), Universiti Teknologi Petronas, Tronoh 31750, Perak, Malaysia; rashid@utp.edu.my

[3] Advance Fluids Focus Group, Faculty of Mechanical Engineering, Universiti Malaysia Pahang, Kuantan 26600, Malaysia

[4] Automotive Engineering Centre, Universiti Malaysia Pahang, Kuantan 26600, Malaysia

* Correspondence: ftwi@ump.edu.my; Tel.: +60-942-463-67

Abstract: Energy sustainability and environmental issues pose greater challenges on different primary energy sectors as the global energy demand increases and it is projected to further increase with an upsurge in population. On the other hand, energy sources from conventional fossil-based fuels are depleting, forcing explorations in challenging and difficult locations. As a result, the use of alternative fuels received dramatic consideration to substitute these conventional fuels, of which natural gas took the significant share. However, the share of natural-gas vehicles in the current vehicle market is quite small, and it is estimated to be below 5%. This paper reviews the current resource scenarios including proven and potential reserves, current production, and consumption, along with the fueling infrastructure, distribution, and storage. It also provides summary of the development of fuel-injection technologies aimed to enhance the performance of gas engines. More attention was also given to natural-gas engines and their limitations. Parameters affecting the performance and combustion of compressed natural gas (CNG) in spark-ignition (SI) engines are thoroughly assessed, among which compression ratio and injection timing play major roles in the optimization of CNG-fueled engines. Furthermore, different technologies that help close the performance gap between conventional liquid-fuel and natural-gas engines and future directions of the research are presented.

1. Introduction

Due to an increase in pollution from automotive vehicles running on conventional liquid fuels, alternative fuels that could result in similar performance became potential candidates to be used as substitutes in short and long-term plans [1]. In the upcoming years, alternative fuels are expected to substitute conventional fuels concerning environmental and energy security issues. While the future trend in the transportation sector is inclining toward electric vehicles, a leap jump is unlikely due to existing infrastructure and resources. There is a need for an alternative transitional fuel that can lead toward 21st century ambitions of zero-carbon emission. As a result, natural gas has become the leading candidate to fill the gap in recent trends [2].

Natural gas has been used as vehicle fuel since the 1920s. Significant development of natural gas was seen during the oil shocks in 1974 and 1979. Natural gas has become the most favorable energy source capable of matching the energy density and combustion-related issues in the engine [3]. Natural gas is also a leading candidate for transportation vehicles in many countries mainly due

to its vast abundance, its price, lower emission rates, and suitability of use in conventional diesel and gasoline engines. In fact, natural-gas combustion produces the lowest greenhouse-gas emissions of fossil fuels, together with a minimal level of suspended particles [4]. As a result, natural gas received great acceptance for fueling vehicles in recent years, and this is likely to rise in the coming years [5]. Over the last few years, the discovery of shale gas and an advancement in unconventional gas production prompted further focus to natural gas. The discovery of natural gas geographically and globally diversified the production of natural gas. According to the International Energy Outlook 2016 (IEO2016) and Annual Energy Outlook 2016 (AEO2016), shale gas is expected to claim up to 30% of the global natural-gas production share by 2040.

Despite all the advantages of fuel and its increasing volume of production, the market share of natural-gas vehicles is too low, comprising only 1.27% [6], and the growth rate is forecasted at 5–7% annually [7]. This weak growth does not match the rapidly increasing growth of transportation vehicles. The attributes to this are a common misconception, operational problems associated with retrofitted engines, storage size, and safety, in addition to a lack of advancement in fuel-conversion technologies, and a greater expectation for the fuel-conversion efficiency in a pollution and energy-saving context being among other contributing factors. Over a two-decade period, there was significant research work to overcome such challenges. Moreover, there were a few review works compiling the works that highlighted the investigation and development of natural-gas vehicles, mainly based on the fuel-conversion technologies and their limitations [8–11]. However, these reviews barely touched the research data in the last decade, except for an effort by Khan et al. (2016) in their bibliographic review [12].

Therefore, the aim of the current review is to highlight the progress on the development of natural-gas-fueled engines for the transportation sector and their technological limitations. This review work targeted the expanding global resource of natural gas, the fueling infrastructure development, the natural-gas fuel-conversion technologies and their technical and operational limitations, and finally, in the conclusions and perspective section, focused on the latest advanced technologies and future technological trends.

2. Natural-Gas Resources: Global Perspective

The world's energy demand increased in last decade, and different energy sources are utilized to fulfill the need [13,14]. Conventional fossil fuels, including coal and oil, took the lion's share of the energy sources over the last few years [15]. However, this proved to have many disadvantages in terms of emission and human health, especially in cities with high population [16,17]. Many efforts were made to combat this growing issue, one of which was the use of alternative fuels in different sectors [18,19]. Table 1 shows world energy consumption by fuel over the past 15 years. Globally, natural gas is the third major energy source, where its use increased over the last decade as opposed to coal and oil. Supply from the major shareholders of energy sources, coal and oil, was observed to decrease in the last ten years, from 33.49% to 32.94% for oil and from 29.84% to 29.20% for coal.

Table 1. Global energy consumption by fuel in 2005, 2010, and 2015 adapted from the World Energy Council (WEC) [20].

Fuel Type	Consumption in Percentage		
	2005	2010	2015
Oil	35.96	33.49	32.94
Gas	22.89	23.7	23.85
Hydro	6.05	6.44	6.79
Solar	1.01	0.06	0.45
Coal	28.61	29.84	29.20
Nuclear	5.73	5.14	4.44
Wind	0.22	0.63	1.44
Other renewables	0.54	0.70	0.89

Due to the reduced reserves of petroleum resources, alternative fuels such as natural gas would lighten the dependency on conventional fossil fuels. This was predicted to increase the natural-gas demand by up to 50% in 2035 from 2010 [21]. Natural gas is a cleaner energy source that reduces the carbon emissions by 20–30% as compared to conventional fuels. Moreover, natural gas is regarded as the primary fuel source for gaining energy security in the long term [22,23]. It was reported that natural gas would be a potential fuel for sustainable energy sources after 2050 [24,25].

2.1. Proven Natural-Gas Reserves

Globally, there is an abundance of natural resources [26]. Table 2 shows a comparison of natural-gas reserves between 2005, 2015, and 2017. Natural-gas reserves amounted to 186.9 trillion cubic meters (tcm) in 2015, and there were 157.3 tcm in 2005, showing more than a 15% increase in a decade. The largest reserve in 2015 was found in the Middle East, which holds 42.8%, followed by Europe and Eurasia (30.4%), the Asia-Pacific (8.4%), Africa (7.5%), North America (6.8%), and South and Central America (4.1%). Many end sectors are motivated by the abundant resources of natural gas [27]. The proven reserves are much greater than that for conventional liquid fuels in 2017: 193.5 tcm versus 270 billion cubic meters (bcm), which further encourages the comprehensive utilization of natural gas.

Table 2. Global proven natural-gas reserves, in percentage: comparison between 2005, 2015, and 2017, adapted from British Petroleum (BP) [28].

Region	Proven Reserves in Percentage		
	Year 2005	Year 2015	Year 2017
Middle East	46.2	42.8	40.9
Europe and Eurasia	27.3	30.4	32.1
Asia-Pacific	8.2	8.4	10.0
Africa	8.9	7.5	7.1
North America	5.0	6.8	5.6
South and Central America	4.4	4.1	4.2
Total (in trillion cubic meters)	157.3	186.9	193.5

Natural gas is being discovered in different geographical regions of the globe [29]. There are two forms of natural-gas reserves: conventional and unconventional [30]. Unconventional natural-gas reserves are categorized into four: coalbed methane or coal-seam gas, shale gas, gas from tight sandstones or tight gas, and methane hydrates (least known). Conventional gas is produced from permeability reservoirs, while shale gas is produced from lower permeable mudstone. Coalbed methane is expensive due to the requirement of water disposal, while tight sands need high developmental costs. Among proven global natural-gas reserves, 4% of them are unconventional gas, including shale gas, coal-seam gas, and tight gas. The Asia-Pacific holds 30% of the unconventional gas reserves, North America holds 25%, and 17% of the total unconventional reserves were found in the former Soviet Union. This increased unconventional gas shares to 15% from 12% in 2007 [31].

2.2. Global Potential Reserves

Natural-gas resources are believed to be enormous with vast recoverable reserves worldwide. The global natural-gas reserves were estimated to be 186.9 tcm in 2015, as shown in Table 2, representing only 22% of the total gas reserves worldwide according to Economides et al. (2011). According to this report, there is a potential of 662.33 tcm of gas reserves that can be recovered, and this amounts to 78% of the world's total proven plus potential reserves [32]. The substantial quantity of natural-gas resources emboldens applications of natural gas in different sectors.

Despite the enormous amount of recoverable gas available worldwide, there are technical challenges that are encountered during gas production. Recent advancement of technologies, such as hydraulic fraction and horizontal drilling, are widely utilized to alleviate the problems. As a result,

a huge amount of shale gas is being produced. Song et al. [33] studied how natural gas can be produced from methane hydrates via thermal stimulation or depressurization, and using both simultaneously. With advanced technology in many countries, the use of natural gas as an energy source is feasible and expected to intensify significantly, which would finally support countries in shifting from coal and oil dependencies soon. Chong et al. [34] stated that natural gas is a strong candidate for an energy source in the future compared to coal and oil. They highlighted that natural gas could also be explored from hydrate resources, which are considered as the largest sources of carbon.

2.3. Current Production Capacity and Consumption

Production of natural gas was instigated from coal in Britain in 1785, followed by drilling from the earth's core [35]. Fei et al. [36] described that natural gas could be produced from fossil resources or anthropogenic resources. Currently, natural gas is produced from both unconventional and conventional gas resources. Hydraulic fracturing (HF), which involves removing gas from the rock following drilling in depth, contributed to the higher production of natural gas recently [37]. Natural-gas production grows by an average of 2.5% every year. Almost equivalently, world natural-gas consumption also increased in the last decade [38]. The global consumption growth was estimated at 1.7% in 2015. Natural-gas production and consumption were both observed to increase in the last decade at averages of 2.4% and 2.3%, respectively. The highest production growth was observed in North America with an estimate of 3.9% in 2015.

The huge production in North America was mainly due to shale gas, which accounts for approximately 32% of the total reserves in the United States (US) [32]. The development of shale technology (a mechanism of recovering reserves which were thought to be unrecoverable) strengthens the production of natural gas in North America [39]. Table 3 shows the top five natural-gas-producing countries in 2015. The largest producer of natural gas was the US with 767.3 bcm, followed by Russia (573.3 bcm), Iran (192.5 bcm), Qatar (181.4 bcm), and Canada (163.5).

Table 3. Top five natural-gas-producing countries in 2015 [28].

Country	Production Amount (bcm) in 2015
United states	767.3
Russia	573.3
Iran	192.5
Qatar	181.4
Canada	163.5

Natural-gas production is increasing in many other countries. Nwaoha et al. [40] indicated a decline in the production of oil, but growth in the utilization of natural gas globally. However, production dropped by 1.7% in Europe and Eurasia [41]. Though domestic natural-gas production is decreasing in Europe, consumption has increased with a higher number of imports, making it 15.3% of the total global consumption in 2011 [42]. Dilaver et al. [43] reported an increase in natural-gas consumption in Europe, and their model showed an increasing trend in the future long-term natural-gas demand. Their analysis revealed that natural-gas consumption of the Organization for Economic Co-operation and Development (OECD)-Europe would be in the range of 572 to 646 bcm by 2020, indicating that natural gas would remain as a primary fuel source in the region. Natural-gas consumption for the European Union (EU) would be 641 bcm in 2020 [44]. Different policies related to the environment supported the wider usage of natural gas in various sectors in the region [45].

Natural gas would play a significant role as a fuel for satisfying the energy demands due to its advantage in the long term in terms of price and its benefit in alleviating climate changes [46–48]. The last half of a decade saw dramatic growth in natural-gas production with the new technology of recovering reserves that were once thought to be unrecoverable reserves [49]. Two new extraction techniques, hydraulic fracturing and horizontal drilling, which allows the drill shaft

to move horizontally underground, resulted in a boom in natural-gas production recently [50,51]. Melo-Martín et al. [52] reported growth in natural-gas production from unconventional sources using recent technologies. Natural-gas production and consumption increased in many parts of the world, and it is projected to further increase in the years to come [53].

Figure 1 compares the production of natural gas by type in the US, China, and Canada in the year 2012 and 2040. It reveals how shale technology would further increase natural-gas production worldwide. The production of natural gas from shale reserves was almost nil in China and Canada, as opposed to that in the United States in 2012. However, it was predicted that the production of gas from this reserve would be practical in many countries in 2040, increasing world natural-gas production in the coming years. Asche et al. [54] discussed that significant production of shale gas, currently considered an unconventional gas, would probably be regarded as a conventional reserve. Bazilian et al. [55] also stated the massive production of shale gas in North America and recommended researches on applicability.
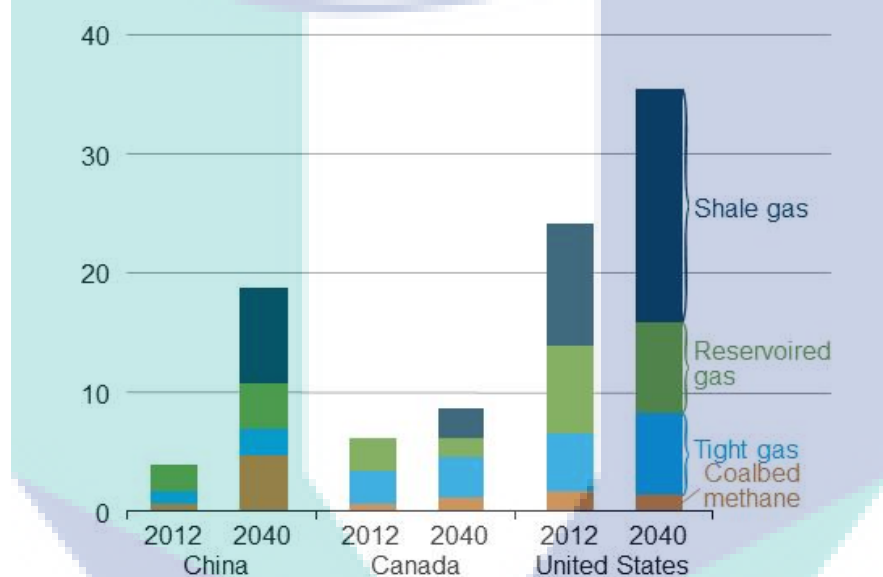

Figure 1. Production of natural gas by type in the United States, China, and Canada: comparison between 2012 and 2040 (trillion cubic feet) [56].

Shale gas is predicted to take over the dominant share in US natural-gas consumption, from 0.396 bcm/day in 2011 to 0.62 bcm/day in 2020 [32]. The production of shale gas increased tenfold annually in the US over the last half of a decade [57], and it is expected to reach three times the current production in 2020. Fukui et al. [58] showed the experience curve for hydraulic fracturing of unconventional natural-gas production, and reported that hydraulic fracturing increased the production of natural gas and lowered wellhead gas price recently. Arora et al. [59] conducted a simulation study showing the growth in world economic activity from 2014 to 2035 as a result of natural-gas production from shale reserves and exports from the US.

Heidari et al. [60] surveyed natural-gas consumption in Iran, and concluded that natural gas has a significant impact on the country's economic growth. Clark et al. [61] showed an increased consumption of natural gas in the US by about 4.8% due to a different policy encouraging the use of natural gas. China's numerous policies supporting the use of natural gas led to significant demand and progress [62]. As a result, the annual natural-gas output increased by 12.1% in China from 2000 to 2014, while consumption grew by 15.1% annually. Cabalu et al. [63] indicated that increasing gas efficiency in addition to developing technologies for the vast production of natural gas would reduce imports and improve the energy security of Asian region.

Figure 2 depicts the global consumption of natural gas by sector from 2014 to 2020. An integrated equilibrium modeling system and a large-scale simulation model were used by the US Energy Information Administration (EIA) and International Energy Agency (IEA), respectively, to forecast natural-gas consumption. Natural gas provides the second major energy source for power generation. Natural gas consumption in the transport sector was estimated to be 11%, and this is projected to increase in the future. As the global greenhouse emissions emanate from the transportation sector, representing 20% of total emissions, natural gas is being considered as an alternative fuel in the transportation sector with minimal greenhouse-gas (GHG) emissions. Economic benefit and energy security encourages the use of natural gas as vehicle fuel [64,65].
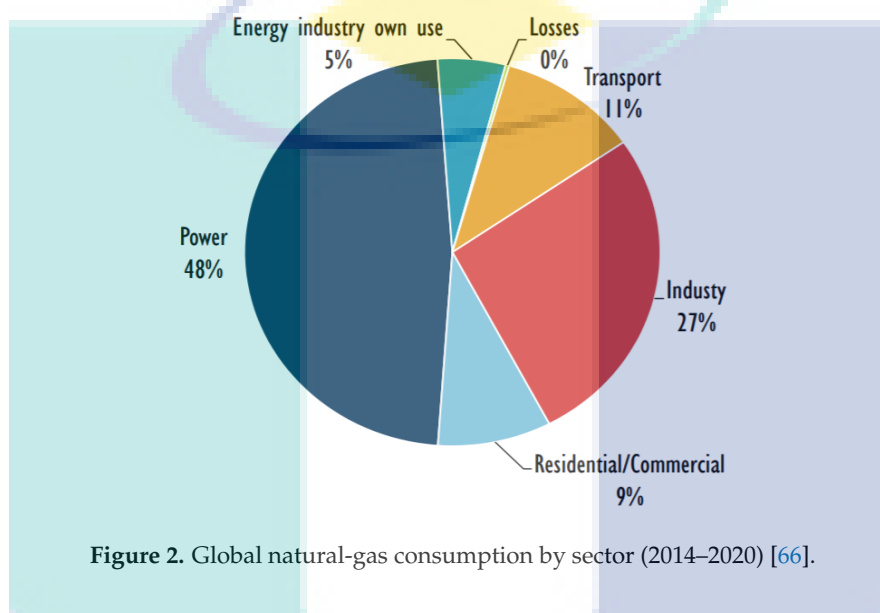

Figure 2. Global natural-gas consumption by sector (2014–2020) [66].

The technology of using natural gas in vehicles is widely adopted and well established. Moreover, the competitive price of natural gas is also another factor attracting more natural-gas vehicles [67,68]. For instance, the European Union's Green Paper is set to substitute 20% of the fossil-fuel consumption for alternative fuels in the year 2020 [69]. In tandem, China is encouraging the broad adoption of natural gas in vehicles as the country faces higher urban pollution. China's fossil fuels resulted in higher GHG emissions, representing 26.4% of the global emissions [70,71]. The country plans to replace 10% of the energy source with natural gas by 2020. Among many applications of natural gas, which include industrial use, commercial use, fertilizer production, power generation, and residential use, priority is given to natural-gas vehicles as this would reduce major urban pollution and improve quality of life. Moreover, to meet high-population needs, there will be substantial growth in the number of transportation vehicles [72]. This raises energy sustainable issues and environmental challenges [73]; thus, the country largely promotes the use of natural-gas vehicles.

2.4. Natural Gas in the Transportation Sector

Natural gas as vehicle fuel is the most promising way of achieving sustainable transport systems [74]. The abundance of natural gas could satisfy the fuel needed by transportation sectors [39]. Moreover, natural gas would offer reduced emissions of 20–30% for CO_2, 70–90% for CO, 75–95% for NO_2, 89% for volatile organic compounds, 90% for particulate matter, and 99% for SO_2 than that of diesel fuel. Moreover, natural gas is considered as an efficient and clean fuel [75,76]. As a result, more than 86 countries are using natural gas to power vehicles [77].

Natural-gas vehicles are increasing in number worldwide. Figure 3 shows the number of global natural-gas vehicles over the last two decades. There were around 26.13 million natural-gas vehicles worldwide in June 2018. The number of vehicles was only 9.5 million in 2009, and this was only 1% of the total number of vehicles in the same year. It was predicted that the number of natural-gas

vehicles will be more than 30 million by 2021, getting more attention as an energy source for the transportation sector.
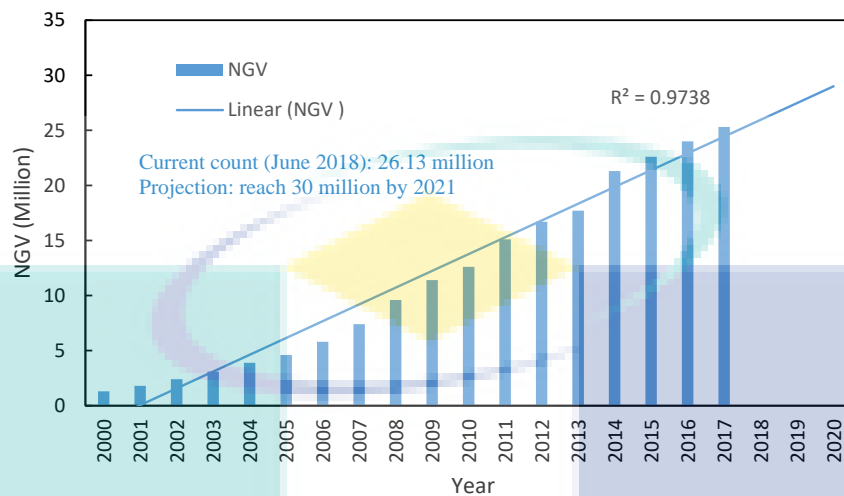

Figure 3. Total worldwide number of natural-gas vehicles from 2000 to June 2018 [78].

Figure 4 shows the statistics of the number of global natural-gas vehicles (NGVs) by region. The number of NGVs is highest in the Asia-Pacific, followed by South America, North America, Europe, the Middle East, and Africa. Around 15 million natural-gas vehicles are found in the Asia-Pacific, where the region saw significant growth in the number of NGVs over the last decade. In contrast, even though natural-gas consumption increased by 4% in 2015 compared to 2014 in Europe, amounting to 426.3 bcm produced [79], the share of NGVs is extremely small compared to other sectors: residential, industry, and power. Engerer et al. [80] studied the options of using natural gas in vehicles in Europe, where natural-gas vehicles are few compared to their number in Asia and Latin America, due to its dependence on gas imports. As a result, the transportation sector is almost completely fueled by conventional liquid fuel, covering approximately 90% [81]. Osorio-Tejada et al. [82] reported that one-quarter of the GHG emissions in Europe emanate from the transport sector. Recently, European countries widely encourage the use of natural gas as a vehicle fuel to combat the overgrowing greenhouse-gas emissions. The governments have tax-reduction incentives in place, encouraging consumers to use natural-gas vehicles widely. In terms of import issues, it was proposed that an improved efficiency of natural gas would reduce the consumption and import costs at times of deficit, thereby expanding the broad adoption of NGVs in the region. Bilgin et al. [83] recommended that energy policies allowing more and diversified suppliers of natural gas could be regarded as one of the options to improve energy security in Europe.

The number of vehicles in Latin America has increased over the last decade. The motive of reducing imports of oil led to some Latin American countries searching for natural-gas vehicles in 1980. However, the advancement came with some incentives, such as reducing taxes compared to gasoline and diesel vehicles. In areas of highly polluted cities, the ban on the use of conventional fuels is inclusive of natural gas too. More importantly, shifting conventional liquid-fuel engines to compressed natural gas (CNG)-fueled engines does not affect the appearance of the vehicle, and as a result, it does not change the physical appearance for customer consideration.

Table 4 shows the top 10 countries by natural-gas vehicle population. The largest number of NG vehicles is found in China, totaling around six million and representing 23.2% of the total number of NGVs worldwide. Hao et al. [84] reviewed natural-gas vehicles in China. They reported that natural gas would be a potential fuel for sustainable transportation in China. The growth is substantial in the Asia-Pacific and Latin America, where more attention was placed on using NG as a vehicle fuel in different countries. For instance, a high increase in the number of CNG-fueled vehicles was

observed in Thailand, an increase of 400,000 NGVs from 2008 to 2010, where most of them were buses and cabs [80]. The lower price of natural gas, more than half of that of diesel and gasoline, contributed to NGV growth. Iran is the most significant user of natural gas in the Middle East, where the country has the second largest reserves. The growth in the number of natural-gas vehicles in Asia is due to a noticeable investment in infrastructure public-sector intervention and support programs. In Columbia, natural gas was first used in public transport, before it got attention for private cars, and the country encouraged stimulus incentives for the conversion of conventional vehicles to NGVs, which finally increased the NGV fleet from 11,500 in 2003 to 72,100 in the year 2006. Likewise, oil-producing countries encouraged the use of natural-gas vehicles to improve their oil export volume. Price reduction, allowance for the conversion from liquid-fuel vehicles to NGVs, and tax cuts were some of the measures taken by various countries, though different policies were used in many countries to encourage the usage of natural gas.
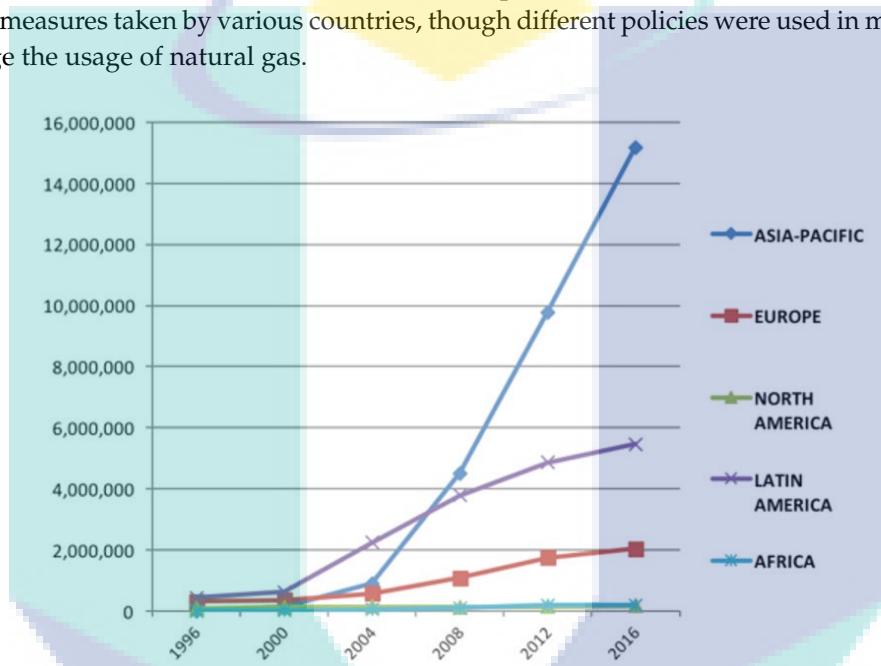

Figure 4. Natural-gas vehicles by region from 1996 to 2016 [78].

Table 4. Top 10 countries by natural-gas vehicle (NGV) population [78].

Country	NGV Population	% of NGVs Globally	Data Month/Year
China	6,080,000	23.2%	January 2018
Iran	4,502,000	17.2%	October 2017
India	3,090,139	11.8%	March 2018
Pakistan	3,000,000	11.5%	November 2016
Argentina	2,185,000	8.4%	October 2016
Brazil	1,859,300	7.1%	November 2015
Italy	1,004,982	3.8%	March 2018
Columbia	571,668	2.2%	March 2018
Thailand	474,486	1.8%	July 2016
Uzbekistan	450,000	1.8%	June 2013

In many countries, natural-gas conversion mainly occurs in diesel-fueled vehicles such as bus fleets and large trucking operations. It was assumed that natural gas will meet 50% of diesel demand by 2020, overtaking a 20-year diesel demand growth of 3.7% [32]. Moreover, the price of natural gas is lower than that of diesel fuel, which would help NG take over the diesel market in the future. Small modifications in fuel injection and ignition systems can contribute to a change from conventional gasoline vehicles to natural-gas vehicles. However, the biggest problem relies on fueling infrastructure, which is considerably smaller than that for conventional fuels.

3. Natural-Gas Fueling Infrastructure

The natural-gas supply system is the main feature considered when it comes to intensifying the number of natural-gas vehicles, for which refueling stations play the leading role [39]. Natural-gas refueling stations are the primary concern for users of natural-gas vehicles [85]. Fueling stations are also the main hindrance for the widespread use of natural-gas vehicles. However, a higher growth in the number of refueling stations was observed and reported. There were more than 28,955 fueling stations at the end of 2016, and a linear increase was foreseen for the coming years. The global trend in the number of natural-gas refueling stations over the last two decades is shown in Figure 5a. Higher growth was observed in the last decade, before which the number of fueling stations was quite small. With the growth in the number of NGVs, the number of fueling stations is increasing rapidly in many regions. Figure 5b illustrates the number of refueling stations by region as of 2016. The Asia-Pacific has more than 16,000 fueling stations, making it the region with most number of stations. This geographic region also saw fast growth in the number of natural-gas fueling stations. In contrast, slow growth was observed in other regions, which, in one way or another, affected the broad adoption of natural gas as a vehicle fuel. Engerer et al. [80] discussed the influence of lack of infrastructure on the growth rate of the number of NGVs in Europe as the region, except for Italy, experienced a slower growth rate in the number of NGVs during the last decade.
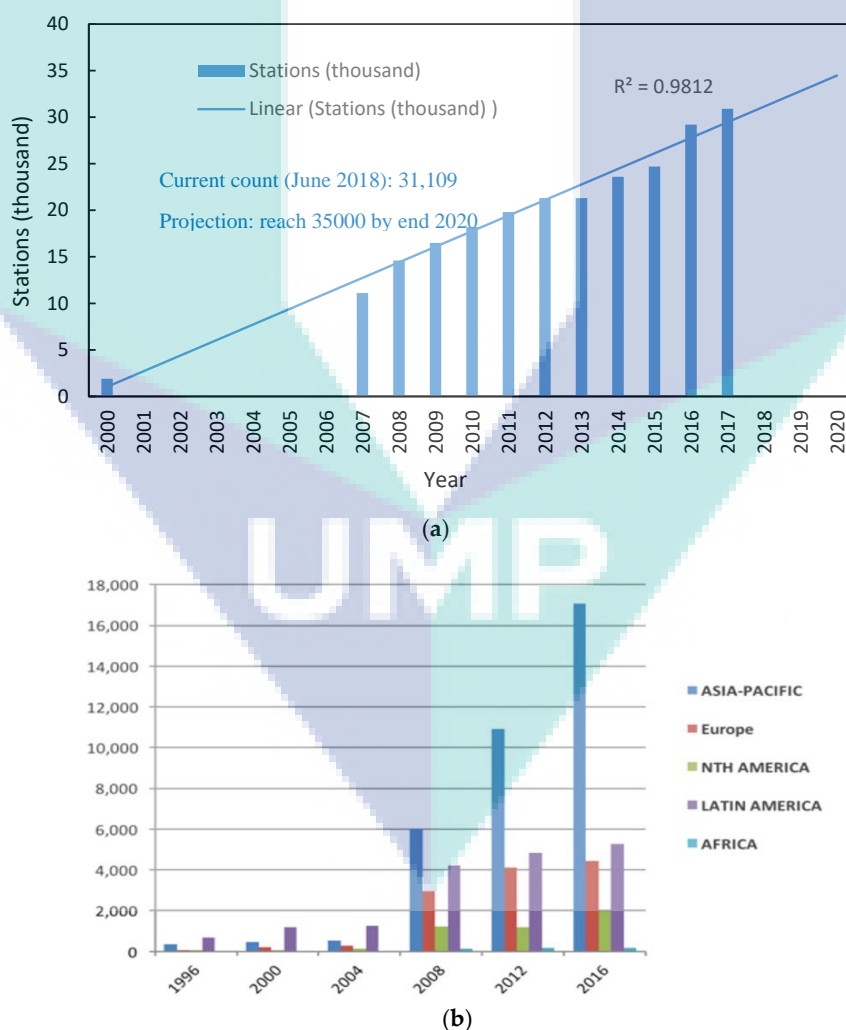

(a)

(b)

Figure 5. The number of natural-gas fueling stations: (**a**) worldwide and its projection; (**b**) growth by region [78].

Table 5 shows the top 10 countries in terms of refueling stations. Currently, China has the highest number of fueling stations with around 8400 reported in January 2018, with more stations undergoing construction. However, this is considerably smaller than the number of refueling stations for gasoline and diesel fuels in the country. The number of refueling stations in Pakistan represents approximately 11.5% of the total number of stations present globally, and reached over 3416 in November 2016. Semin et al. [86] highlighted the expansion of the natural-gas refueling infrastructure in Malaysia and reported a higher growth rate in the number of natural-gas vehicles in the country. Furthermore, replacing liquid fuel would reduce GHG emissions in the country. The number of vehicles per fueling station (the ratio of vehicles to fueling stations) is the main aspect to be considered when determining the expansion in the number of natural-gas vehicles. Refueling time and waiting duration are another two key issues encountered when adopting the use of natural vehicles. A number of refueling stations approximately 10–20% of that for gasoline would eliminate the refueling issues, as the price of NG is usually 40–60% lower than that of gasoline [87]. The smaller ratio of vehicles to fueling stations would also encourage automotive manufacturers to develop dedicated CNG vehicle models.

Table 5. Top 10 countries by the number of fueling stations [78].

Country	NGV Population	Fueling Stations	Ratio of Vehicles to Stations
China	6,080,000	8400	724
Iran	4,502,000	2400	1875
India	3,090,139	1424	2170
Pakistan	3,000,000	3416	878
Argentina	2,185,000	2014	1085
Brazil	1,859,300	1805	1030
Italy	1,004,982	1219	824
Columbia	571,668	813	703
Thailand	474,486	502	945
Uzbekistan	450,000	213	2113

3.1. Types of Refueling Station

Similar to the vehicle performance parameters, refueling stations and services could be of importance for NG vehicle operation. There are two types of natural-gas fueling station: CNG refueling stations and liquid natural gas (LNG) refueling stations. CNG refueling stations require additional infrastructure compared to gasoline or diesel stations. This mainly includes large compressor and cooling systems to compress the gas to 24 MPa, which increases the initial construction cost of CNG stations [74]. It was reported that constructing one refueling station requires a huge amount of investment. LNG fueling stations cost twice that required for CNG fueling stations, making it a barrier for developing the infrastructure. CNG can also be filled by LNG, whereby L-CNG refueling stations are used involving gasification prior to CNG sales machines [88].

Unlike CNG refueling stations, LNG refueling stations do not require a compressor. As a result, there is less noise emission than CNG stations. Moreover, it is comparatively compact in shape and requires easier installation as the parts can also be assembled in a factory. The number of LNG refueling stations is increasing in many countries. The number of refueling stations in the US and China rose by 3% and 32%, respectively, in the years from 2010 to 2015 [89]. Supplying LNG through LNG tankers is more economical than on-site liquefaction. CNG can also be supplied to LNG stations if there is a small-scale liquefaction plant. Arteconi et al. [69] investigated the use of LNG in vehicles, and problems existed with supply systems. It was reported that solving the limitation of refueling stations through either government subsidies or incentives could help natural gas meet the demand required by the transportation sector, and this could be achieved with limited additional investment. For instance, a European project called GasHighWay is aiming to solve refueling barriers [90]. The European commission plans on building LNG fueling stations at every 400 km, and it is targeting to alleviate the barrier of using LNG as an alternative fuel for heavy-duty vehicles in the region [91].

3.2. Natural Gas Quality

Natural gas is non-toxic to human beings and animals. In the event of leakage, it tends to disperse into the atmosphere due to its lightweight characteristics as compared to air. If the leakage also happens in a confined space, the displacement of oxygen is expected, which may slightly affect respiration; however, its lightweight nature helps make lower points have sufficient oxygen, while displacement is only expected at the highest point. Its energy-to-carbon ratio is the high compared to other fossil fuels. Its octane number is the highest (110/130) [92] compared to diesel (92/96) and gasoline (95/98), which helps increase the compression ratio, thus leading to higher efficiency [93]. Its autoignition temperature is approximated to be 540 °C, whereas it is 225 °C for diesel. More importantly, it is insensitive to climate conditions as it does not freeze until −165 °C. Bakar et al. [10] reviewed the advantages of CNG with vehicles regarding environmental issues. On average, there is more than 50% reduction in emissions, excluding CO_2, reported with the combustion of natural gas, with almost zero little matter [11,94]. The noise level was also detected to be quite small, and natural gas further reduces noise by about −5 to −8 decibels, which improves quality of life in urban areas. It is easily incorporated with biomethane produced from biomass without modification in the engine design or infrastructure. It has higher calorific values, which, in some regions, results in it being named H-gas referring to high-calorific gas [95].

Natural gas is mainly composed of methane with an approximate percentage of 99% [96]. In many samples, methane constitutes 92% of natural gas, whereas the remaining components are higher-level hydrocarbons and some contaminants [97,98]. A composition of methane as low as 70% can also be found in natural gas [99]. Table 6 shows the compositions of different samples of natural gas.

Table 6. Composition of natural gas in different samples [10].

Composition (Formula)	Volume Fraction (%)			
	Sample 1	Sample 2	Sample 3	Sample 4
Methane (CH_4)	94	92.07	94.39	91.82
Ethane (C_2H_6)	3.3	4.66	3.29	2.91
Propane (C_3H_8)	1	1.13	0.57	Nil
Iso-butane (i-C_4H_{10})	0.15	0.21	0.11	Nil
N-butane (n-C_4H_{10})	0.2	0.29	0.15	Nil
Iso-pentane (i-C_5H_{12})	0.02	0.1	0.05	Nil
N-pentane (n-C_5H_{12})	0.02	0.08	0.06	Nil
Nitrogen (N_2)	1	1.02	0.96	4.46
Carbon dioxide (CO_2)	0.3	0.26	0.28	0.81
Hexane ($C_6 + (C_6H_{14})$)	0.01	0.17	0.13	Nil
Oxygen (O_2	Nil	0.01	<0.01	Nil
Carbon monoxide (CO)	Nil	<0.01	<0.01	Nil
Total	100	100	100	100

Natural gas also receives more attention in safety, environmental, and efficiency contexts compared to conventional fuels [100]. Liu et al. [101] reported that synthetic natural gas could be used in CNG vehicles. Currently, an increase in natural-gas demand motivated higher synthetic natural-gas production.

Natural-gas properties play a significant role in gas engineering, among which density is the main property. Esfahani et al. [102] used a least-square support vector modeling approach to determine the density of natural gas. The density of natural gas was predicted as a function of molecular weight, temperature, and pressure. The model predicted the density of natural gas in pressures ranging from 1 to 690 bar, temperatures from −3.9 to 238 °C, and gas molecular weights from 16 to 130. They observed higher effects of molecular weight on gas density compared with the consequences of pressure and temperature. Jarrahian et al. [99] illustrated the measurement of viscosity of natural gas at high temperature and pressure. They predicted the viscosity of natural gas in a wide range of temperatures

(up to 444 K), pressures (up to 138 MPa), and compositions, which helps during the design process of surface facilities and the management of natural gas [103]. Major effects of the molecular weight of gas on viscosity compared to pressure and temperature were also observed by Yousefi et al. [104], who developed a model that predicted the viscosity of natural gas. Another critical parameter that affects natural-gas transportation in the pipeline is the dew point, which causes condensation and pressure drop, thereby affecting transportation efficiency. Skylogianni et al. [105] developed a model to measure and predict the dew point of natural gas, so s to avoids hydrocarbon condensation and increase transportation efficiency. Pezhman et al. [5] investigated the thermophysical properties of natural gas, so as to optimize natural-gas production. Table 7 shows the properties of CNG as compared to the two conventional transport fuels.

Table 7. Combustion and physical properties of compressed natural gas (CNG), diesel, and gasoline.

Properties		CNG	Diesel	Gasoline
Composition, weight %	Carbon	75.0	82.5 [106] 84–87 [107]	87.0 85–88 (c) [107]
	Hydrogen	25.0	12.75 [108] 33–16 [107]	13.0 12–15 [107]
	Oxygen	0.0	0.0	0.0
	Nitrogen	0.0	0.0	0.0
Molecular weight (g/mol)		16.04	184.43 [106] ~200 [107]	100–105 [107]
Density at 15 °C and 1 atm (kg/m^3) [107]		0.75	803–887	719–779
Specific gravity at 15 °C and 1 atm [107]		0.424	0.81–0.89	0.72–0.78
Stoichiometric air–fuel ratio	Molar Basis	9.7	50.03 [1]	59.5 [2]
	Mass Basis [107]	17.2	14.7	14.7
Stoichiometric volume occupation in cylinder, %		9.35	N/A	2 [3]
Lower calorific value	MJ/Nm^3	38.0	36,046	32,317
	MJ/kg	47.1	44.41	42.9
Stoichiometric mixture energy density (MJ/Nm^3)	Mixture aspirated	2.9	3.61 [4]	3.55 [5]
	Air Aspirated	3.60	N/A	N/A
Flammability limit, % vol. of fuel in air [107]	Lower	5.3	1	1.4
	Higher	15.0	6	7.6
Laminar flame velocity (cm/s)		38 [11]	82.17 [109]	48.93 [110]
Latent heat of vaporization at 15 °C, MJ/Nm^3 [107]		N/A	26.08	33.5
Latent heat of vaporization at 15 °C, MJ/kg [107]		N/A	0.233	0.35
Theoretical adiabatic flame temperature, K		2220	2300–2350 [111]	2411
Autoignition temperature, K [107]		813.15	588.7	530.37
Octane number [107]	Research octane number (R)	>127 [112]	N/A	90–100
	Motor octane number (M)	122 [112]	N/A	81–90
	Mean ((R + M)/2)	N/A	N/A	86–94
Cetane number [107]		N/A	40–55	5–20
Minimum ignition energy in air, MJ [113]		0.285	0.243	0.243
Storage pressure, MPa		20.6	0.1	0.1
Boiling point (atmospheric pressure), °C		−162	250–350	35–200

[1] Calculated from diesel fuel with 86.5% C and 13.25% H. [2] Calculated from gasoline with C_8H_{18}. [3] Volume percentage of fuel in vaporized stoichiometric mixture [107]. [4] Heating value of stoichiometric mixture, a mixture in vapor state [107]. [5] Heating value of stoichiometric mixture, a mixture in vapor state [107].

3.3. Fuel Treatment and Distribution

The transmission of natural gas through pipelines is one of the major challenges for the popular utilization of NGVs. The presence of carbon dioxide and hydrogen sulfide along with water forms an acidic solution, which is very corrosive and leads to severe damage in the pipelines, and hence, leakage of the natural gas. The presence of water, on the other hand, would cause slug flow following condensation

in pipelines. As high as 70% CO_2 could be present in some natural-gas fields. Therefore, it is necessary to remove some acidic gas prior to transportation to meet pipeline specifications of 2–3% CO_2 or not more than 50 ppm CO_2 in LNG production. By removing the acidic gases, the gas volume reduces, and the sold gas stream calorific value can be increased [114]. Currently, there are some mechanisms to remove these acidic gases via sweetening technologies to prevent corrosion. The utilization of these technologies depends on natural-gas feed conditions, size and location of natural-gas treatment plants, plant economics, ambient conditions, process control, and environmental aspects [115].

There are some mechanisms that are popular in this area, such as physical and chemical absorption, membrane separation, and low-temperature separation. The most suitable process for the removal of CO_2 from LNG is low-temperature separation as the distillation temperature for the gaseous products and dehydration is achieved. Moreover, CO_2 can be solidified and removed at a temperature below its solidification temperature, and achieves a higher degree of fractionation by adding additives. Membrane processes are also another eco-friendly alternative with little loss of amine solution. The most common membrane used is cellulose acetate, and the process depends on the gas components, membrane material, and the process conditions [116]. This technology is able to remove chemical species without phase change, and requires low thermal energy and simple process flow [117]. Membrane technology is normally used for purification and desalination of water, and is widely used to remove carbon dioxide, nitrogen, and hydrogen sulfide, which is highly toxic and corrosive. Higher compression-gas pressure is also required to overcome the hydrodynamic resistance caused by the permeation of acidic gases through nanoscale pores [118]. In the amine absorption process, the crude natural gas enters the separator in order to remove the free liquid prior to entering the absorber. The lean amine solution then enters the absorber and reacts with acidic gases and dissolves in the liquid phase. The acidic gas stream is cooled and flashed back to recapture water, which is then flowed back into the regeneration column to prevent water loss. However, the disadvantages of this process are the occurrence of corrosion during absorption, degradation when oxygen combines with amine solutions, and foaming due to condensed hydrocarbons, suspended solids, and other impurities [119].

Furthermore, inorganic solvents in carbonate-based absorption can chemically absorb CO_2. The process is regenerable, requiring low desorption energy; however, it has a lower rate of carbon-dioxide absorption that can be enhanced by adding piperazine. In addition, the gas stream can also be passed through trays with caustic solution in sodium-hydroxide-based absorption. The CO_2 forms a non-regenerable solution (Na_2CO_3) that must be removed in the process. The liquid desiccant absorption process (physical or chemical) is the most common technology used in the removal of acidic gases from natural gas worldwide. The acidic gas reacts with aqueous alkaline amine solution, and hence, purifies the processed gas. This process is mainly enhanced by lower temperatures, higher amine concentrations, and circulation rate. Furthermore, solid desiccant adsorption processes can handle lower gas-processing capacities. Its working principle involve either adhesive force or a chemical process [118].

The production of natural gas can be increased; however, the ability to distribute to the end user needs significant attention and consideration. The distribution of natural gas is one of the concerns. Natural gas can be transported to refueling stations either via pipeline or LNG tanker. The transportation of NG is mainly performed via underground pipeline to minimize the harmful effects [95]. Pipelines are an efficient way of transporting natural gas [120]. The transportation of natural gas via pipelines is common, which reduces the cost of liquefying the natural gas, and also reduces the transportation risk on the road [121]. Moreover, liquefaction requires advanced technology. Pipelines are generally the main pathways for transporting natural gas domestically and across countries [122]. To fulfill the increasing number of vehicles run by natural gas, there are many pipelines under construction in many regions. Recently, a higher growth in the number of pipelines was also observed worldwide. For instance, the overall length of China's pipelines reached 50,000 km from 16,000 km in ten years, and is expected to reach 100,000 km in 2020. Different policies are also in effect to boost the distribution line, and a higher pipeline utilization rate would help meet increasing natural-gas demands [123].

Distribution systems play a significant role for natural gas to be widely used. Natural gas can also be transported as LNG. LNG involves the use of a liquefaction plant to convert gas into a liquid phase, after which it is stored in a cryogenic tank at −160 °C [124–126]. LNG transportation is frequent in many regions [127]. Three-quarters of Asia's imported natural gas is as LNG, 50% of which belongs to Japan [128]. LNG imports are also increasing in Europe. Dorigoni et al. [129] predicted a tremendous increase in natural-gas usage in Europe by 2025 and compared the effectiveness of LNG imports, where the current LNG cost is higher than that of pipeline transport. However, their model also predicted a lower LNG price than that of pipeline gas if liquefaction, transportation, and regasification costs could be reduced in the future. The increase in LNG infrastructure across Europe was also reported in another study [130].

Currently, though there is a huge supply of natural gas from unconventional reserves, liquefaction facilities hinder the export capacity [131]. Wang et al. [132] studied the potential of natural-gas transport in Asia. They reported that pipelines carry 70% of the natural gas, and the remaining 30% is transported as LNG. CNG pipelines are mentioned as not being a good option for long-term utilization. As such, LNG could be considered a better option. However, this depends on the market demand and consumption capacity. It was reported that transporting natural gas in pipelines is more efficient [133]. For unforeseen circumstances and problems in pipelines, LNG is a better consideration, and its usage recently increased [134,135]. This diversification could potentially minimize issues related to supply [136]. Similarly, natural-gas storage plays a significant role in the development of NG vehicles. As the global consumption of NG increases, constructing a bigger storage system is required to alleviate deficiency issues, especially during times of peak demand.

Table 8 shows LNG and pipeline shares in the global gas market. The LNG share in the global gas trade market is increasing and was forecasted to overtake that of pipelines after 2020, resulting in an increase in the number of LNG vehicles. Wang et al. [137] proposed that there would be a dramatic growth in the number of LNG vehicles in China. A higher rate of LNG export from the US as a result of shale-gas production was forecasted [138,139]. The distribution phase is one of the main bottlenecks for LNG vehicles, though the technology of refueling, storage, and burning are well established. Two methods can be used to supply LNG to the refueling station. The first method is through purchase at regasification terminals, which depend on distance, and it was found not to be economical for very long distances, as heat can change the liquid to gas. The second method is through liquefaction on site [69]. For long distances, the latter might be an economical and feasible option; however, the main issue involves the availability of small-scale liquefaction.

Table 8. Liquid natural gas (LNG) and pipeline shares on the global gas trade market, adapted from Reference [140].

Natural Gas Transport Type	Year		
	2000	**2015**	**2040**
LNG	26%	40%	53%
Pipeline	74%	60%	47%
Total (tcm)	525	695	1150

3.4. Fuel Storage and Range

The storage of natural gas raises some disadvantages compared to liquid fuel, as it is in gaseous form at standard temperature and pressure conditions. The energy content per unit volume (storage energy) of natural gas is lower than liquid fuels. Natural gas can be made ready for use in vehicles in two forms: compressed natural gas (CNG) and liquid natural gas (LNG). LNG and CNG both indicate the stored forms of natural gas [141,142]. Most natural-gas vehicles worldwide operate with CNG as opposed to LNG [4]. Anderson et al. [39] illustrated that liquefying natural gas is an option to consider for enhancing the performance of natural gas, which lacks initial energy content in

its normal condition. LNG was found to result in a similar performance to that of diesel-fueled engines, and as a result, it was found attractive for heavy-duty vehicles. A cryogenic tank is required to store LNG at −165 °C. Another option of restraining natural gas to an adequate size is by compressing it to 20–22 MPa, which reduces its standard gaseous volume 100-fold. Pressurizing the CNG in a sealed storage container increases the energy density closer to that of liquid fuels. By doing so, it reduces the need for a larger tank in the car. Compressing the gas to the level mentioned above requires a hard certified tank, such as one made from steel or carbon fiber. Moreover, testing every five years is required to reduce accidents caused by cylinders. As the energy density of natural gas is 25% lower than that of gasoline, the tank usually takes up more space in the trunk of vehicles. The compression of natural gas, therefore, alleviates the issue of spacing in vehicles. It was reported that space problems in small vehicles is no longer an issue as small fuel tanks are suitable for storage in small vehicles [143]. CNG fuel characteristics are listed in Table 7.

Table 9 shows differences between CNG and LNG. LNG vehicles (1% of the total number of vehicles) are lesser in number compared to CNG vehicles (5% of the total number of vehicles). Hao et al. [84] reported that China started using LNG as vehicle fuels in 2009, whereas CNG was widely used beforehand. Eighty percent of CNG vehicles were modified from gasoline-fueled vehicles, while 20% were initially manufactured as CNG vehicles due to consumer cost contemplation. Modifications involve the installation of a CNG tank and an engine retrofit. Modified CNG vehicles were found to be more attractive than manufactured CNG vehicles as the follow-up costs were higher in the case of the latter. For LNG vehicles, 70% were heavy-duty transports (HDTs), and the other 30% were buses. Comparatively, LNG vehicles are more expensive (20% higher than diesel), typically due to the cost incurred by LNG tanks.

Table 9. Differences between compressed natural gas (CNG) and LNG [132].

Properties	CNG	LNG
Fluid state	Gas	Liquid
Pressure	100 to 250 bar	1 bar
Temperature	30 °C to −40 °C	−163 °C
Loading	Dehydrate, compress	Treat, liquefy, store
Loading/Offloading	Gas under pressure	As liquid
Compression Ratio	~250–350:1	~600/1
Containment D/t	~25 to 60	~1000
Material	Fine-grain normalized C-Mn steel, Fibre-reinforced plastic (FRP)	Aluminum, Stainless, Ni Steel

Storage capacity plays a significant role in the range of CNG vehicles. CNG vehicles have reduced driving distance, typically between 150 and 200 km, and the gas tank takes 10–20% of the luggage space. Upon replacing gasoline engines, CNG vehicles must cover a minimum range of 450 km, compensating for the coverage range of gasoline vehicles between 450 km and 800 km with a storage capacity of 45 to 110 L [85]. The storage capacity and pressure determines the range of vehicles following the optimization of engine efficiency. The pressure at the filling station of CNG is usually 24 MPa [144]. To achieve the range mentioned above, the storage capacity needs to be in the range of 170 to 280 L, which is almost three times that of the average of its gasoline counterpart, thereby reducing space for passengers and cargo. Moreover, the storage tank should also withstand mechanical damage due to accidents, and external degradation due to environmental conditions, including heat.

CNG vehicles still currently lack individual consumer market penetration. Decreased range, the reduced number of refueling stations, purchasing price, and difficulties during servicing are some of the barriers for adopting CNG as a vehicle fuel [39]. The purchasing price is higher for CNG than for gasoline. For example, the price for a Honda Civic was 18,500 USD for gasoline, while it was USD 26, 500 for a factory CNG vehicle. The lower cost of fuel is believed to offset the initial purchase price of the vehicle, and this is more feasible in a larger fleet, as there would be bulk purchase

sharing refueling and maintenance facilities. CNG does require modification when used in gasoline engines. Converting gasoline vehicles to CNGVs is technically possible by separately fitting a fuel supply system and injecting into the same cylinder. It can also be used in a diesel engine with small modifications. However, the theoretical performance of CNG may not be achieved, as engine internals have some effects. The simpler conversion of conventional vehicles into CNG vehicles augmented the number of natural-gas vehicles by 2.5% per year over the last four decades in different vehicle types, including light or heavy vehicles, commercial trucks, street sweepers, trains, and buses. A significant regulator is required when delivering CNG from storage to four-stroke engines, and a gas injector assisted by a metering valve is also needed for injecting gas into the combustion chamber.

3.5. Natural Gas from Other Sources (Renewable CNG and Biomethane)

In addition to the promising reserves and relatively low prices, some countries also decided to produce biomethane for transportation to avoid potential problems related to supply to the international market. This is widely practiced in some regions in an effort to tackle energy and supply security caused by geopolitical pressure and instability, and as a result, the use of biogas in different parts of the world is estimated to double current production in 2022 [145]. Biogas is produced via anaerobic digestion, which is a biochemical conversion mechanism of biomass into useful fuel. The process involves the digestion of human, animal, and plant waste with anaerobic organisms in the absence of oxygen in the digester [146,147]. Biogas can also be produced via anaerobic fermentation in landfill, which is referred to as landfill gas. There are three main stages in biogas production: hydrolysis, acidification, and methane formation. Consequently, the product contains methane in prime amounts ranging from 50% to 60%, while the remainder is mostly composed of CO_2 comprising 30% to 40%. It has a small amount of other impurities including water, albeit not exceeding 4%. As the methane content in biogas is high, it can be directly used for heat and electricity generation. However, as the methane concentration determines the energy content, upgrading to a higher proportion of methane, called biomethane, is vital for its application as a transport fuel. Upgrading biogas to biomethane removes CO_2, which purifies the gas and constitutes its energy content as a fossil-fuel-derived natural gas. Biomethane production was reported to be suitable for different engine modes, and its share in the transportation sector is estimated to reach 27% by 2050 from a 2% share at present [148]. Moreover, it was found that the application of biomethane in the transportation sector is as economically competitive as heat and electricity generation from biogas [149].

Membrane separation, chemical and physical absorption, pressure swing adsorption (PSA), and cryogenic processes are some recent technologies being used to upgrade biogas to biomethane. In conjunction with these technologies, a prior stage is required to remove or reduce other impurities including H_2O, siloxanes, and H_2S. Absorption relies on the solubility of compositions in the biogas. As CO_2 is more soluble than CH_4, it can be separated via absorption, which can be categorized into high-pressure water scrubbing, organic physical scrubbing, and chemical scrubbing. The category is based on the solvent used for the absorption process. Water is used as the solvent in water scrubbing, organic solvents, such as selexol, are used in organic physical scrubbing for dissolving purposes, while chemical scrubbing uses chemicals to absorb and chemically react with CO_2 [148]. In pressure swing adsorption, CO_2 due to its lower molecular size compared to CH_4 can be removed into the adsorbent material using elevated pressure and separated from CH_4. Regeneration processes would then help remove the adsorbed CO_2 by applying lower pressure [150]. Currently, membrane separation has a larger market due to its economic benefits. The principle of cryogenic separation mainly arises from different boiling temperatures of CO_2 ($-78.2\,^{\circ}$C) and methane ($-161.5\,^{\circ}$C) at 1 bar; thus, the separation of the two gases can be achieved while liquefying [151]. Biomethane with above 95% methane content was achieved using these technologies, which is then suitable to be used as vehicular fuel.

There is a recent initiative of producing methane through power to a gas solution in view of storing excess renewable electricity [152], CO_2 capture, and flue gas treatment [153]. Methane can be produced through this solution in two steps. A surplus of electricity is supplied to the electrolysis process where high-temperature steam is injected, and oxygen and hydrogen are separated.

Hydrogen is then combined with carbon dioxide in a methanation reaction. The technological, economic, and environmental feasibility of such an initiative is still under investigation. The methane produced from this process is another potential alternative fuel for internal combustion engines.

4. Natural-Gas Engines and Their Limitations

Since the 1940s, natural gas has been used as a source of energy for heat and electricity, and as a raw material in the chemical industry. In the transportation sector, it has been used to fuel vehicles for decades. This was intensified in the last two decades due to the mass production of lightweight high-pressure storage cylinders [11]. However, the market share of natural-gas vehicles is low, amounting to only 15.2 million of the 1.2 billion total vehicles [6]. This is in contrast to the multifaceted benefits of the fuel and its abundant availability. Even though research shows a growing trend in the market share of natural-gas vehicles in the next 20 years, with an annual growth of 5–7% pushing the market share to 35 million in 2025 [7], natural gas is far below the capacity of replacing other fuels in transportation sector. This section presents the types of engine using natural gas as a source of energy, and their limitations. Natural gas is commonly used in automotive vehicles with two methods of fueling, compressed natural gas (CNG) and liquid natural gas (LNG). Details of these two fuels are stated in Section 3, Table 9. This section focuses on CNG-powered engines and their limitations.

CNG is most commonly utilized in spark-ignition (SI) engines. This is due to the higher autoignition temperature, as shown in Table 7, requiring higher ignition energy only attainable through a spark. In recent studies, there were efforts to utilize CNG as a diesel substitution in compression-ignition (CI) engines in a dual-fueling mode. This was mainly motivated by the higher emissions of particulate matter (PM) and nitrogen oxides (NOx) in diesel-fueled compression-ignition engines. Figure 6 shows the various combustion modes for CNG in internal combustion (IC) engines [154]. The utilization of CNG in compression-ignition (CI), dual-fueling compression-ignition (DFCI), and homogeneous-charge compression-ignition (HCCI) engines, along with their recent progress, is the focus of a separate review. The current work focuses on the utilization of natural gas in spark-ignition engines and its technological and operational challenges. The latest advancements in research and development using CNG in diesel engines is also briefly discussed.
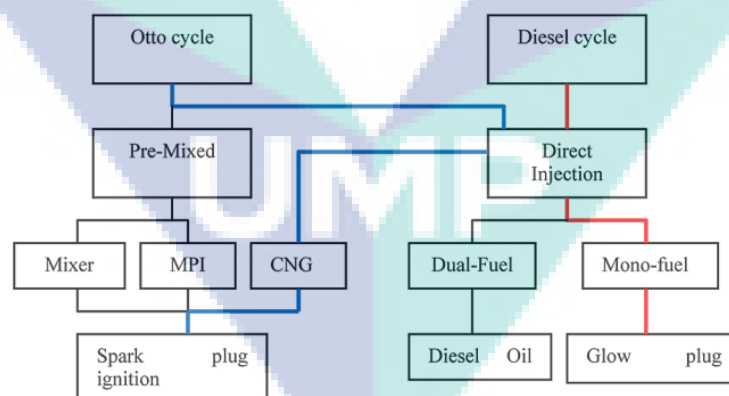
Figure 6. Combustion modes for compressed natural gas (CNG) in internal combustion (IC) engines [154].

The ignition and flame initiation process of an SI engine should be discussed in detail for a better picture of the combustion phenomenon of both liquid and gaseous fuels. In an SI engine, combustion is initiated by a spark discharge, which is imposed by an electrical ignition system. The initiation and formation of a self-sustaining flame kernel in the combustion of such an engine comprise complex processes that can have many phases. These stages are categorized as pre-breakdown, and the plasma and initial combustion phases [155–157]. The fundamental requirements for the ignition system are to create a self-sustaining flame kernel to have enough voltage to break the gap resistance between the electrodes. The ignition system should have enough energy-storage capacity to create a sufficiently

sized ignition kernel, and there should be a sufficient duration of voltage release [155]. The minimum ignition energy required by different fuels in air varies. As shown in Table 7, the minimum ignition energy required by CNG is higher than that of gasoline. The required minimum energy of ignition systems can be the function of an equivalence ratio (φ). For a lean local air/fuel mixture, the required minimum ignition energy can be higher. The mixture φ does not directly affect the initial plasma kernel; however, the inflammation process and thickness are significantly affected by the local φ. Hence, a lean mixture demands a larger plasma kernel before inflammation becomes apparent. The work of Aleiferis et al. [158] also showed that, for a given spark energy, the longest discharge duration produced the highest initial flame-kernel growth rate.

The regular combustion process of SI engine can be categorized into three distinct phases according to the energy release and fuel burn rate as shown in Figure 7a,b, and as discussed in Reference [155]. The first phase is the flame development process, during which a small fraction of fuel is burned (up to 10%). The flame size in this phase, especially in the early stages, is tiny and highly influenced by the turbulent flow surrounding it, by the φ of the mixture, and by heat transfer due to early flame contact with spark electrodes. The turbulent flame then propagates at a fast rate until the combustion chamber limits its expansion. Up to 90% of the total fuel energy is released at the end of the fast-burning phase [155]. The process ends with the completion phase, which can be long or unable to achieve a complete combustion depending on the φ of the mixture and other factors.

(a)

(b)
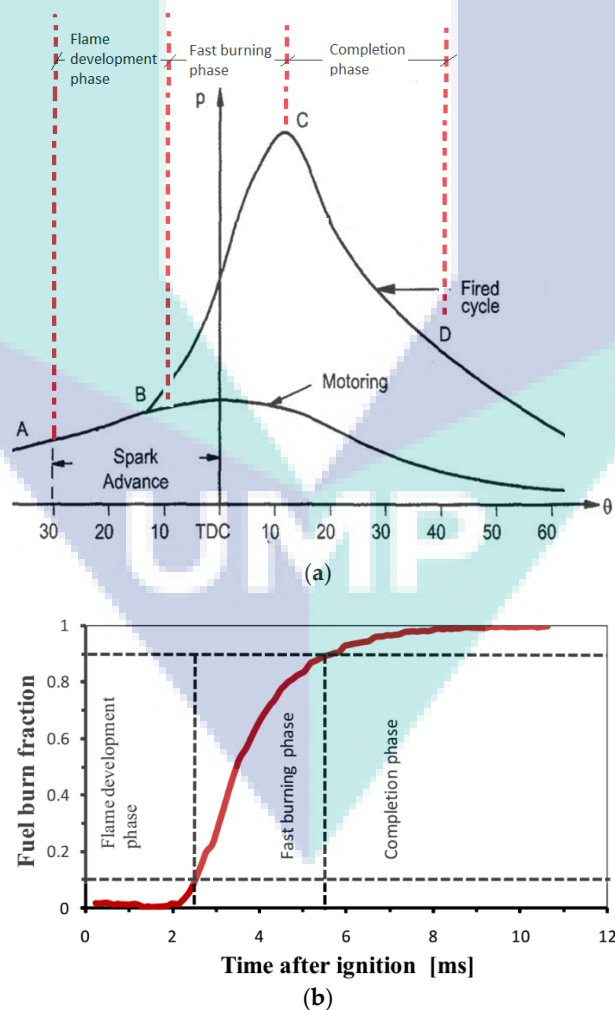
Figure 7. Spark-ignition (SI) engine combustion stages: (**a**) combustion pressure versus crank angle; (**b**) burn fraction of a homogeneous CNG combustion [159].

The performance parameters that affect the combustion of fuels in SI engines are the φ or its inversely proportional air–fuel ratio (λ). It increases along with the ratio of the actual fuel–air ratio to the chemically correct (stoichiometric) fuel–air ratio. Accordingly, mixtures can be lean ($\varphi < 1$), rich ($\varphi > 1$), or chemically correct (stoichiometric) ($\varphi = 1$). The ratio of the total volume (also known as maximum cylinder volume) to the clearance volume (minimum volume) of the engine cylinder is defined as the compression ratio (γ). The compression ratio is an influential parameter in both spark-ignition and compression-ignition engines, heavily affecting thermal efficiency. Even though thermal efficiency increases with an increase in compression ratio for both spark- and compression-ignition engines, the typical γ for a gasoline engine is traditionally limited to the range of 8–11, and 12–23 for a diesel engine. With an increase in the γ of an SI engine, the temperature of the air–fuel mixture rises above the autoignition temperature of the fuel-in-air mixture, leading to knock and surface pre-ignition. The compression ratio of diesel engines, however, is limited by the strength of the engine cylinder and the engine block material.

A proper understanding of the thermodynamic process of internal combustion engines depends on the accuracy of experimental work. Pressure and temperature measurement are the most common tools to analyze the combustion process that can be obtained through experiment. Other experimental observations need complicated and expensive measurement systems and devices, such as flame imaging, to understand the development, in-cylinder flow, spray behavior, and mixture distribution. The most widely used equipment to measure the combustion pressure is a pressure transducer that enables the study of pressure variation throughout the cycle. Observations and detailed analysis of pressure readings from a pressure transducer are utilized to gather further information about the rate of heat release (HRR), indicated mean effective pressure (IMEP), mass fraction burn (MFB), and combustion efficiency. In-cylinder pressure (P) is usually presented against degree crank angle (CAD) or cylinder volume (V). The pressure is built during the compression stroke (also called motoring pressure) and increases drastically due to the combustion process (also known as combustion pressure). It then drops as soon as the expansion stroke starts, and the built-up pressure is transformed into mechanical power, before the exhaust valve opens.

The area inside the cycle is considered IMEP. IMEP is defined as the average pressure exerted on the piston head during the working cycle developed by the combustion. The pressure difference between the pressure developed during the motoring cycle and the pressure generated during the working cycle is defined as the pressure built by the combustion process, used to calculate the heat released from the combustion.

4.1. CNG in Spark-Ignition Engines

Gasoline is used in spark-ignition engines. The transportation sector is currently under close surveillance due to an increase in emissions of CO_2, CO, hydrocarbon (HC), and NOx from the exhaust tail of these engines. Even though liquid fuels have advantages over their gaseous counterparts, such as a higher calorific value [160], ease of storage and transportation, and requiring smaller combustion chamber volumes, they are under scrutiny due to the gaseous emissions, as stated above. From Table 7, it can be seen that CNG as a fuel has a lower carbon content compared to its gasoline counterpart, leading to lower emissions of CO_2 in addition the fact that CNG is utilized in an air-tight fueling system. The evaporative emissions from CNG are minimal compared to those of liquid fuels used in SI engines. Likewise, gaseous fuels such as CNG take a brief time to fully atomize with the air. On the other hand, liquid fuels need more time for the air–fuel atomization. This is due to extra time required for the evaporation of spray droplets (physical delay). As a result, liquid fuels emit more HCs, especially with an increase in engine speed. It is said that CNG/LNG vehicles emit 10–20% lower GHGs compared to gasoline vehicles [161].

4.1.1. Mixture-Aspirated SI Engine

The supply of air–fuel ratio in spark-ignition engines is either via a carburetor, old technology, or through a fuel-injection system [162]. In the carburetor system, a mixture of air and fuel proportionated by the pressure difference in the venturi of the carburetor is inducted into the combustion chamber [163]. On the other hand, air alone enters through the inlet manifold and fuel is injected into the port or directly into the combustion chamber in the injection system [162]. The carburetor is completely replaced by a mixing chamber where CNG and air are mixed [164]. These types of engines are retrofitted from carburetor-type gasoline-fueled spark-ignition engines to use CNG. Such engines may operate as dual-fuel arrangements, where a CNG mixing chamber is installed after the carburetor, which is controlled by a solenoid switch valve. Since the engine is designed for liquid gasoline, it has a lower compression ratio. This is because of gasoline having a lower octane rating compared to CNG.

Table 7 shows the octane rating comparison of CNG and gasoline. When CNG is fueled in a retrofitted gasoline engine, the combustion efficiency drops and combustion stability is highly compromised. Jahirul et al. [165] reported a 19.25% reduction in brake power and 15.96% reduction in brake-specific fuel consumption (BSFC) at 50% throttle position for the speed range of 1500–5500 rpm. A 15.5% reduction in brake power and 9% reduction in BSFC were also reported by Rezapour et al., as shown in Figure 8 [166]. Moreover, fueling CNG in a retrofitted SI engine requires modifications to the ignition system, valve trains, storage, and fueling system. Such limitations are addressed when using diesel engines for a retrofitted CNG engine in SI engine mode, thereby allowing a high-compression-ratio combustion chamber to be attained [167]. A comparative analysis of CNG and gasoline on such retrofitted engines could not be found in the literature as base data for such engines are available only with diesel fuel.
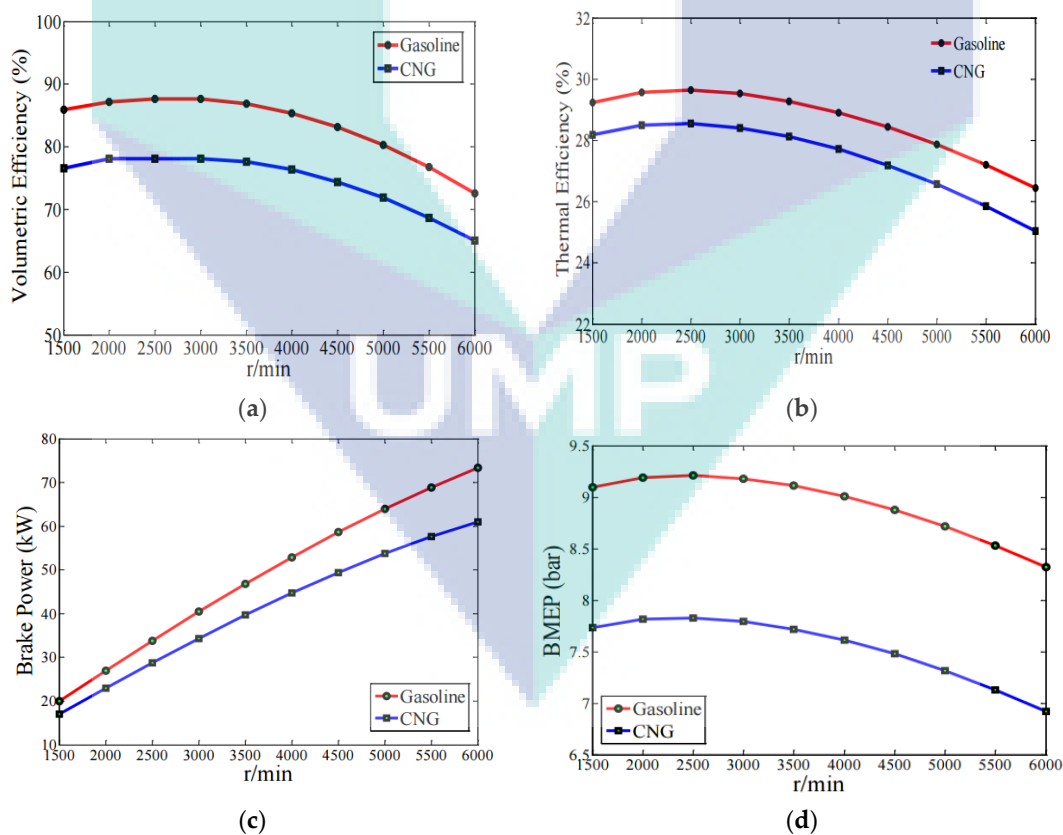
Figure 8. Performance comparison of CNG and gasoline in a retrofitted dual-fuel gasoline engine: (**a**) volumetric efficiency; (**b**) thermal efficiency; (**c**) brake power; (**d**) brake mean effective pressure (BMEP) [166].

In regular service, natural-gas engines consume 25–35% more energy than their diesel counterparts [168]. Engines retrofitted from diesel engines for CNG fueling can only be operated in mono-fuel operation, as fueling gasoline in such engines leads to severe knock and other operation hurdles. The high compression ratio of an engine retrofitted from diesel results in higher NOx emissions [169,170]. In addition to the issue of the compression ratio, as CNG displaces the air during the fuel–air mixing, there is an enormous compromise in the volumetric efficiency in the carbureted and indirect-injection fueling systems [11,171–174]. Specifically, in the carburetor system, there is air restriction due to the throttling effect. Therefore, the application of CNG in a mixture-aspirated SI engine is coupled with engine performance reduction. It was reported that natural gas gives 10% lower power output compared to equivalent gasoline-fueled vehicles [175–177]. On top of this, the precision of controlling the air–fuel mixture through a carburetor system was in question for a longer period. Adding electronic components did not show improvement; rather, the construction of such a system proved to be challenging [178]. It was at this point that the fuel-injection system was adopted from the compression-ignition engine fueling system. There are other mechanisms which improve the performance of CNG-fueled engine with a direct-injection (DI) fueling system, discussed in detail in the next section.

4.1.2. Spark-Ignition Direct-Injection Engines

Fuel delivery systems have seen various changes throughout the years, and recently incorporated advanced technologies. The development of fuel delivery started from a conventional carburetor system before arriving at the recent DI system. The limitations of a carburetor system are discussed in Section 4.1.1, and are examined further in References [179,180]. In the fuel-injection technology, fuel-and-air mixing is performed by forcing the fuel through a narrow nozzle with the help of high pumping pressure. The fuel injection system for SI engines is broadly classified as direct and indirect injection. The direct-injection system injects the fuel at high pressure directly into the combustion chamber, while, in the indirect-injection system (port-injection, manifold-injection, and multipoint fuel-injection systems), the fuel injector delivers fuel at some point near the combustion chamber. All indirect-injection systems like the carburetor fueling system have performance loss issues when they are fueled with gaseous fuels. The fuel-injection design would avoid problems related to balancing multiple carburetors and would gain even distribution in the inlet manifold. Some advantages of the fuel-injection system involve higher volumetric efficiency, high precision with air–fuel mixture control, and thereby, a better response to change, better fuel distribution and atomization, ability to integrate with feedback control, and the use of greater overlap [181]. Furthermore, the introduction of post-combustion control of emissions, such as catalytic converters and oxygen sensors, demanded a closed-loop control system and precise metering of the fuel–air mixture [182]. Electronic fuel injection systems now supersede the early injection systems that are mechanical. Single-point fuel injection (SPI) came after the carburetor system, followed by multipoint injection (MPI), and direct injections. The technological trend of the development of fuel-injection systems is shown in Figure 9.

The injector in a single-point injection system sprays fuel at atmospheric pressure, and as a result, the pressure regulator can constantly maintain gauge pressure. The single-point fuel-injection system (throttle-body fuel injection) is considered cheaper than multipoint fuel injection. It can result in a power reduction of 10% compared to a multipoint injection system [170]. CNG engines with single-point injection systems encounter lower IMEP, amounting to 13.8% at rated speeds compared to gasoline engines [183]. The fueling level of multipoint injection is controlled by the duration of injection pulses and fuel supply pressure, allowing for multipoint injection to gain higher power output compared to single-point injection (SPI) [184]. The fuel injector of the multipoint-injection systems senses the inlet manifold unlike the single-point-injection system, so as to maintain a constant differential pressure across the injection [179]. Moreover, the MPI system uses a more sophisticated system compared to SPI, one of which is the engine control unit (ECU) that monitors and controls the injection parameters, including injection timing, injection duration, and the amount of fuel required by

each cylinder [9]. It was reported that CNG engines employing MPI systems resulted in 3 to 5% better performance than SPI CNG systems. However, CNG engines employing MPI had a 10.4% lower IMEP than gasoline engines using MPI systems [36]. Multipoint fuel injection is not uncommon in today's vehicles. Multipoint injection suffers at high load, where uniform fuel distribution cannot be achieved. As a result, the direct-injection system (DI) is considered as the most recent sophisticated fuel-injection system [185]. A typical spark-ignition direct-injection (SIDI) engine consists of a high-pressure fuel pump, injector, and ECU, where the ECU controls the amount of fuel injection and injection parameters, such as injection pressure and injection time [186]. It was reported that DI CNGs had increased engine torque at all engine speeds compared to MPI CNGs, due to higher volumetric efficiency, enhanced in-cylinder flow motion, and improved combustion with faster flame propagation [187]. The direct injection of CNG offers advantages regarding power output, an extension of lean limit, and unburned hydrocarbon (UHC) emission levels; it also increases IMEP by between 9% and 15% of that generated by the manifold injection [188,189].

Direct fuel injection leads to much better control of charge stratification, while simultaneously allowing homogeneous stoichiometric or lean mixtures to be formed by injecting fuel early during the induction stroke. This flexibility of controlling the timing and quantity of fuel injection electronically has advantages of reducing exhaust emissions while maintaining high power output with much better fuel economy than conventional port-injected engines [190,191]. The advanced high-pressure fuel injection in the DI system helps the engine operate efficiently with short response times and with injection quantities appropriate for a broad range of engine sizes. While regulating injection parameters such as injection pressure, injection timing, and spray angle controlling the mixture preparation, it also helps reduce emission and increases the power output of the engine [192].
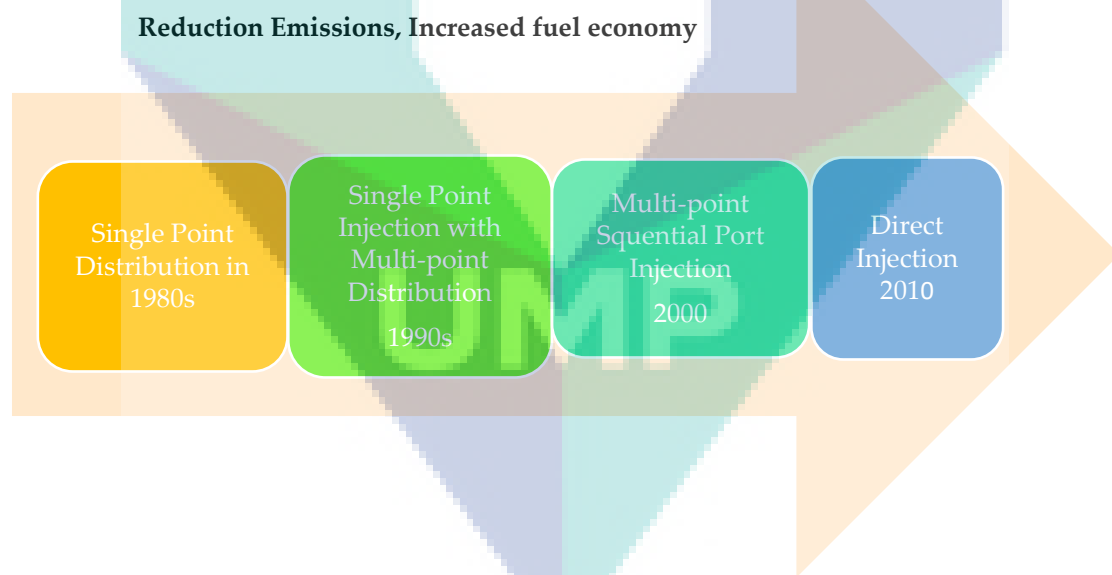
Figure 9. Technological development of fuel-injection systems [193].

The previous research and development of NGVs relied on retrofitting existing engine set-ups. Due to extensive studies on fueling technology and CNG in general, original equipment manufacture (OEM) engines are more reliable [194]. Direct-injection CNG engines are mostly designed based on the fuel properties of CNG, thereby eliminating performance loss associated with engine retrofitting [195]. However, CNG has a low flame speed (38 cm/s) and narrow combustible range (5.3–15%), and it requires a high ignition energy (0.285 MJ), as shown in Table 7. These factors lead to incomplete

combustion, and thus, lower performance and higher CO and total hydrocarbon (THC) emissions [154]. Such outcomes are more exaggerated at lower speeds and low-load operation conditions [192]. There were different improvement strategies employed over the years to optimize the performance and emissions of CNG-fueled SIDI engines. Section 4.2 discusses the relevant strategies and their success rates.

4.2. Performance and Emission Optimization Strategies of CNG Fuel in the Latest SI Engines

Due to this fuel being abundant and having superior benefits to the environment, there are multiple efforts to optimize the engine-operating parameters, based on the limitations of the fuel properties. The parameters taken in to account for the optimization of the performance of DI CNG engines include compression ratio, fuel-injection timing and duration, lean combustion, fuel stratification, ignition timing and energy control, injection pressure, exhaust gas recirculation (EGR), boost pressure, optimization of intake and exhaust valve lift, and adding more flammable fuels (hydrogen and syngas).

4.2.1. Effect of Compression Ratio

Increasing the compression ratio of the engine affects the pressure and temperature of the cylinder before the fuel is injected and combustion begins. This further influences the thermal efficiency, and thus, the fuel economy and emissions. Different researchers studied the effect of compression ratio on the combustion, performance, and emissions of CNG fueling in direct-injection spark-ignition engines [196–199]. Damrongkijkosol and Kerdsuwan (2006) investigated the effects of compression ratio on the performance and emissions of CNG fuel in a four-cylinder four-stroke engine retrofitted from a diesel engine. The compression ratio varied from 9.0 to 10.5 with 0.5 intervals. The engine was operated in the range of 1000 to 4000 rpm. The CNG fuel performance and emissions at four different compression ratios were compared, and a further comparative evaluation was done with the base diesel fuel. Figure 10 shows the brake power of the retrofitted engine with CNG and diesel fueling. With an increase in compression ratio and engine speed, the brake power increased [199].
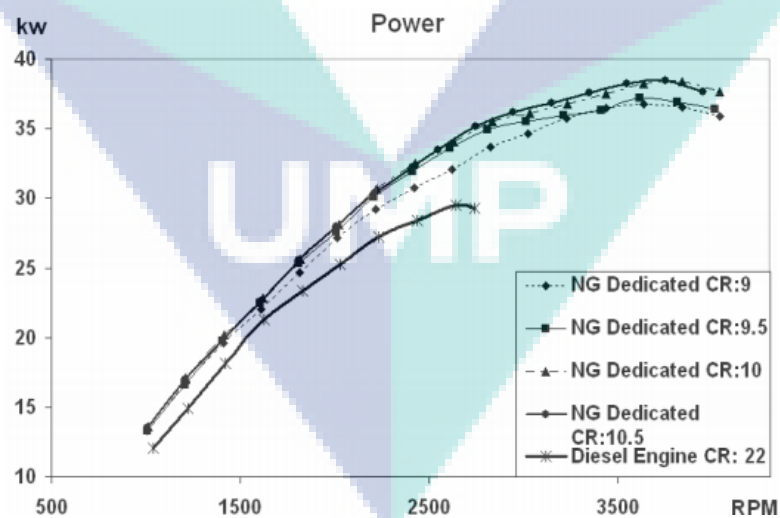
Figure 10. Brake power of CNG fuel at four different compression ratios and of diesel fuel [199].

Similarly, the effect of compression ratio on the combustion, performance, and emissions of a retrofitted single-cylinder engine (rated power was 4.5 kW at 1800 rpm in petrol mode, and 3.5 kW at 1500 rpm in diesel mode) fueled with CNG was investigated by Ramachandran and Waghmare [196]. The engine was operated at engine speeds ranging from 1200 to 1800 rpm. The compression ratio varied from 8:1 to 13:1 with an interval of 1. It was reported that the engine did not experience

knock over the range of compression ratios. Moreover, the peak pressure increased from 28.5 bar at a compression ratio of 8:1 to 43 bar at a compression ratio of 13:1, as shown in Figure 11. In terms of performance and emission, a similar trend to the findings of Damrongkijkosol and Kerdsuwan [199] was reported [198]. Based on the autoignition temperature of CNG (813.15 K as shown in Table 7), the compression ratio often goes as high as 17–18, based on the pressure–volume–temperature (P–V–T) polytrophic compression relationship ideal gas. However, the maximum compression ratio for CNG is bounded by the design of mechanical parts (mainly spark-electrode erosion) and the thermodynamic efficiency of the engine. Most researchers agree that the maximum working compression ratio in SI engines is 15 [8,9].
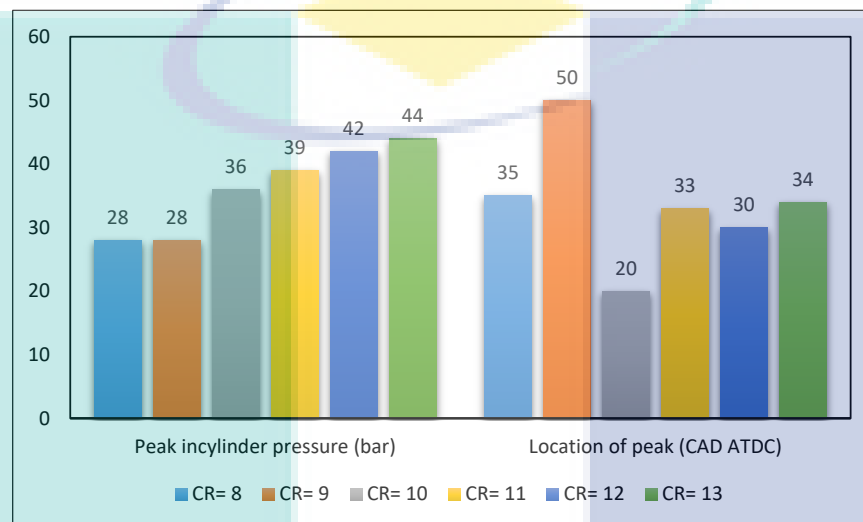
Figure 11. Peak in-cylinder pressure and its respective location of CNG under various compression ratios, modified from Reference [198].

4.2.2. Effect of Lean Charge Strategy

Another trend from diesel-engine operation in the CNG SIDI engines is the lean operation strategy. In the search for reduced greenhouse gas emissions and overall fuel consumption, the lean combustion strategy is an option explored in the research domain [192,200–202]. Lean combustion strategy works under both homogeneous and stratified charge depending on the extent of leanness. When the overall air–fuel ratio is maintained extremely lean, near to the lower flammability limit, the probability of an ignited mixture having a sustained flame is small [203]. In such cases, the strategy is mainly modified to have a fuel-stratification mechanism, so that a variable air–fuel ratio occurs around the combustion chamber. The stratification provides a relatively rich mixture near the igniter and a uniformly mixed ultra-lean mixture throughout the cylinder. Hagos et al. [192] reported an extension of the lean limit of CNG fuel with the use of a stratification fueling strategy. An extension of the lean limit of up to 10% was also reported by Evans et al. [204], as shown in Figure 12 for a partially stratified charge engine with a speed of 2000 rpm. Furthermore, the lean-burn strategy has superior performance with regards to emissions, NOx in particular [200]. The challenges with lean charge involve engine stability, as a result of reduced burning rate [9,200,202], and suitability only for part-load conditions and low-MEP operation [8]. Even though gaseous fuels are known for their lower emission of THC, lean-burn CNG has relatively higher emissions of THC, resulting from the unburned mixture in the end zone [205]. The effect of the air–fuel ratio on the combustion efficiency and emissions is shown in Figure 13. According to the review by Cho and He [9], the combustion instability under the lean-burn strategy can be further improved by optimizing certain parameters. These are the in-cylinder air motion, ignition energy, quality of natural gas, moisture content of induced air, residual fraction, and mixture temperature during ignition, which is a function of the compression ratio.
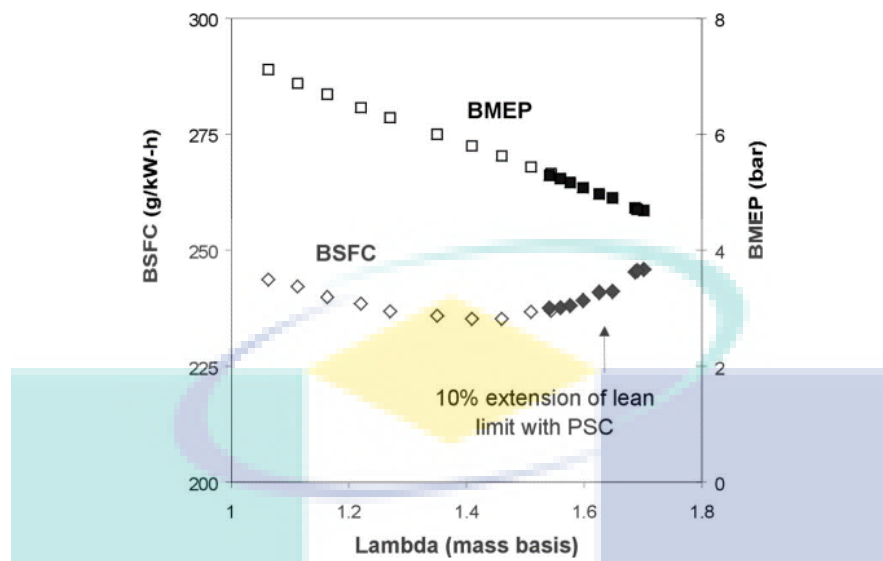
Figure 12. Extension of lean limit by partially stratified charge at 2000 rpm [204].
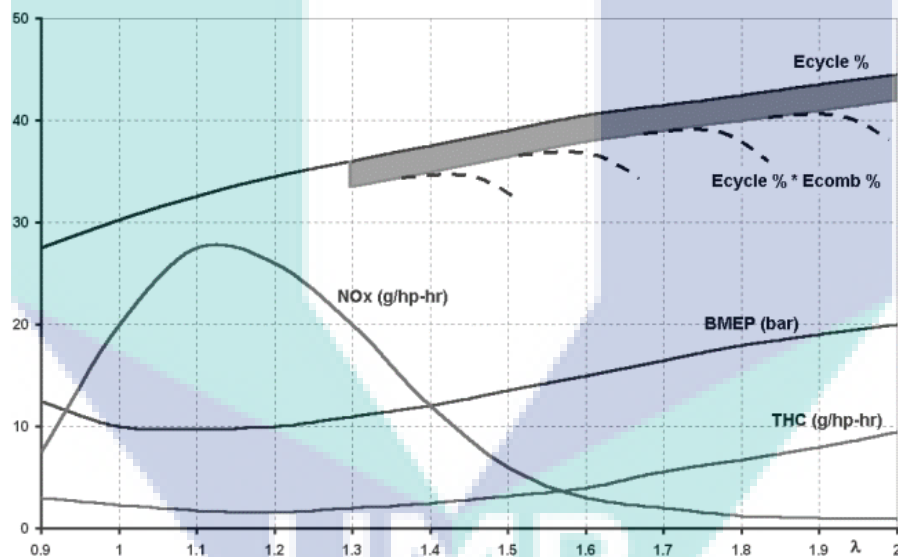
Figure 13. Effect of air–fuel ratio of natural gas [205].

4.2.3. Effect of Injection Timing and Injection Pressure

There are various efforts reported in the literature to improve the performance of CNG SIDI engines by injecting the fuel late after the inlet valve closes (IVC), thereby improving the volumetric efficiency drop [162,206–210]. When fuel is injected after the inlet valve closes (IVC), the air-breathing capacity of the engine does not get influenced by the type of fuel. However, there is insufficient time for the fuel to completely mix with the air when the fuel is injected late, leading to a slow combustion rate. For fast-burning fuels such as hydrogen and syngas, this fuel-injection strategy is adopted and it currently attracts attention [159,211,212]. Aziz et al. (2010) used a dedicated CNG engine for the study of the effect of injection timing on the combustion, performance, and emissions of SIDI engines. The engine test-bed was a single-cylinder research engine (SCRE) with a compression ratio of 14. The test was conducted at full-load conditions with the ignition point set at maximum brake torque (MBT) for speeds of 2000–5000 rpm. A high-pressure injector (18 bar) was used in a central injection system. The air–fuel ratio was set at the stoichiometric condition of 17.4 for CNG gas. Furthermore,

300° before top dead center (BTDC) injection timing was used as a baseline to simulate port-injection systems as a comparison for other direct-injection systems. By applying 300° BTDC injection timing, fuel was injected during intake stroke, which is assumed to have the same mixture properties as port injection systems. On the other hand, 180° BTDC was used to simulate direct injection and 120° BTDC was used to simulate late injection after the IVC. Figure 14 shows the injection-duration mapping for the three injections, with reference to the valve inlet valve opening and closing, and the start of ignition. They reported that direct injection performed better across most operation conditions, while port injection and late injection performed better at higher and lower speeds, respectively. Figures 15 and 16 show the performance and combustion trends of different injection timings, respectively [162].
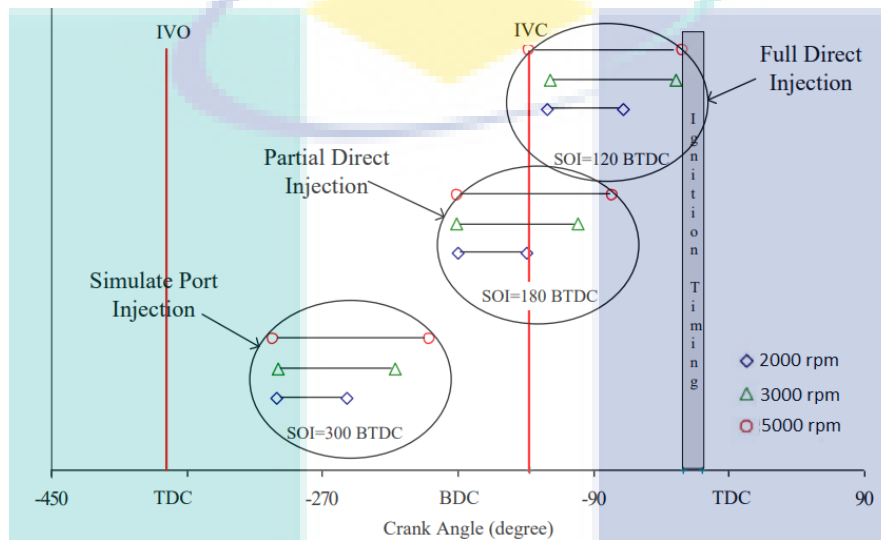
Figure 14. Injection duration for different injection timings for engine speeds 2000 rpm, 3000 rpm, and 5000 rpm [162].
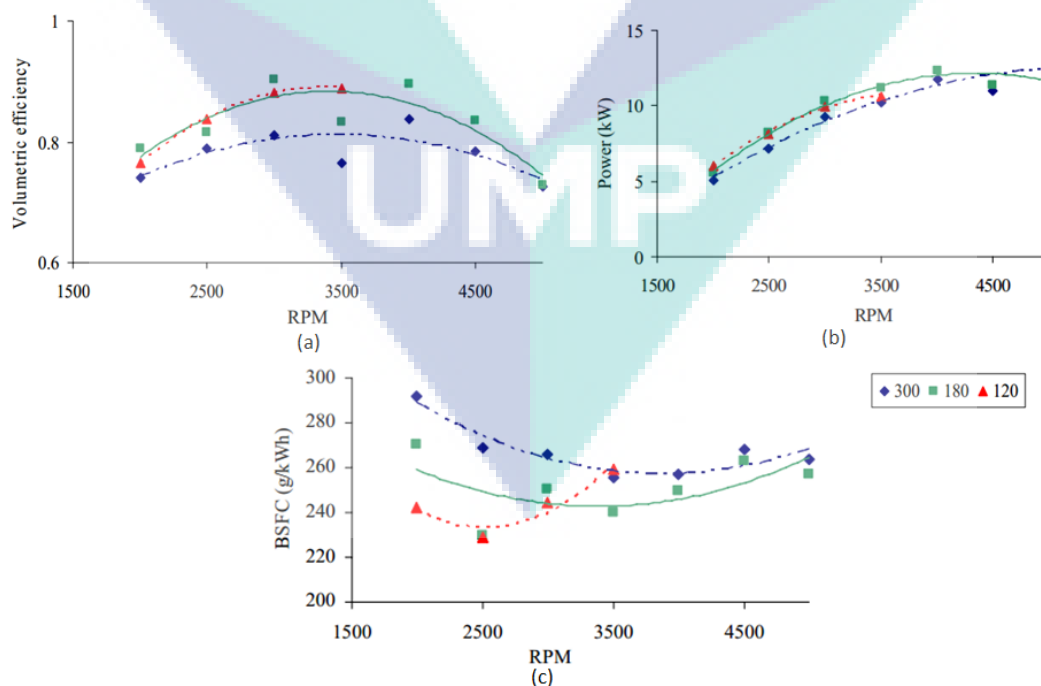
Figure 15. Volumetric efficiency (**a**), brake power (**b**), and brake-specific fuel consumption (BSFC) (**c**) of different injection timings at various engine speeds [162].

A similar study was conducted by Aljamali et al. [206] on a four-stroke four-cylinder direct-injection spark-ignition engine by varying the injection timings on 120° BTDC, 180° BTDC, 300° BTDC, and 360° BTDC. The speed was varied from 1500 rpm to 4000 rpm with an interval of 500 rpm. Maximum performance was found with the 120° BTDC at most engine speeds tested. At 4000 rpm, 180° BTDC was reported to perform better than the other injection timings. Better volumetric efficiency and higher performance were reported when fuel was injected near the IVC [210].
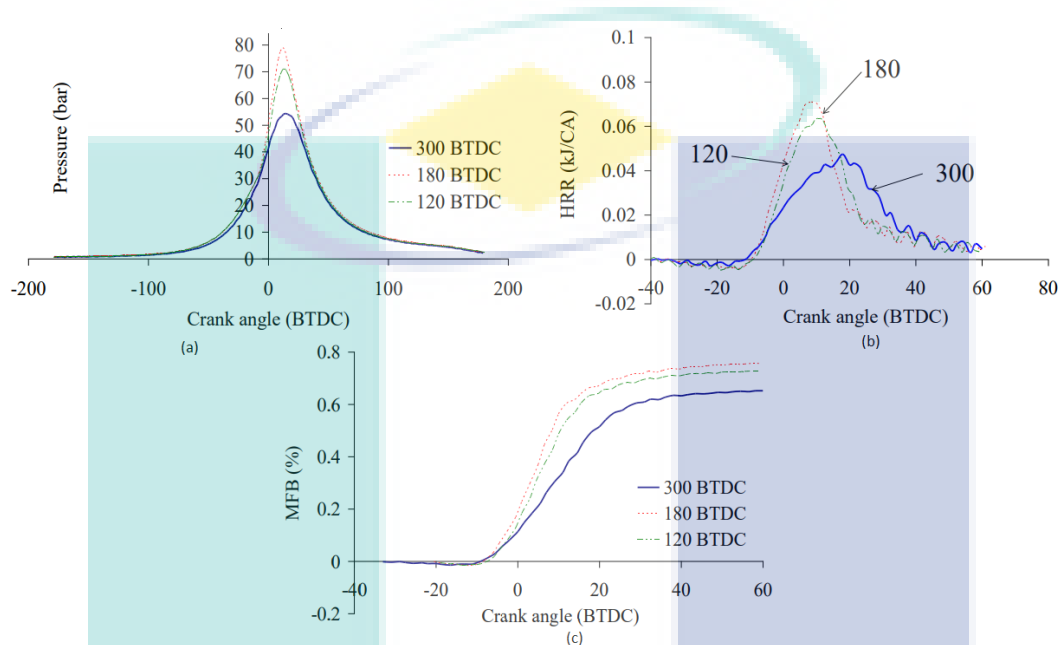
Figure 16. In-cylinder pressure (**a**), heat release rate (**b**), and mass fraction burned (**c**) for different injection timings at an engine speed of 3000 rpm [213].

Zeng et al. [208] investigated the effect of injection timing on the combustion characteristics of CNG fueling in an SIDI engine. The compression ratio of the engine under study was 8:1, and the throttle was kept at 70% open. The engine was operated at 1200 rpm, and the ignition advance was kept at 32° BTDC. Unlike the two studies discussed earlier, the injection duration was held constant, and the start of injection was varied from 150 to 210° BTDC with a 10° crank angle (CA). The maximum pressure, a higher heat release rate, and the shortest heat release duration were observed with 180° BTDC, similar to the observations of Aziz et al. [164] and Aljamali et al. [206]. They reported that injection timing had considerable influence over the combustion characteristics, for late injection in particular. Late injection affects the air-and-fuel mixing, as there is insufficient time before the onset of ignition. A similar observation was also reported elsewhere by Aziz et al. [162] and Aljamali et al. [206]. Late injection was also reported to be associated with higher emissions of HC and CO.

Firmansyah (2007) investigated the effect of fuel-injection pressure on the combustion, performance, and emissions of a CNG SIDI engine with a compression ratio of 14. The engine was operated at wide-open throttle, and the speed was varied from 2000 to 5000 rpm. The injection pressures considered in the study were 7.5 kPa, 12 kPa, and 18 kPa. It was shown that an injection pressure of 18 kPa had better performance at speeds below 3500 rpm, while 12 kPa showed superior performance at engine speeds higher than 3500 rpm. For the combustion process, IMEP values at 18 kPa were found to be the highest for all engine speeds, despite showing a slower burning rate compared to that at 12 kPa. Furthermore, 18 kPa showed greatest variation at lower speeds, decreasing as engine speed increased [213]. However, an insignificant effect was reported on the combustion characteristics by a change in injection pressure by Song et al. (2017). The experiment was conducted using various injection pressures of 5 kPa, 8 kPa, and 11 kPa [210].

4.2.4. Effect of Ignition Timing and Ignition Energy Control

In addition to the optimization of injection timing and injection pressure, there are various research studies on the optimization of ignition timing and ignition energy control. Ignition advances for maximum brake torque (MBT) affect the properties of the fuel, the equivalence ratio, and the burned-gas mixture. The engine design and operating conditions also have a significant impact on the optimal conditions. As shown in Figure 7, combustion in SI engines starts slightly before the compression of TDC and continues until slightly after TDC, ending after the point of peak pressure [155]. All stages of combustion (flame development, flame propagation, and the secure termination), as well as the length of the flame travel path across the chamber, influence ignition advances for MBT. There is a lack of consistency on ignition advances for MBT of CNG in the literature. Bell et al. (1993), as cited by Ehsan (2006), reported it as 15–20° CA more than that of gasoline [214,215]. This value was contradicted by Cho and He (2007), placing it at 2–10° CA more than that of gasoline [9]. This is mainly due to the lower laminar flame speed of CNG compared to gasoline (38 cm/s for CNG compared to 49 cm/s for gasoline, as shown in Table 7). Maximum brake torque is attained by igniting the fuel–air mixture so as to attain peak pressure at slightly after TDC, thereby maximizing the transfer of expansion work from the combustion gas to the piston, while reducing the transfer of compression work from the piston to the gas [155]. Figure 17 shows the effect of ignition advances on the conversion efficiency of CNG fuel, as observed by Dimopoulos et al. [216]. The optimal ignition advance for maximum fuel-conversion efficiency of CNG was reported to be from 28–32° BTDC. This result was similar to results obtained by Bell et al. [215]. In a separate study, Khan et al. (2014) investigated the effect of ignition timing on CNG at two different injection timings (60° BTDC and 90° BTDC). The 8.5:1 compression ratio two-cylinder four-stroke engine was run at 3000 rpm, and the ignition timings evaluated were 50, 44, 34, 24, 22, and 20° BTDC. The performance and emissions of the engine were studied. Ignition advances for MBT was reported at 40° BTDC and 34° BTDC for injection timings of 60° BTDC and 90° BTDC, respectively. The work did not specify the air–fuel ratio of the charge used in the study [217]. Similarly, ignition advances for MBT increase with a decrease in fuel–air ratio (φ) from the stoichiometric fuel–air ratio ($\varphi = 1$) [9]. This is due to the decrease in laminar flame speed with an increase in the air–fuel ratio [218]. Figure 18 shows the variation in laminar flame speed of CH_4 and NG under atmospheric conditions. The maximum laminar flame speed for NG (around 38 cm/s, as also stated in Table 7) was obtained at $\varphi = 1.1$. The amount of energy and the rate of energy release decreased with an increase in fuel–air mixture leanness. As a result, the laminar flame speed decreased. With a lower laminar flame speed, the mixture required a longer duration to reach peak pressure. If ignition timing is not well advanced, the position of peak pressure gets pushed far away from TDC, leading to a decrease in the transfer of expansion work from the combustion gas [155].
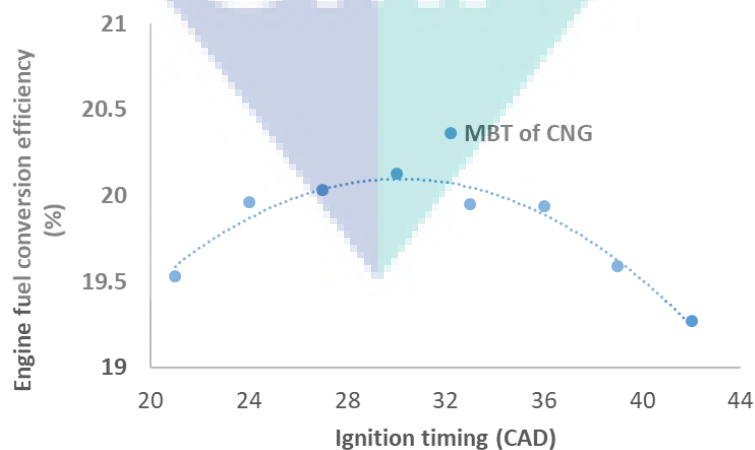
Figure 17. Ignition advance for maximum brake torque (MBT) extracted from Reference [216].
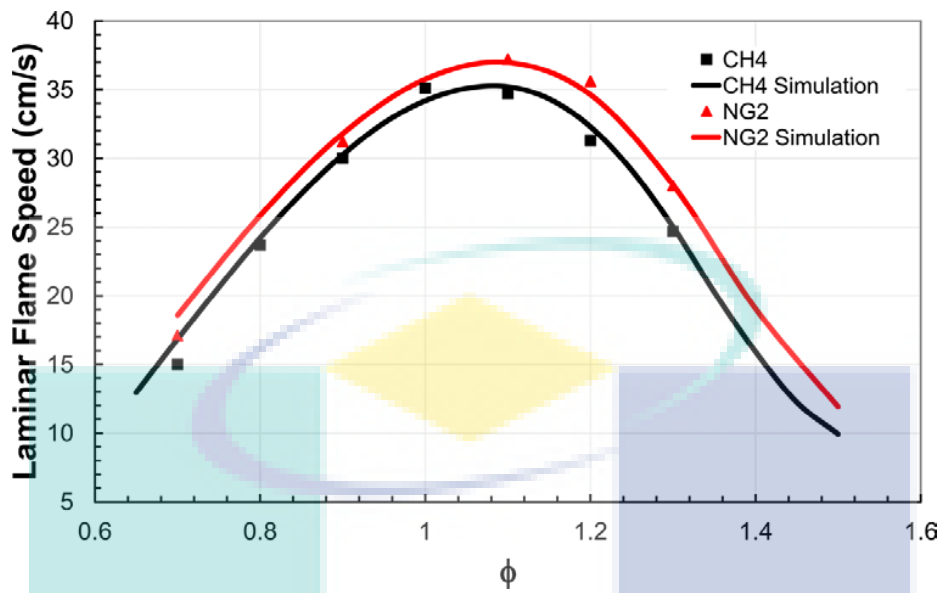
Figure 18. Laminar flame speed (cm/s) versus equivalence ratio (φ) for CH_4 and NG under atmospheric conditions [218].

4.2.5. Effect of Boost Pressure

The volumetric efficiency loss due to the displacement of air by gaseous fuels can be compensated by boosting the induced air, thereby increasing the breathing efficiency of the engine [219]. The volumetric efficiency of gaseous-fuel engines is also affected by the lack of evaporative cooling that is associated with liquid fuels [220,221]. In terms of the fuel properties, CNG has a lower laminar flame speed and a lower energy density compared to its liquid counterpart, as shown in Table 7. By doing so, the fuel economy of the engine, and thus, the pollutant emissions from the engine can be reduced. According to Hillstrom [222], CNG is the best candidate for such an optimization due to its higher octane number. There are a number of studies on the effect of boost pressure on the performance and emissions of CNG fuel in spark-ignition engines [92,169,222,223]. As cited in Cho and He [9], due to a high boost pressure is needed to overcome the performance loss of CNG fueling in SIDI engines, this forces the spark plug to work under more stress, leading to frequent failure [224]. As a result, Chala et al. [92] recommended the use of lower boost pressure, in the range of 7.5 kPa, combined with optimal fuel-injection timing for better performance and emissions, as shown in Figure 19.
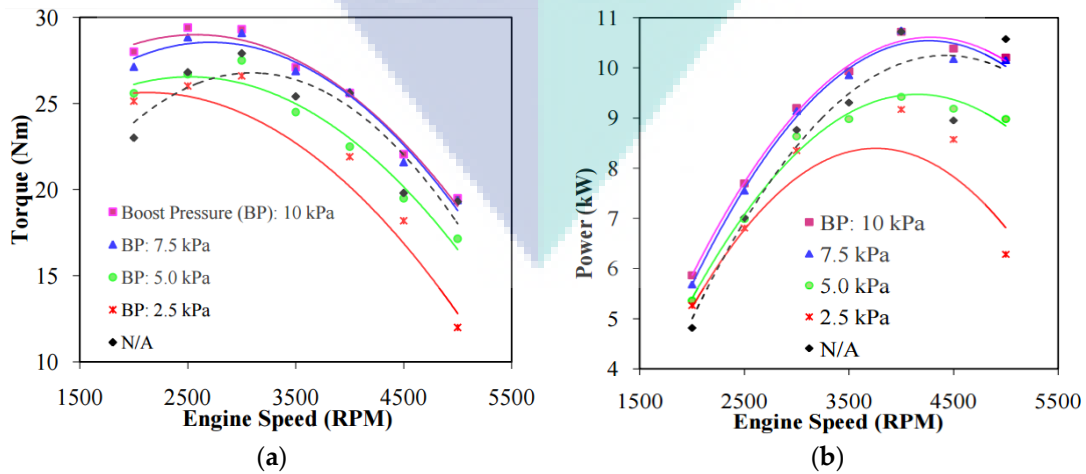
Figure 19. *Cont.*
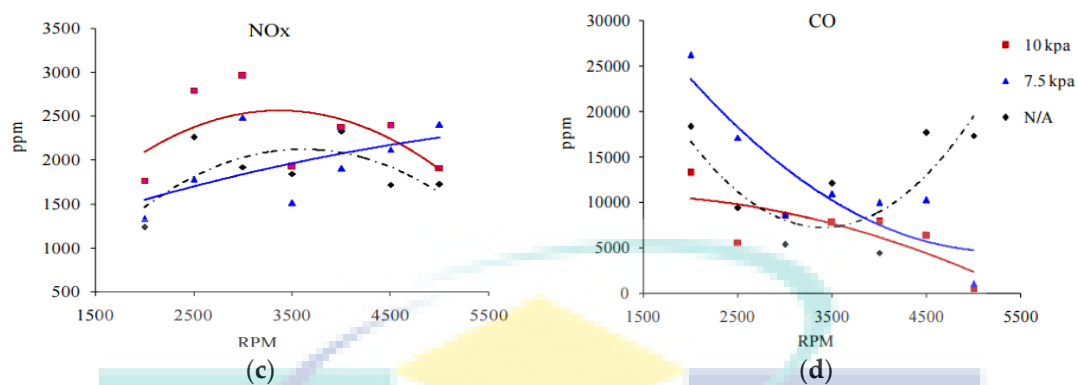
Figure 19. Performance (brake torque (**a**) and brake power (**b**)) and emissions (nitrogen oxides (NOx) (**c**) and CO (**d**)) of a CNG spark-ignition direct-injection (SIDI) engine at lower boost pressure [92].

4.2.6. Effect of EGR

The use of exhaust gas recirculation (EGR) was also on the cards for CNG-fueled SI engines. EGR in lean-burn CNG-fueled SI engines is not suitable, as it severely affects the stability of combustion. This is caused by dilution of the fuel–air mixture with EGR creating trouble for the early flame to sustain and develop. In a stoichiometric air–fuel ratio, however, there are numerous studies on the effect of EGR on the combustion, performance, and emissions, both experimental and numerical [225–228]. Ibrahim and co-authors employed EGR with low and high boost pressure at 13 (intake pressure of 113 kPa), 100 (intake pressure of 200 kPa), and 150 kPa (intake pressure of 250 kPa). The EGR was cooled down before it was diluted with the mixture. They reported a decrease in NOx emissions, an increase in engine performance, and improved fuel economy [225,226]. Sen et al. [227] investigated the effect of EGR on the combustion cycle-to-cycle variation of CNG fueling at a stoichiometric ratio by varying the EGR from 0–20% in 5% intervals. The engine was operated at 2000 rpm. The result indicated an increase in the cyclic variation of IMEP with an increase in the percentage of EGR.

4.2.7. Effect of Valve Lift and Valve Timing

Among the engine hardware-based studies, intake and exhaust valve-lift optimization is believed to enhance the combustion characteristics, engine performance, and emissions of CNG-fueled engines. Optimization of the intake and exhaust valve lift contributes to the extent of turbulence on the engine mainly during the early flame-development stage, leading to a sustained flame and stable combustion [203,229]. Soid et al. [230] numerically investigated the effect of different valve timings on the performance of a methane-fueled small engine. This was done by varying the inlet and exhaust valve openings. A 5–10% improvement in performance was reported by retarding the exhaust valve opening by 10° CA. The effect of dissimilar valve timings on the turbulence in the combustion chamber and its impact on the flame propagation stage were investigated by Ramasamy et al. [229]. An improvement in the combustion characteristics (peak pressure) and flame propagation were reported with the use of dissimilar valve timings.

4.2.8. Effect of Fuel Blending

Fuel blending is common in liquid fuels for both SI and CI engines. This is mainly done for fossil-fuel substitution and oxygenation. In gaseous fuels, with CNG in particular, the lower laminar-flame-speed characteristics attracted researchers to add higher laminar-flame-speed fuels, such as hydrogen and syngas [218,231–235]. Figure 20 shows the effect of hydrogen blending in natural gas over a range of equivalence ratios. The addition of a small quantity of hydrogen was found to have less effect on the laminar flame speed. However, Mohammed et al. [233] reported a significant influence on the performance, emissions, and combustion of a CNG DI engine upon blending a

small quantity of hydrogen, as shown in Figure 21. There are different success rates reported in the literature with hydrogen blending. Almost all research findings have a consensus that, technically, the enriching of natural gas with higher laminar-flame-speed fuels improves the combustion and performance of the engine [236]. However, this fuel-based improvement has operational limitations. Hydrogen and hydrogen-rich syngas have storage-related concerns. They are associated with hydrogen embrittlement. On the other hand, accompaniment with another high-pressure storage tank for the high laminar-flame-speed fuels would lead to space limitations and high inertia.
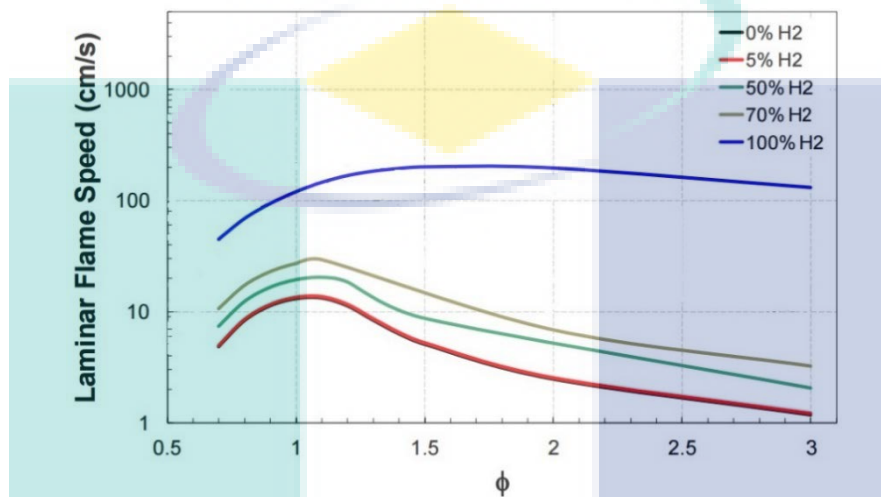
Figure 20. Effect of blending hydrogen in natural gas on the laminar flame speed at 15 kPa and 300 K, extracted from Reference [218].
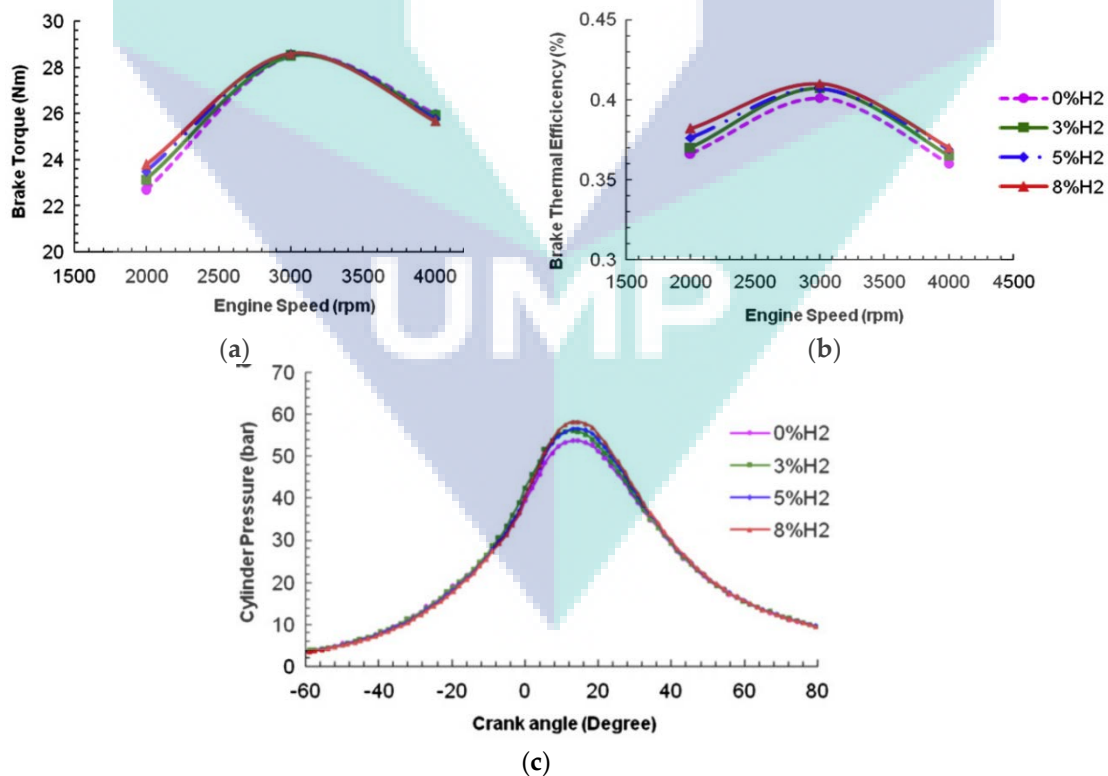
Figure 21. *Cont.*
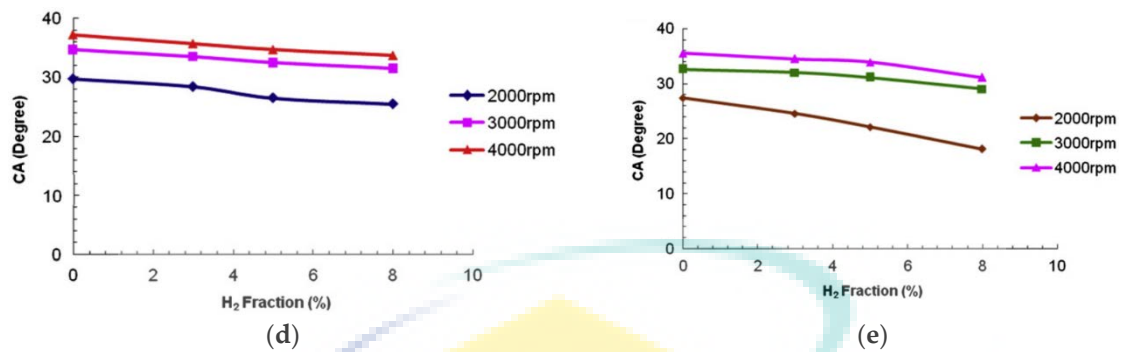
Figure 21. Effect of adding a small fraction of hydrogen on the performance and combustion of a CNG SI engine. (**a**) Brake torque versus engine speed; (**b**) brake thermal efficiency (BTE) versus engine speed; (**c**) in-cylinder pressure versus crank angle for various hydrogen-blending ratios; (**d**) flame-development duration versus H_2 percentage; (**e**) rapid-combustion duration versus H_2 percentage [233].

4.3. CNG in CI Engines

The various strategies employed in the performance improvement of SIDI engines are mostly effective at low loads. However, with stringent emission regulations in high-torque diesel engines, significant interest is arising in dedicated CNG engines for heavy-duty transport applications. It is impossible to achieve ignition in compression-ignition engines due to the fact that CNG has a higher autoignition temperature. Therefore, CNG should be blended with a low-autoignition-temperature fuel such as diesel so as to achieve ignition in CI engines. Such arrangements can be done by either a mixed-fuel or dual-fuel arrangement. The US Environmental Protection Agency designates these two arrangements as similar. Technically, a small quantity of diesel is added in a mixed-fuel arrangement, which is sufficient only for the initiation of ignition, while up to 90% of the fuel induced is CNG. The Cummins Westport ISX12 is the latest engine running with a mixed-fuel-mode CNG engine. This engine is the latest CNG engine suitable for heavy-duty applications [237]. The engine is designed to run on CNG, liquid petroleum gas (LPG), and biomethane, and it is equipped with a maintenance-free three-way catalyst after the treatment of gas. The engine is designed to work under stoichiometric conditions with cooled-EGR technology, thereby combining the benefits of a stoichiometric ratio and lean-burn combustion [237]. In a dual-fuel arrangement, however, CNG is used for diesel substitution while the engine is still able to run using 100% diesel mode. The main motivation in using CNG and other gaseous fuels in a diesel engine is for the possible substitution of diesel by a gaseous fuel, thereby reducing cost, minimizing pollutant emissions such as NOx and particulate matter, and further increasing the performance of the engine. One of the engine technologies in dual-fuel mode, approved by the US Environmental Protection Agency in 2013, is the Detroit Diesel S60 12.7-L engine. It was claimed that up to 60% diesel replacement, noise and PM reduction by 40%, and smoke reduction by 50% are some of the benefits [238]. However, Wagemakers and Leermakers [239] reviewed the effect of the dual fueling of diesel and various gaseous fuels on performance and emission. CNG, LPG, syngas, and hydrogen are some of the gaseous fuels considered in their review. They reported that all gaseous fuels, when applied to diesel-fuel combustion as a dual fuel, could decrease soot emissions except for syngas. A reduction in NOx emissions was reported when both CNG and LPG were used as primary fuels. However, syngas and hydrogen increased NOx levels compared to diesel combustion. Unburned hydrocarbons and CO demonstrated an increased trend with all gaseous fuels. With regards to the effect of these fuels on efficiency, hydrogen and LPG had a positive effect, while syngas and CNG had a negative effect.

5. Conclusions and Perspectives

In the current review work, recent works focusing on natural-gas utilization in IC engines, particularly spark-ignition engines, were discussed. Progress on the development of engine technology, as well as influencing engine parameters and their impact on engine performance and emissions, and the socio-economic prospect of the fuel were evaluated. Recently, in the automotive industry, the application of CNG in SI engines is more customary than before. The driving force for such movement is due to the technical superiority of the fuel as compared to its conventional counterparts. Technological advantages under spotlight are the higher octane number, higher autoignition temperature, high hydrogen-to-carbon ratio, gaseous phase under atmospheric conditions, and wider flammability limit. The higher octane number of natural gas allows for high compression of the engine, which in turn, results in enhanced power and higher total combustion efficiency. CNG/LNG vehicles reduce GHG emissions by 10–20% compared to gasoline vehicles. The lower number of particulates from CNG also results in reduced wear of the parts in relative motion compared to liquid fuels, and this, in turn, reduces the maintenance of CNG engines, despite the higher compression ratio and higher combustion temperature potentially slightly raising stress in the moving parts. The lower frictional loss in CNG vehicles could also result in reduced noise. Moreover, natural gas has lower fuel consumption, which is considered as economical for use as a fuel. In addition to the technical advantages, natural gas is abundantly available. The recent expansion in the production of natural gas from shale (shale gas) further increased the relevance of the fuel in the transportation sector. Globally, the production potential and capacity advanced in recent years. As a result, the natural-gas resource potential map is regularly being revised, even though such trends are marred by geopolitical complexities. On the other hand, conventional fuels are having trouble complying with the ever-increasing emission restrictions. This situation provides an upper hand to natural gas in tackling the GHG emission concerns.

The research and development of natural-gas-fueled IC engines focused on modified gasoline engines. Consequently, the perception of the fuel with researchers and end users was slightly negative, despite it having enormous economic, technical, and environmental benefits. The use of natural gas can result in a significant reduction in maximum power, torque, and volumetric efficiency at fully open throttle operation, which is attributed to the displacement of air by natural gas and the absence of evaporation cooling. Natural-gas engines have a lower power output than gasoline-fueled engines, mainly due to the lower energy content of natural gas, the displacement of air, and longer combustion durations. CNG vehicles have a 10–20% reduction in power compared to their gasoline counterparts after modification/retrofit. Comparatively, the natural-gas engine conversion from gasoline-fueled engines requires some modifications on the ignition system and valve trains, as well as the storage and fueling systems. Our transportation system was 100% reliant on conventional fuels. As a result, our technological development and infrastructure are tailored to that mode. In designing alternative or replacement fuels, the existing technological set-up and infrastructure should be taken into account. There are close to 1.2 billion cars in operation. In addition to designing a new engine based on its fuel characteristics, the adaptation and retrofitting of existing engines to accommodate CNG in either a standalone mode or as a dual fuel is on the rise.

Low engine efficiency and power output are issues encountered with retrofitted natural-gas engines. It was reported that natural gas results in a 10% lower power output compared to equivalent gasoline-fueled vehicles. In regular service, natural-gas engines consume 25–35% more energy than their diesel counterparts. Pumping loss and lower volumetric efficiency could arise due to the gaseous nature of natural gas. More unburned fuel could also result as CNG burns slower than conventional liquid fuels. Moreover, the cooling effect produced due to the vaporization of liquid fuel is absent when using CNG. The higher temperature due to the higher compression ratio of CNG engines usually results in higher NOx emissions. A sluggish start-up is another disadvantage of natural-gas engines, although this effect could be minimized by adding hydrogen as a secondary fuel.

Since the development of tailored direct-injection CNG engines, optimal engine-operating conditions were specified, and the performance and emissions of CNG DI engines became on par

with their gasoline counterpart. Due to CNG being a gaseous fuel, fuel-and-air mixing is not an issue. As a result, injection timing can be varied with the appropriate design of an injector. An injector with a narrow-angle design was found to be suitable for natural-gas fuel by different researchers.

There are different mechanisms deployed in order to overcome the efficiency deficit when using natural gas, such as working toward lean-burn combustion, supercharging, optimizing fuel-injection parameters (injection timing, injection pressure, and injection duration), optimizing ignition energy, ignition timing, and the optimization of valve timing. All these strategies have their strengths and weaknesses, as discussed in Section 4.2 in detail. Lean-burn technology would increase engine efficiency, and hence, the vehicle capacity range. Moreover, electronics like variable valve timing, skip-fire, and new engine technologies can help enhance the performance of gas engines. However, these enhancements are at the cost of engine torque. As a result, they are only suitable for small-load and low-speed operations. Similarly, improvements resulting from late injection of the fuel were associated with increased emissions of CO and HC. The combined effect of the engine-based mechanisms mentioned above could slightly improve SI engine efficiency. However, this improvement cannot beat the expectation of energy security and GHG emission concerns. As a result, fuel-based improvements, such as mixing CNG with high laminar-speed fuels and coupling engines with steam reformers for inline syngas mixing (research in its early stage), are on the table. A radical line of thinking currently in the research-and-development stage is the use of CNG in high-pressure DI diesel engines. This is achieved through mixed- and dual-fueling modes, where both CNG and diesel are injected into the cylinder at various times. The pilot fuel (diesel) is injected to initiate the ignition. In this arrangement, a maximum diesel replacement of up to 90% could be attained. The use of natural gas in automotive engines is expected to accelerate in the coming years due to the stringent regulations on liquid-fuel-based engines and the emergence of the latest strategies in fueling systems and combustion mechanisms.

Conflicts of Interest: The authors declare no conflict of interest. The founding sponsors had no role in the design of the study; in the collection, analyses, or interpretation of data; in the writing of the manuscript, and in the decision to publish the results.

References

1. Hesterberg, T.; Bunn, W.; Lapin, C. An evaluation of criteria for selecting vehicles fueled with diesel or compressed natural gas. *Sustain. Sci. Pract. Policy* **2009**, *5*, 20–30. [CrossRef]
2. Thipse, S.S.; Sonawane, S.B.; D'Souza, A.F.; Rairikar, S.D.; Kavathekar, K.K.; Marathe, N.V. *Injection Strategies, Optimization and Simulation Techniques on DI CNG Technology*; SAE Technical Paper No. 2015-26-0046; SAE International: Warrendale, PA, USA, 2015.
3. Soldo, B.; Potočnik, P.; Šimunović, G.; Šarić, T.; Govekar, E. Improving the residential natural gas consumption forecasting models by using solar radiation. *Energy Build.* **2014**, *69*, 498–506. [CrossRef]
4. Yue, T.; Chai, F.; Hu, J.; Jia, M.; Bao, X.; Li, Z.; He, L.; Zu, L. Gaseous emissions from compressed natural gas buses in urban road and highway tests in China. *J. Environ. Sci.* **2016**, *48*, 193–199. [CrossRef] [PubMed]
5. Ahmadi, P.; Chapoy, A.; Tohidi, B. Density, speed of sound and derived thermodynamic properties of a synthetic natural gas. *J. Nat. Gas Sci. Eng.* **2017**, *40*, 249–266. [CrossRef]
6. AFDC. Natural gas vehicles. In *Alternative Fuels Data Center*; US Department of Energy: Washington, DC, USA, 2017.
7. FMI. Automotive natural gas vehicle market: Global industry analysis and opportunity assessment 2015–2025. In *Future Market Insites*; FMI: Washington, DC, USA, 2017.

8.   Bhandari, K.; Bansal, A.; Shukla, A.; Khare, M. Performance and emissions of natural gas fueled internal combustion engine: A review. *J. Sci. Ind. Res.* **2005**, *64*, 333–338.

9.   Cho, H.M.; He, B.-Q. Spark ignition natural gas engines—A review. *Energy Convers. Manag.* **2007**, *48*, 608–618. [CrossRef]

10. Bakar, R.; Ismail, A.R. Green engines development using compressed natural gas as an alternative fuel: A review. *Am. J. Environ. Sci.* **2009**, *5*, 1–11.

11. Semin, R.A.B. A technical review of compressed natural gas as an alternative fuel for internal combustion engines. *Am. J. Eng. Appl. Sci* **2008**, *1*, 302–311.

12. Khan, M.I.; Yasmeen, T.; Khan, M.I.; Farooq, M.; Wakeel, M. Research progress in the development of natural gas as fuel for road vehicles: A bibliographic review (1991–2016). *Renew. Sustain. Energy Rev.* **2016**, *66*, 702–741. [CrossRef]

13. Matsuo, Y.; Yanagisawa, A.; Yamashita, Y. A global energy outlook to 2035 with strategic considerations for Asia and Middle East energy supply and demand interdependencies. *Energy Strategy Rev.* **2013**, *2*, 79–91. [CrossRef]

14. Su, M.; Zhang, M.; Lu, W.; Chang, X.; Chen, B.; Liu, G.; Hao, Y.; Zhang, Y. ENA-based evaluation of energy supply security: Comparison between the Chinese crude oil and natural gas supply systems. *Renew. Sustain. Energy Rev.* **2017**, *72*, 888–899. [CrossRef]

15. Mahmood, A.; Javaid, N.; Zafar, A.; Ali Riaz, R.; Ahmed, S.; Razzaq, S. Pakistan's overall energy potential assessment, comparison of LNG, TAPI and IPI gas projects. *Renew. Sustain. Energy Rev.* **2014**, *31*, 182–193. [CrossRef]

16. Shaikh, F.; Ji, Q.; Fan, Y.; Shaikh, P.H.; Uqaili, M.A. Modelling an optimal foreign natural gas import scheme for China. *J. Nat. Gas Sci. Eng.* **2017**, *40*, 267–276. [CrossRef]

17. Kerzmann, T.L.; Buxton, G.A.; Preisser, J. A computer model for optimizing the location of natural gas fueling stations. *Sustain. Energy Technol. Assess.* **2014**, *7*, 221–226. [CrossRef]

18. Peters, J.C. Natural gas and spillover from the us clean power plan into the Paris agreement. *Energy Policy* **2017**, *106*, 41–47. [CrossRef]

19. Pourhoseini, S.H.; Asadi, R. An experimental study on thermal and radiative characteristics of natural gas flame in different equivalence ratios by chemiluminescence and IR photography methods. *J. Nat. Gas Sci. Eng.* **2017**, *40*, 126–131. [CrossRef]

20. WEC. Energy resource: Gas. In *World Energy*; World Energy council: London, UK, 2016.

21. Wood, D.A.; Nwaoha, C.; Towler, B.F. Gas-to-liquids (GTL): A review of an industry offering several routes for monetizing natural gas. *J. Nat. Gas Sci. Eng.* **2012**, *9*, 196–208. [CrossRef]

22. Vivoda, V. LNG import diversification in Asia. *Energy Strategy Rev.* **2014**, *2*, 289–297. [CrossRef]

23. Zhang, Q.; Li, Z.; Wang, G.; Li, H. Study on the impacts of natural gas supply cost on gas flow and infrastructure deployment in China. *Appl. Energy* **2016**, *162*, 1385–1398. [CrossRef]

24. Kumar, S.; Kwon, H.-T.; Choi, K.-H.; Hyun Cho, J.; Lim, W.; Moon, I. Current status and future projections of LNG demand and supplies: A global prospective. *Energy Policy* **2011**, *39*, 4097–4104. [CrossRef]

25. Kumar, S.; Kwon, H.-T.; Choi, K.-H.; Lim, W.; Cho, J.H.; Tak, K.; Moon, I. LNG: An eco-friendly cryogenic fuel for sustainable development. *Appl. Energy* **2011**, *88*, 4264–4273. [CrossRef]

26. Ruble, I. European union energy supply security: The benefits of natural gas imports from the eastern Mediterranean. *Energy Policy* **2017**, *105*, 341–353. [CrossRef]

27. Al-Sobhi, S.A.; Elkamel, A. Simulation and optimization of natural gas processing and production network consisting of LNG, GTL, and methanol facilities. *J. Nat. Gas Sci. Eng.* **2015**, *23*, 500–508. [CrossRef]

28. BP. *BP Statistical Review of World Energy*; BP: London, UK, 2016.

29. Siddig, K.; Grethe, H. No more gas from Egypt? Modeling offshore discoveries and import uncertainty of natural gas in Israel. *Appl. Energy* **2014**, *136*, 312–324. [CrossRef]

30. Kang, Z. Natural gas supply-demand situation and prospect in China. *Nat. Gas Ind. B* **2014**, *1*, 103–112. [CrossRef]

31. Leather, D.T.B.; Bahadori, A.; Nwaoha, C.; Wood, D.A. A review of Australia's natural gas resources and their exploitation. *J. Nat. Gas Sci. Eng.* **2013**, *10*, 68–88. [CrossRef]

32. Economides, M.J.; Oligney, R.E.; Lewis, P.E. U.S. Natural gas in 2011 and beyond. *J. Nat. Gas Sci. Eng.* **2012**, *8*, 2–8. [CrossRef]

33. Song, Y.; Cheng, C.; Zhao, J.; Zhu, Z.; Liu, W.; Yang, M.; Xue, K. Evaluation of gas production from methane hydrates using depressurization, thermal stimulation and combined methods. *Appl. Energy* **2015**, *145*, 265–277. [CrossRef]

34. Chong, Z.R.; Yang, S.H.B.; Babu, P.; Linga, P.; Li, X.-S. Review of natural gas hydrates as an energy resource: Prospects and challenges. *Appl. Energy* **2016**, *162*, 1633–1652. [CrossRef]

35. Soldo, B. Forecasting natural gas consumption. *Appl. Energy* **2012**, *92*, 26–37. [CrossRef]

36. Fei, Q.; Guarnieri, M.T.; Tao, L.; Laurens, L.M.L.; Dowe, N.; Pienkos, P.T. Bioconversion of natural gas to liquid fuel: Opportunities and challenges. *Biotechnol. Adv.* **2014**, *32*, 596–614. [CrossRef] [PubMed]

37. Bahadori, A. Chapter 1—overview of natural gas resources. In *Natural Gas Processing*; Gulf Professional Publishing: Boston, MA, USA, 2014; pp. 1–22.

38. Shaffer, B. Natural gas supply stability and foreign policy. *Energy Policy* **2013**, *56*, 114–125. [CrossRef]

39. Anderson, B.E.; Uz, V. Compressed natural gas as a feasible replacement fuel for U.S. Transportation. *J. Def. Model. Simul.* **2014**, *12*, 67–78. [CrossRef]

40. Nwaoha, C.; Wood, D.A. A review of the utilization and monetization of Nigeria's natural gas resources: Current realities. *J. Nat. Gas Sci. Eng.* **2014**, *18*, 412–432. [CrossRef]

41. Egging, R.; Pichler, A.; Kalvø, Ø.I.; Walle–Hansen, T.M. Risk aversion in imperfect natural gas markets. *Eur. J. Oper. Res.* **2017**, *259*, 367–383. [CrossRef]

42. Honore, A. *European Natural Gas Demand, Supply, and Pricing: Cycles, Seasons, and the Impact of LNG Price Arbitrage*; Oxford University Press: Oxford, UK, 2011.

43. Dilaver, Ö.; Dilaver, Z.; Hunt, L.C. What drives natural gas consumption in Europe? Analysis and projections. *J. Nat. Gas Sci. Eng.* **2014**, *19*, 125–136. [CrossRef]

44. Eurogas. *Eurogas Statistical Report 2015*; Eurogas: Brussels, Belgium, 2016.

45. Holz, F.; von Hirschhausen, C.; Kemfert, C. A strategic model of European gas supply (gasmod). *Energy Econ.* **2008**, *30*, 766–788. [CrossRef]

46. Aloui, R.; Aïssa, M.S.B.; Hammoudeh, S.; Nguyen, D.K. Dependence and extreme dependence of crude oil and natural gas prices with applications to risk management. *Energy Econ.* **2014**, *42*, 332–342. [CrossRef]

47. Ríos-Mercado, R.Z.; Borraz-Sánchez, C. Optimization problems in natural gas transportation systems: A state-of-the-art review. *Appl. Energy* **2015**, *147*, 536–555. [CrossRef]

48. Kafood, A.H. CNG application in Qatar. In Proceedings of the International Petroleum Technology Conference (IPTC 2014), Bangkok, Thailand, 14–16 November 2014.

49. Wang, Q.; Chen, X.; Jha, A.N.; Rogers, H. Natural gas from shale formation—The evolution, evidences and challenges of shale gas revolution in united states. *Renew. Sustain. Energy Rev.* **2014**, *30*, 1–28. [CrossRef]

50. Brigida, M. The switching relationship between natural gas and crude oil prices. *Energy Econ.* **2014**, *43*, 48–55. [CrossRef]

51. Koh, D.-Y.; Kang, H.; Lee, J.-W.; Park, Y.; Kim, S.-J.; Lee, J.; Lee, J.Y.; Lee, H. Energy-efficient natural gas hydrate production using gas exchange. *Appl. Energy* **2016**, *162*, 114–130. [CrossRef]

52. de Melo-Martín, I.; Hays, J.; Finkel, M.L. The role of ethics in shale gas policies. *Sci. Total Environ.* **2014**, *470–471*, 1114–1119. [CrossRef] [PubMed]

53. Fernández, R.; Palazuelos, E. The future of Russian gas exports to east Asia: Feasibility and market implications. *Futures* **2011**, *43*, 1069–1081. [CrossRef]

54. Asche, F.; Oglend, A.; Osmundsen, P. Gas versus oil prices the impact of shale gas. *Energy Policy* **2012**, *47*, 117–124. [CrossRef]

55. Bazilian, M.; Brandt, A.R.; Billman, L.; Heath, G.; Logan, J.; Mann, M.; Melaina, M.; Statwick, P.; Arent, D.; Benson, S.M. Ensuring benefits from north American shale gas development: Towards a research agenda. *J. Unconv. Oil Gas Resour.* **2014**, *7*, 71–74. [CrossRef]

56. US Energy Information Administration. *International Energy Outlook 2016*; US Energy Information Administration: Washington, DC, USA, 2016.

57. Moryadee, S.; Gabriel, S.A.; Avetisyan, H.G. Investigating the potential effects of U.S. LNG exports on global natural gas markets. *Energy Strategy Rev.* **2014**, *2*, 273–288. [CrossRef]

58. Fukui, R.; Greenfield, C.; Pogue, K.; van der Zwaan, B. Experience curve for natural gas production by hydraulic fracturing. *Energy Policy* **2017**, *105*, 263–268. [CrossRef]

59. Arora, V.; Cai, Y. U.S. Natural gas exports and their global impacts. *Appl. Energy* **2014**, *120*, 95–103. [CrossRef]

60. Heidari, H.; Katircioglu, S.T.; Saeidpour, L. Natural gas consumption and economic growth: Are we ready to natural gas price liberalization in Iran? *Energy Policy* **2013**, *63*, 638–645. [CrossRef]

61. Clark, D.E.; Dybicz, C.; Hanson, A.; Nourzad, F. "No shut-off" policies and natural gas consumption. *Resour. Energy Econ.* **2017**, *48*, 19–29. [CrossRef]

62. Dong, X.; Pi, G.; Ma, Z.; Dong, C. The reform of the natural gas industry in the Republic of China. *Renew. Sustain. Energy Rev.* **2017**, *73*, 582–593. [CrossRef]

63. Cabalu, H. Indicators of security of natural gas supply in Asia. *Energy Policy* **2010**, *38*, 218–225. [CrossRef]

64. Ogunlowo, O.O.; Bristow, A.L.; Sohail, M. Developing compressed natural gas as an automotive fuel in Nigeria: Lessons from international markets. *Energy Policy* **2015**, *76*, 7–17. [CrossRef]

65. Von Rosenstiel, D.P.; Heuermann, D.F.; Hüsig, S. Why has the introduction of natural gas vehicles failed in Germany?—Lessons on the role of market failure in markets for alternative fuel vehicles. *Energy Policy* **2015**, *78*, 91–101. [CrossRef]

66. International Energy Agency. *Mid Term Market Report 2015*; International Energy Agency: Paris, France, 2015.

67. Xian, H.; Karali, B.; Colson, G.; Wetzstein, M.E. Diesel or compressed natural gas? A real options evaluation of the U.S. Natural gas boom on fuel choice for trucking fleets. *Energy* **2015**, *90*, 1342–1348. [CrossRef]

68. Curran, S.J.; Wagner, R.M.; Graves, R.L.; Keller, M.; Green, J.B., Jr. Well-to-wheel analysis of direct and indirect use of natural gas in passenger vehicles. *Energy* **2014**, *75*, 194–203. [CrossRef]

69. Arteconi, A.; Polonara, F. LNG as vehicle fuel and the problem of supply: The Italian case study. *Energy Policy* **2013**, *62*, 503–512. [CrossRef]

70. Wang, H.; Fang, H.; Yu, X.; Wang, K. Development of natural gas vehicles in China: An assessment of enabling factors and barriers. *Energy Policy* **2015**, *85*, 80–93. [CrossRef]

71. Paltsev, S.; Zhang, D. Natural gas pricing reform in China: Getting closer to a market system? *Energy Policy* **2015**, *86*, 43–56. [CrossRef]

72. Hao, H.; Wang, H.; Ouyang, M.; Cheng, F. Vehicle survival patterns in China. *Sci. Chin. Technol. Sci.* **2011**, *54*, 625–629. [CrossRef]

73. Hao, H.; Geng, Y.; Li, W.; Guo, B. Energy consumption and GHG emissions from China's freight transport sector: Scenarios through 2050. *Energy Policy* **2015**, *85*, 94–101. [CrossRef]

74. Ma, L.; Geng, J.; Li, W.; Liu, P.; Li, Z. The development of natural gas as an automotive fuel in china. *Energy Policy* **2013**, *62*, 531–539. [CrossRef]

75. Li, J.; Dong, X.; Shangguan, J.; Hook, M. Forecasting the growth of china's natural gas consumption. *Energy* **2011**, *36*, 1380–1385. [CrossRef]

76. Halova Wolfe, M.; Rosenman, R. Bidirectional causality in oil and gas markets. *Energy Econ.* **2014**, *42*, 325–331. [CrossRef]

77. Khan, M.I.; Yasmin, T. Development of natural gas as a vehicular fuel in Pakistan: Issues and prospects. *J. Nat. Gas Sci. Eng.* **2014**, *17*, 99–109. [CrossRef]

78. Perry, D. *Current Natural Gas Vehicle Statistics*; NGV Global: Auckland, New Zealand, 2017.

79. Holmala, J.; Isaksson, J. *Metso-Supplied World's Largest Biomass Gasification Plant Inaugurated in Finland*; Metso Corporation: Helsinki, Finland, 2013.

80. Engerer, H.; Horn, M. Natural gas vehicles: An option for Europe. *Energy Policy* **2010**, *38*, 1017–1029. [CrossRef]

81. Kuby, M.; Capar, I.; Kim, J.-G. Efficient and equitable transnational infrastructure planning for natural gas trucking in the European union. *Eur. J. Oper. Res.* **2017**, *257*, 979–991. [CrossRef]

82. Osorio-Tejada, J.L.; Llera-Sastresa, E.; Scarpellini, S. Liquefied natural gas: Could it be a reliable option for road freight transport in the EU? *Renew. Sustain. Energy Rev.* **2017**, *71*, 785–795. [CrossRef]

83. Bilgin, M. Geopolitics of European natural gas demand: Supplies from Russia, Caspian and the Middle East. *Energy Policy* **2009**, *37*, 4482–4492. [CrossRef]

84. Hao, H.; Liu, Z.; Zhao, F.; Li, W. Natural gas as vehicle fuel in China: A review. *Renew. Sustain. Energy Rev.* **2016**, *62*, 521–533. [CrossRef]

85. DeVos, K. *A Review of Compressed Natural Gas as a Viable Alternative Fuel for Passenger Vehicle, Spark Ignition, Four-Stroke Engines*; Rensselaer Polytechnic Institute: Troy, NY, USA, 2014.

86. Idris, S.; Abu Baker, R. An overview of compressed natural gas as an alternative fuel and Malaysian scenario. *Eur. J. Sci. Res.* **2009**, *34*, 6–15.

87. Yeh, S. An empirical analysis on the adoption of alternative fuel vehicles: The case of natural gas vehicles. *Energy Policy* **2007**, *35*, 5865–5875. [CrossRef]
88. Chen, S.P.; Xie, G.F.; Li, Q.Y.; Chang, K. Comparison among LNG, CNG and l-CNG filling stations. *Gas Heat* **2007**, *7*, 006.
89. Sharafian, A.; Talebian, H.; Blomerus, P.; Herrera, O.; Mérida, W. A review of liquefied natural gas refueling station designs. *Renew. Sustain. Energy Rev.* **2017**, *69*, 503–513. [CrossRef]
90. Gashighway. Available online: http://www.gashighway.net/ (accessed on 17 June 2017).
91. Commission, E. *Eu Launches Clean Fuel Strategy*; European Commission: Bruxelles, Belgium, 2013.
92. Chala, G.; Aziz, A.; Hagos, F. Combined effect of boost pressure and injection timing on the performance and combustion of CNG in a di spark ignition engine. *Int. J. Automot. Technol.* **2017**, *18*, 85–96. [CrossRef]
93. Yang, B.; Xi, C.; Wei, X.; Zeng, K.; Lai, M.-C. Parametric investigation of natural gas port injection and diesel pilot injection on the combustion and emissions of a turbocharged common rail dual-fuel engine at low load. *Appl. Energy* **2015**, *143*, 130–137. [CrossRef]
94. McTaggart-Cowan, G.P.; Jones, H.L.; Rogak, S.N.; Bushe, W.K.; Hill, P.G.; Munshi, S.R. The effects of high-pressure injection on a compression–ignition, direct injection of natural gas engine. *J. Eng. Gas Turbines Power* **2006**, *129*, 579–588. [CrossRef]
95. Amrouche, F.; Benzaoui, A.; Harouadi, F.; Mahmah, B.; Belhamel, M. Compressed natural gas: The new alternative fuel for the algerian transportation sector. *Procedia Eng.* **2012**, *33*, 102–110. [CrossRef]
96. Srinivasan, K.K.; Krishnan, S.R.; Singh, S.; Midkiff, K.C.; Bell, S.R.; Gong, W.; Fiveland, S.B.; Willi, M. The advanced injection low pilot ignited natural gas engine: A combustion analysis. *J. Eng. Gas Turbines Power* **2006**, *128*, 213–218. [CrossRef]
97. Korakianitis, T.; Namasivayam, A.; Crookes, R. Natural-gas fueled spark-ignition (SI) and compression-ignition (ci) engine performance and emissions. *Prog. Energy Combust. Sci.* **2011**, *37*, 89–112. [CrossRef]
98. De Carvalho, R.D.B.; Valle, R.M.; de Magalhães, F.E. *Performance and Emission Analysis of the Turbocharged Spark-Ignition Engine Converted to Natural Gas*; 0148-7191; SAE Technical Paper; SAE International: Warrendale, PA, USA, 2003.
99. Jarrahian, A.; Aghel, B.; Heidaryan, E. On the viscosity of natural gas. *Fuel* **2015**, *150*, 609–618. [CrossRef]
100. Ocelík, P.; Osička, J. The framing of unconventional natural gas resources in the foreign energy policy discourse of the Russian federation. *Energy Policy* **2014**, *72*, 97–109. [CrossRef]
101. Liu, Z.; Norbeck, J.M.; Raju, A.S.K.; Kim, S.; Park, C.S. Synthetic natural gas production by sorption enhanced steam hydrogasification based processes for improving ch4 yield and mitigating CO_2 emissions. *Energy Convers. Manag.* **2016**, *126*, 256–265. [CrossRef]
102. Esfahani, S.; Baselizadeh, S.; Hemmati-Sarapardeh, A. On determination of natural gas density: Least square support vector machine modeling approach. *J. Nat. Gas Sci. Eng.* **2015**, *22*, 348–358. [CrossRef]
103. Heidaryan, E.; Moghadasi, J.; Salarabadi, A. A new and reliable model for predicting methane viscosity at high pressures and high temperatures. *J. Nat. Gas Chem.* **2010**, *19*, 552–556. [CrossRef]
104. Yousefi, S.H.; Azamifard, A.; Hosseini, S.-A.; Shamsoddini, M.-J.; Alizadeh, N. Toward a predictive model for predicting viscosity of natural and hydrocarbon gases. *J. Nat. Gas Sci. Eng.* **2014**, *20*, 147–154. [CrossRef]
105. Skylogianni, E.; Novak, N.; Louli, V.; Pappa, G.; Boukouvalas, C.; Skouras, S.; Solbraa, E.; Voutsas, E. Measurement and prediction of dew points of six natural gases. *Fluid Phase Equilib.* **2016**, *424*, 8–15. [CrossRef]
106. Mesquita, F.; Feitosa, F.; Do Carmo, F.; de Santiago-Aguiar, R.; de Sant'Ana, H. Viscosities and viscosity deviations of binary mixtures of biodiesel + petrodiesel (or n-hexadecane) at different temperatures. *Braz. J. Chem. Eng.* **2012**, *29*, 653–664. [CrossRef]
107. Walsh, M.P. Property of fuels. In *Car Lines*; Michael, P., Ed.; Car Lines: Arlington, ND, USA, 2006.
108. Acevedo, H.; Mantilla, J. Performance and emissions of a heavy duty diesel engine fuelled with palm oil biodiesel and premium diesel. *Dyna* **2011**, *78*, 152–158.
109. Chong, C.T.; Hochgreb, S. Measurements of laminar flame speeds of liquid fuels: Jet-a1, diesel, palm methyl esters and blends using particle imaging velocimetry (PIV). *Proc. Combust. Inst.* **2011**, *33*, 979–986. [CrossRef]
110. Dirrenberger, P.; Glaude, P.-A.; Bounaceur, R.; Le Gall, H.; da Cruz, A.P.; Konnov, A.; Battin-Leclerc, F. Laminar burning velocity of gasolines with addition of ethanol. *Fuel* **2014**, *115*, 162–169. [CrossRef]

111. Glaude, P.-A.; Fournet, R.; Bounaceur, R.; Molière, M. Adiabatic flame temperature from biofuels and fossil fuels and derived effect on NO$_x$ emissions. *Fuel Process. Technol.* **2010**, *91*, 229–235. [CrossRef]

112. Ahlvik, P. Natural gas. In *Diesel NET*; ECOpoint Inc.: Mississauga, ON, Canada, 2003.

113. Mishra, S. *Biogas from Wholesale Vegetable and Fruit Market Waste in the Indian Cities: Truely Sustainable and Renewable Transport Fuel*; Green Cosmos Energy Solutions Pvt. Ltd.: Bangalore, India, 2012.

114. Mazyan, W.; Ahmadi, A.; Ahmed, H.; Hoorfar, M. Market and technology assessment of natural gas processing: A review. *J. Nat. Gas Sci. Eng.* **2016**, *30*, 487–514. [CrossRef]

115. Berstad, D.; Nekså, P.; Anantharaman, R. Low-temperature CO$_2$ removal from natural gas. *Energy Procedia* **2012**, *26*, 41–48. [CrossRef]

116. Peters, L.; Hussain, A.; Follmann, M.; Melin, T.; Hägg, M.B. CO$_2$ removal from natural gas by employing amine absorption and membrane technology—A technical and economical analysis. *Chem. Eng. J.* **2011**, *172*, 952–960. [CrossRef]

117. Rufford, T.E.; Smart, S.; Watson, G.C.Y.; Graham, B.F.; Boxall, J.; Diniz da Costa, J.C.; May, E.F. The removal of CO$_2$ and N$_2$ from natural gas: A review of conventional and emerging process technologies. *J. Pet. Sci. Eng.* **2012**, *94–95*, 123–154. [CrossRef]

118. Alcheikhhamdon, Y.; Hoorfar, M. Natural gas quality enhancement: A review of the conventional treatment processes, and the industrial challenges facing emerging technologies. *J. Nat. Gas Sci. Eng.* **2016**, *34*, 689–701. [CrossRef]

119. Faramawy, S.; Zaki, T.; Sakr, A.A.E. Natural gas origin, composition, and processing: A review. *J. Nat. Gas Sci. Eng.* **2016**, *34*, 34–54. [CrossRef]

120. Ahmadian Behrooz, H. Managing demand uncertainty in natural gas transmission networks. *J. Nat. Gas Sci. Eng.* **2016**, *34*, 100–111. [CrossRef]

121. Nagayama, D.; Horita, M. A network game analysis of strategic interactions in the international trade of russian natural gas through ukraine and belarus. *Energy Econ.* **2014**, *43*, 89–101. [CrossRef]

122. Qu, Z.; Wang, Y.; Yue, H.; An, Y.; Wu, L.; Zhou, W.; Wang, H.; Su, Z.; Li, J.; Zhang, Y. Study on the natural gas pipeline safety monitoring technique and the time-frequency signal analysis method. *J. Loss Prev. Process Ind.* **2017**, *47*, 1–9. [CrossRef]

123. Üster, H.; Dilaveroğlu, Ş. Optimization for design and operation of natural gas transmission networks. *Appl. Energy* **2014**, *133*, 56–69. [CrossRef]

124. Ertas, A.; Anderson, E. Review of methanol and compressed natural gas (CNG) as alternative for transportation fuels. *J. Energy Resour. Technol* **1991**, *113*, 101. [CrossRef]

125. Koza, D.F.; Ropke, S.; Boleda Molas, A. The liquefied natural gas infrastructure and tanker fleet sizing problem. *Transp. Res. Part E Logist. Transp. Rev.* **2017**, *99*, 96–114. [CrossRef]

126. Shi, G.-H.; Jing, Y.-Y.; Wang, S.-L.; Zhang, X.-T. Development status of liquefied natural gas industry in china. *Energy Policy* **2010**, *38*, 7457–7465. [CrossRef]

127. Wood, D.A. A review and outlook for the global LNG trade. *J. Nat. Gas Sci. Eng.* **2012**, *9*, 16–27. [CrossRef]

128. Vivoda, V. Natural gas in Asia: Trade, markets and regional institutions. *Energy Policy* **2014**, *74*, 80–90. [CrossRef]

129. Dorigoni, S.; Graziano, C.; Pontoni, F. Can LNG increase competitiveness in the natural gas market? *Energy Policy* **2010**, *38*, 7653–7664. [CrossRef]

130. Dorigoni, S.; Portatadino, S. LNG development across Europe: Infrastructural and regulatory analysis. *Energy Policy* **2008**, *36*, 3366–3373. [CrossRef]

131. Erdős, P. Have oil and gas prices got separated? *Energy Policy* **2012**, *49*, 707–718. [CrossRef]

132. Wang, X.; Marongiu Porcu, M. The Potential of Compressed Natural Gas Transport in Asia. In Proceedings of the International Petroleum Technology Conference, Kuala Lumpur, Malaysia, 3–5 December 2008.

133. Hafner, M.; Karbuz, S.; Esnault, B.; Andaloussi, H.E. Long-term natural gas supply to Europe: Import potential, infrastructure needs and investment promotion. *Energy Environ.* **2008**, *19*, 1131–1153. [CrossRef]

134. Talus, K. Long-term natural gas contracts and antitrust law in the European union and the united states. *J. World Energy Law Bus.* **2011**, *4*, 260–315i. [CrossRef]

135. Castillo, L.; Majzoub Dahouk, M.; Di Scipio, S.; Dorao, C.A. Conceptual analysis of the precooling stage for lng processes. *Energy Convers. Manag.* **2013**, *66*, 41–47. [CrossRef]

136. Zhou, S.; Gao, J.; Yang, Y.; Li, B.; Petro, P. Development, problems and market share of the LNG industry in China. *Int. Pet. Econ.* **2013**, *6*, 3.

137. Wang, Z.; Rao, L.; Yang, Y.; Gao, H. Natural gas vehicles will develop greatly in china. In Proceedings of the International Petroleum Technology Conference (IPTC 2013), Beijing, China, 26–28 March 2013.

138. Medlock, K.B.; Jaffe, A.M.; O'Sullivan, M. The global gas market, LNG exports and the shifting us geopolitical presence. *Energy Strategy Rev.* **2014**, *5*, 14–25. [CrossRef]

139. Paltsev, S. Scenarios for Russia's natural gas exports to 2050. *Energy Econ.* **2014**, *42*, 262–270. [CrossRef]

140. Birol, F. G7 energy ministerial meeting. In Proceedings of the G7 Energy Ministerial Meeting, Rome, Italy, 9–10 April 2017.

141. Thomas, S.; Dawe, R.A. Review of ways to transport natural gas energy from countries which do not need the gas for domestic use. *Energy* **2003**, *28*, 1461–1477. [CrossRef]

142. Wang, X.; Economides, A.M.; Porcu, M.M.; Economides, M.J. Compressed natural gas for Indonesia. In Proceedings of the Asia Pacific Oil and Gas Conference & Exhibition, Jakarta, Indonesia, 4–6 August 2009.

143. Khan, M.I.; Yasmin, T.; Shakoor, A. Technical overview of compressed natural gas (CNG) as a transportation fuel. *Renew. Sustain. Energy Rev.* **2015**, *51*, 785–797. [CrossRef]

144. Melaina, M.; Bremson, J. Refueling availability for alternative fuel vehicle markets: Sufficient urban station coverage. *Energy Policy* **2008**, *36*, 3233–3241. [CrossRef]

145. Patrizio, P.; Leduc, S.; Chinese, D.; Dotzauer, E.; Kraxner, F. Biomethane as transport fuel—A comparison with other biogas utilization pathways in northern Italy. *Appl. Energy* **2015**, *157*, 25–34. [CrossRef]

146. Salman, C.A.; Schwede, S.; Thorin, E.; Yan, J. Enhancing biomethane production by integrating pyrolysis and anaerobic digestion processes. *Appl. Energy* **2017**, *204*, 1074–1083. [CrossRef]

147. Görling, M.; Larsson, M.; Alvfors, P. Bio-methane via fast pyrolysis of biomass. *Appl. Energy* **2013**, *112*, 440–447. [CrossRef]

148. Ullah Khan, I.; Hafiz Dzarfan Othman, M.; Hashim, H.; Matsuura, T.; Ismail, A.F.; Rezaei-DashtArzhandi, M.; Wan Azelee, I. Biogas as a renewable energy fuel—A review of biogas upgrading, utilisation and storage. *Energy Convers. Manag.* **2017**, *150*, 277–294. [CrossRef]

149. Patterson, T.; Esteves, S.; Dinsdale, R.; Guwy, A. An evaluation of the policy and techno-economic factors affecting the potential for biogas upgrading for transport fuel use in the UK. *Energy Policy* **2011**, *39*, 1806–1816. [CrossRef]

150. Augelletti, R.; Conti, M.; Annesini, M.C. Pressure swing adsorption for biogas upgrading. A new process configuration for the separation of biomethane and carbon dioxide. *J. Clean. Prod.* **2017**, *140*, 1390–1398. [CrossRef]

151. Pellegrini, L.A.; De Guido, G.; Langé, S. Biogas to liquefied biomethane via cryogenic upgrading technologies. *Renew. Energy* **2017**, *124*, 75–83. [CrossRef]

152. Götz, M.; Lefebvre, J.; Mörs, F.; McDaniel Koch, A.; Graf, F.; Bajohr, S.; Reimert, R.; Kolb, T. Renewable power-to-gas: A technological and economic review. *Renew. Energy* **2016**, *85*, 1371–1390. [CrossRef]

153. Castellani, B.; Rinaldi, S.; Morini, E.; Nastasi, B.; Rossi, F. Flue gas treatment by power-to-gas integration for methane and ammonia synthesis – energy and environmental analysis. *Energy Convers. Manag.* **2018**, *171*, 626–634. [CrossRef]

154. Hassan, M.H.; Kalam, M.A.; Mahlia, T.I.; Aris, I.; Nizam, M.K.; Abdullah, S.; Ali, Y. Experimental test of a new compressed natural gas direct injection engine. *Energy Fuels* **2009**, *23*, 4981–4987. [CrossRef]

155. Heywood, J.B. *Internal Combustion Engine Fundamentals*; McGraw Hill International: New York, NY, USA, 1988.

156. Arcoumanis, C.; Kamimoto, T. *Flow and Combustion in Reciprocating Engines*; Springer Science & Business Media: Berlin, Germany, 2009.

157. Willems, H.; Sierens, R. Modeling the initial growth of the plasma and flame kernel in SI engines. *Trans. Am. Soc. Mech. Eng. J. Eng. Gas Turbines Power* **2003**, *125*, 479–484. [CrossRef]

158. Aleiferis, P.G.; Taylor, A.M.; Whitelaw, J.H.; Ishii, K.; Urata, Y. *Cyclic Variations of Initial Flame Kernel Growth in a Honda Vtec-E Lean-Burn Spark-Ignition Engine*; SAE Technical Paper 0148-7191; SAE International: Warrendale, PA, USA, 2000.

159. Hagos, F. Combustion, Performance and Emissions Characteristics of Imitated Syngases in Direct-Injection Sparkigntion Engine. Ph.D. Thesis, Universiti Teknologi Petronas, Seri Iskandar, Malaysia, 2013.

160. Gharehghani, A.; Hosseini, R.; Mirsalim, M.; Yusaf, T.F. A comparative study on the first and second law analysis and performance characteristics of a spark ignition engine using either natural gas or gasoline. *Fuel* **2015**, *158*, 488–493. [CrossRef]

161. Ou, X.; Zhang, X. Life-cycle analyses of energy consumption and GHG emissions of natural gas-based alternative vehicle fuels in china. *J. Energy* **2013**, *2013*. [CrossRef]

162. Aziz, A.R.A.; Shahzad, R. Combustion analysis of a CNG direct injection spark ignition engine. *Int. J. Automot. Mech. Eng.* **2010**, *2*, 157–170. [CrossRef]

163. Chandra, R.; Vijay, V.; Subbarao, P.; Khura, T. Performance evaluation of a constant speed IC engine on CNG, methane enriched biogas and biogas. *Appl. Energy* **2011**, *88*, 3969–3977. [CrossRef]

164. Sonthalia, A.; Rameshkumar, C.; Sharma, U.; Punganur, A.; Abbas, S. Combustion and performance characteristics of a small spark ignition engine fuelled with HCNG. *J. Eng. Sci. Technol.* **2015**, *10*, 404–419.

165. Jahirul, M.I.; Masjuki, H.; Saidur, R.; Kalam, M.; Jayed, M.; Wazed, M. Comparative engine performance and emission analysis of CNG and gasoline in a retrofitted car engine. *Appl. Therm. Eng.* **2010**, *30*, 2219–2226. [CrossRef]

166. Rezapour, K.; Mason, B.; Wood, A.S.; Ebrahimi, M. Bi-fuel SI engine model for analysis and optimization. *Univ. J. Mech. Eng.* **2014**, *2*, 71–82. [CrossRef]

167. Poulton, M.L. *Alternative Fuels for Road Vehicles*; WIT Press: Southampton, UK, 1994.

168. Ouellette, P. High pressure direct injection (HPDI) of natural gas in diesel engines. In Proceedings of the ANGVA 2000 Conference, Yokohama, Japan, 7–10 November 2000.

169. Tadesse, G.; Aziz, A.R.A. *Effect of Boost Pressure on Engine Performance and Exhaust Emissions in Direct-Injection Compressed Natural Gas CNG-DI) Spark Ignition Engine*; SAE Technical Paper No. 2009-32-0135; SAE International: Warrendale, PA, USA, 2009.

170. Tadesse, G. Effect of Boost Pressure on Performance, Combustion and Exhaust Emissions in Direct Injection Compressed Natural Gas (CNG) Engine. Master's Thesis, University Teknologi Petronas, Perak, Malaysia, 2009.

171. d'Ambrosio, S.; Spessa, E.; Vassallo, A.; Ferrera, M.; Peletto, C. *Experimental Investigation of Fuel Consumption, Exhaust Emissions and Heat Release of a Small-Displacement Turbocharged CNG Engine*; SAE Technical Paper 0148-7191; SAE International: Warrendale, PA, USA, 2006.

172. Li, H. *An Experimental and Analytical Examination of Gas Fuelled Spark Ignition Engine-Performance and Combustion*; University of Calgary: Calgary, AB, Canada, 2004.

173. Reynolds, C.C.O.; Evans, R.L.; Andreassi, L.; Cordiner, S.; Mulone, V. *The Effect of Varying the Injected Charge Stoichiometry in a Partially Stratified Charge Natural Gas Engine*; SAE Technical Paper 0148-7191; SAE International: Warrendale, PA, USA, 2005.

174. Da Silveira, B.H.; Benvenuti, L.H.; Werninghaus, E.; Coelho, E.P.; Silva, C.D.; de Oliveira, F.R.; Silva, J.C.S. *Development of a Concept Vehicle for Compressed Natural Gas*; SAE Technical Paper 0148-7191; SAE International: Warrendale, PA, USA, 2004.

175. Durell, E.; Allen, J.; Law, D.; Heath, J. Installation and Development of a Direct Injection System for a Bi-Fuel Gasoline and Compressed Natural Gas Engine. In Proceeding of the ANGVA 2000 Conference, Yokohama, Japan, 18–21 July 2000.

176. Abid, F.H. Comparison of performance characteristics of ng and gasoline-fuelled single cylinder SI engine. *Int. J. Comput. Appl. Sci.* **2016**, *1*, 13–20.

177. Melaika, M.; Dahlander, P. *Experimental Investigation of Methane Direct Injection with Stratified Charge Combustion in Optical SI Single Cylinder Engine*; SAE Technical Paper 0148-7191; SAE International: Warrendale, PA, USA, 2016.

178. Ilves, R.; Olt, J. Study of prior art of spark ignition engine fuel supply system. *Argon. Res.* **2012**, *10*, 55–74.

179. Stone, R. *Introduction to Internal Combustion Engines*; Palgrave Macmillan: London, UK, 2012.

180. Mello, P.; Pelliza, G.; Cataluña, R.; da Silva, R. Evaluation of the maximum horsepower of vehicles converted for use with natural gas fuel. *Fuel* **2006**, *85*, 2180–2186. [CrossRef]

181. Tuner, M. *Combustion of Alternative Vehicle Fuels in Internal Combustion Engines*; Report within Project; A Pre-Study to Prepare for Interdisciplinary Research on Future Alternative Transportation Fuels; Financed by The Swedish Energy Agency; Lund University: Lund, Sweden, 2016.

182. Nice, K. How Fuel Injection Systems Work. 2001. Available online: https://www.howstuffworks.com/ (accessed on 17 June 2017).

183. Loukanine, V.N.; Khatchiyan, A.S.; Shishlov, I.G.; Khamidullin, R.K. Analysis of different ways to develop low-emission natural gas engines. In Proceedings of the NGV 2000, Yokohama, Japan, 17–19 October 2000.

184. Czerwinski, J.; Comte, P.; Zimmerli, Y. *Investigations of the Gas Injection System on a HD-CNG-Engine*; SAE Technical Paper 0148-7191; SAE International: Warrendale, PA, USA, 2003.

185. Choi, M.; Lee, S.; Park, S. Numerical and experimental study of gaseous fuel injection for CNG direct injection. *Fuel* **2015**, *140*, 693–700. [CrossRef]

186. Chiodi, M.; Berner, H.-J.; Bargende, M. *Investigation on Different Injection Strategies in a Direct-Injected Turbocharged CNG-Engine*; SAE Technical Paper 0148-7191; SAE International: Warrendale, PA, USA, 2006.

187. Cox, G.; DelVecchio, K.; Hays, W.; Hiltner, J.; Nagaraj, R.; Emmer, C. *Development of a Direct-Injected Natural Gas Engine System for Heavy-Duty Vehicles*; Caterpillar, Inc.: Peoria, IL, USA, 2000.

188. Hayashida, M.; Yamato, T.; Sekino, H.; Sugahara, K. *Investigation of Performance and Fuel Distribution of a Direct Injection Gas Engine Using LIF Measurement*; SAE Technical Paper 0148-7191; SAE International: Warrendale, PA, USA, 1999.

189. Hassaneen, A.E.; Varde, K.S.; Bawady, A.H.; Morgan, A.-A. *A Study of the Flame Development and Rapid Burn Durations in a Lean-Burn Fuel Injected Natural Gas SI Engine*; SAE Technical Paper 0148-7191; SAE International: Warrendale, PA, USA, 1998.

190. Heywood, J. *Internal combustion ENGINE Fundamentals*; McGraw-Hill Education: New York, NY, USA, 1988.

191. Achleitner, E.; Bäcker, H.; Funaioli, A. *Direct Injection Systems for Otto Engines*; SAE Technical Paper 0148-7191; SAE International: Warrendale, PA, USA, 2007.

192. Hagos, F.Y.; Aziz, A.R.A.; Sulaiman, S.A. Combustion characteristics of late injected CNG in a spark ignition engine under lean operating condition. *J. Appl. Sci.* **2012**, *12*, 2368. [CrossRef]

193. Sahari, B.B.; Ali, Y.; Ahmadun, F.L.-R.; Abdullah, S.; Hassan, M.H.; Aris, I.; Abdullah, M.A.; Ahmad, M.F.; Chelliah, V.; Taha, Z. Development of a prototype compressed natural gas direct injection vehicle—A Malaysian experience. In Proceedings of the 12th IANGV Conference and Exhibition, Rome, Italy; 9–12 May 2010.

194. Nijboer, M. *The Contribution of Natural Gas Vehicles to Sustainable Transport*; 2079-2581; International Energy Agency: Paris, France, 2010.

195. Kalam, M.; Masjuki, H. An experimental investigation of high performance natural gas engine with direct injection. *Energy* **2011**, *36*, 3563–3571. [CrossRef]

196. Zheng, J.; Wang, J.; Wang, B.; Huang, Z. Effect of the compression ratio on the performance and combustion of a natural-gas direct-injection engine. *Proc. Inst. Mech. Eng. D-J. Automob. Eng.* **2009**, *223*, 85–98. [CrossRef]

197. Ibrahim, A.; Bari, S. Effect of varying compression ratio on a natural gas SI engine performance in the presence of EGR. *Energy Fuels* **2009**, *23*, 4949–4956. [CrossRef]

198. Ramachandran, A.; Waghmare, A. Experimental investigation of the effect of compression ratio on the performance of a dedicated CNG engine. *Int. Res. J. Eng. Technol.* **2016**, *3*, 312–316.

199. Damrongkijkosol, C.; Kerdsuwan, S. Experiment Study on Influence of Compression Ratio onto Performance and Emission of Compressed Natural Gas Retrofit Engine. Master's Thesis, King Mongkut's Institute of Technology, Bangkok, Thailand, 2006.

200. Manivannan, A.; Chandrasekaran, S.; Ramprabhu, R. *Lean Burn Natural Gas Spark Ignition Engine—An Overview*; SAE Technical Paper 0148-7191; SAE International: Warrendale, PA, USA, 2003.

201. Abbasi Atibeh, P.; Brear, M.J.; Dennis, P.A.; Orbaiz, P.J.; Watson, H.C. Lean limit combustion analysis for a spark ignition natural gas internal combustion engine. *Combust. Sci. Technol.* **2013**, *185*, 1151–1168. [CrossRef]

202. Cartellieri, W.; Chmela, F.; Kapus, P.; Tatschl, R. Mechanisms leading to stable and efficient combustion in lean burn gas engines. In Proceedings of the International Symposium COMODIA, Yokohama, Japan, 11–14 July 1994.

203. Aziz, A.R.A.; Anbese, Y.T.; Hagos, F.Y.; Heikal, M.R. Characteristics of early flame development in a direct-injection spark-ignition CNG engine fitted with a variable swirl control valve. *Energies* **2017**, *10*, 964. [CrossRef]

204. Evans, R. Extending the lean limit of natural-gas engines. *J. Eng. Gas Turbines Power* **2009**, *131*, 032803. [CrossRef]

205. Chen, S.K.; Beck, N.J. *Gas Engine Combustion Principles and Applications*; SAE Technical Paper 0148-7191; SAE International: Warrendale, PA, USA, 2001.

206. Aljamali, S.; Abdullah, S.; Wan Mahmood, W.M.F.; Ali, Y. The effect of injection timings on performance and emissions of compressed natural-gas direct injection engine. *J. Combust.* **2016**, *2016*, 6501462. [CrossRef]

207. Wasiu, A.B.; Aziz, A.R.A.; Heikal, M.R. The effect of injection timing on the performance of natural gas with a high carbon dioxide (CO_2) content in a direct injection (di) gas engine. In *MATEC Web of Conferences*; EDP Sciences: Ulis, France, 2014; p. 02027.

208. Zeng, K.; Huang, Z.; Liu, B.; Liu, L.; Jiang, D.; Ren, Y.; Wang, J. Combustion characteristics of a direct-injection natural gas engine under various fuel injection timings. *Appl. Therm. Eng.* **2006**, *26*, 806–813. [CrossRef]

209. Liu, L.-X.; Huang, Z.-H.; Jiang, D.-M.; Ren, Y.; Wang, J.-H.; Wang, Q. Combustion characteristics of a direct injection natural gas engine under various fuel injection timings. *Trans. CSICE* **2005**, *5*, 14.

210. Song, J.; Choi, M.; Kim, D.; Park, S. Combustion characteristics of methane direct injection engine under various injection timings and injection pressures. *J. Eng. Gas Turbines Power* **2017**, *139*, 082802. [CrossRef]

211. Hagos, F.Y.; Aziz, A.R.A.; Sulaiman, S.A. Methane enrichment of syngas (H_2/CO) in a spark-ignition direct-injection engine: Combustion, performance and emissions comparison with syngas and compressed natural gas. *Energy* **2015**, *90*, 2006–2015. [CrossRef]

212. Hagos, F.Y.; Aziz, A.R.A.; Sulaiman, S.A. Syngas (H_2/CO) in a spark-ignition direct-injection engine. Part 1: Combustion, performance and emissions comparison with CNG. *Int. J. Hydrog. Energy* **2014**, *39*, 17884–17895. [CrossRef]

213. Firmansyah. *Optimization of Injection Parameters in Compressed Natural Gas Direct Injection (CNG-DI) Spark Ignition Engine*; Universiti Teknologi Petronas: Tronoh, Malaysia, 2007.

214. Ehsan, M. Effect of spark advance on a gas run automotive spark ignition engine. *J. Chem. Eng.* **2010**, *24*, 42–49. [CrossRef]

215. Bell, S.R. *Natural Gas as a Transportation Fuel*; SAE Technical Paper 0148-7191; SAE International: Warrendale, PA, USA, 1993.

216. Dimopoulos, P.; Rechsteiner, C.; Soltic, P.; Laemmle, C.; Boulouchos, K. Increase of passenger car engine efficiency with low engine-out emissions using hydrogen–natural gas mixtures: A thermodynamic analysis. *Int. J. Hydrog. Energy* **2007**, *32*, 3073–3083. [CrossRef]

217. Khan, M.A.H.; Qidwai, M.O.; Chausalkar, A. Effect of variable ignition and injection timing on emission characteristics of SI engine using CNG and HCNG as fuel. *Int. J. Adv. Mech. Eng.* **2014**, *4*, 83–94.

218. Brower, M.; Petersen, E.L.; Metcalfe, W.; Curran, H.J.; Füri, M.; Bourque, G.; Aluri, N.; Güthe, F. Ignition delay time and laminar flame speed calculations for natural gas/hydrogen blends at elevated pressures. *J. Eng. Gas Turbines Power* **2013**, *135*, 021504. [CrossRef]

219. Kim, J.; Carley, D. *Development of Direct Injection CNG Engine*; Inha Technical College: Incheon, Korea, 2000.

220. Hagos, F.Y.; Aziz, A.R.A.; Sulaiman, S.A.; Mahgoub, B.K. Low and medium calorific value gasification gas combustion in IC engines. In *Developments in Combustion Technology*; InTech: London, UK, 2016.

221. Tilagone, R.; Venturi, S. Development of natural gas demonstrator based on an urban vehicle with a down-sized turbocharged engine. *Oil Gas Sci. Technol.* **2004**, *59*, 581–591. [CrossRef]

222. Hillstrom, D.R. *Light Duty Natural Gas Engine Characterization*; The Ohio State University: Ohio, CO, USA, 2014.

223. Ahmad, N.; Babu, M.G. *Simulation and Experimental Studies on Combustion and Performance Characteristics for a Turbocharged and Naturally Aspirated Multi-Cylinder Compression Ignition Engine*; SAE Technical Paper 0148-7191; SAE International: Warrendale, PA, USA, 2006.

224. Hupperich, P.; Dürnholz, M. *Time-Controlled Pilot Injection for Stationary and Heavy-Duty Gas Engines*; SAE Technical Paper 0148-7191; SAE International: Warrendale, PA, USA, 1997.

225. Ibrahim, A.; Bari, S.; Bruno, F. *A Study on EGR Utilization in Natural Gas SI Engines Using a Two-Zone Combustion Model*; SAE Technical Paper 0148-7191; SAE International: Warrendale, PA, USA, 2007.

226. Ibrahim, A.; Bari, S. An experimental investigation on the use of EGR in a supercharged natural gas SI engine. *Fuel* **2010**, *89*, 1721–1730. [CrossRef]

227. Sen, A.K.; Ash, S.K.; Huang, B.; Huang, Z. Effect of exhaust gas recirculation on the cycle-to-cycle variations in a natural gas spark ignition engine. *Appl. Therm. Eng.* **2011**, *31*, 2247–2253. [CrossRef]

228. Nitnaware, P.T.; Ganvir, V.M. Design development and analysis of exhaust gas recirculation system for cng fuelled si engine. *IOSR J. Mech. Civ. Eng.* **2015**, *13*, 27–35.

229. Ramasamy, D.; Zainal, Z.; Kadirgama, K.; Briggs, H.W.-G. Effect of dissimilar valve lift on a bi-fuel CNG engine operation. *Energy* **2016**, *112*, 509–519. [CrossRef]

230. Soid, S.; Amir, S.; Ismail, M.; Hamid, M.; Amzari, M.; Said, M. Simulation studies on the performance of small engine fuelled by methane and the effect of various valve timings. *Indian J. Sci. Technol.* **2015**, *8*. [CrossRef]

231. Bell, S.R.; Gupta, M. Extension of the lean operating limit for natural gas fueling of a spark ignited engine using hydrogen blending. *Combust. Sci. Technol.* **1997**, *123*, 23–48. [CrossRef]

232. Suryawanshi, J.G.; Nitnaware, P.T. *An Investigation on si Engine Using Hydrogen and CNG Blends*; Department of Mechanical Engineering, Visvesvaraya National Institute of Technology, Nagpur & DY Patil College of Engineering: Pune, India, 2011.

233. Mohammed, S.E.; Baharom, M.; Aziz, A.R.A. Analysis of engine characteristics and emissions fueled by in-situ mixing of small amount of hydrogen in CNG. *Int. J. Hydrog. Energy* **2011**, *36*, 4029–4037. [CrossRef]

234. Mohammed, S.E.; Baharom, M.; Aziz, A.R.A. The effects of fuel-injection timing at medium injection pressure on the engine characteristics and emissions of a CNG-DI engine fueled by a small amount of hydrogen in CNG. *Int. J. Hydrog. Energy* **2011**, *36*, 11997–12006. [CrossRef]

235. Tunestål, P.; Christensen, M.; Einewall, P.; Andersson, T.; Johansson, B.; Jönsson, O. *Hydrogen Addition for Improved Lean Burn Capability of Slow and Fast Burning Natural Gas Combustion Chambers*; SAE Technical Paper 0148-7191; SAE International: Warrendale, PA, USA, 2002.

236. Hagos, F.; Aziz, A.; Sulaiman, S. Investigation of deposit formation in direct-injection spark-ignition engine powered on syngas. *Int. J. Automot. Technol.* **2015**, *16*, 479–485. [CrossRef]

237. Kamel, M.M. *Advanced Natural Gas Engine Advanced Natural Gas Engine Technology for Heavy Duty Vehicles*; US Department of Energy: Washington, DC, USA, 2014.

238. LandiRenzo. *Epa Approval of Dual Fuel CNG System for Detroit Diesel 12.7l s60 Engine*; Landi Renzo USA: Torrance, CA, USA, 2013.

239. Wagemakers, A.M.L.M.; Leermakers, C.A.J. *Review on the Effects of Dual-Fuel Operation, Using Diesel and Gaseous Fuels, on Emissions and Performance*; SAE Paper 2012-01-0869; SAE International: Warrendale, PA, USA, 2012.

CHAPTER 3

SCOPUS JOURNAL

Title: Application of The Chain Code and Fourier Analysis Techniques for The Investigation of Wrinkles and Distortions on Early Flames

Journal:

International Journal of Automotive and Mechanical Engineering

Volume / Page Number:
15/ 5709-5728

Application of The Chain Code and Fourier Analysis Techniques for The Investigation of Wrinkles and Distortions on Early Flames

A. R. A. Aziz[1], F. Y. Hagos[2,3*], Y. T. Anbese[1], M. R. Heikal[4] and Firmansyah[1]

[1]Center for Automotive Research and Electric Mobility (CAREM),
Universiti Teknologi Petronas, 31750 Tronoh, Perak, Malaysia
[2]Advanced Fluids Focus Group (AFFG), Faculty of Mechanical Engineering,
Universiti Malaysia Pahang, 26600, Pekan, Pahang, Malaysia
*Email: ftwi@ump.edu.my
Phone: +6094246367; Fax: +6094246222
[3]Automotive Engineering Center (AEC), Universiti Malaysia Pahang, 26600, Pekan,
Pahang, Malaysia,
[4]School of Computing, Engineering and Mathematics, University of Brighton

ABSTRACT

The study of flame commencement and growth in SI engine has attracted the attention of many researchers due to its strong dependence to the in-cylinder flow and its capability to influence flame propagation characteristics in SI engines. Optical visualisation has been one of the prominent techniques utilized in this study of the early flame properties. This work shows the application of Elliptic Fourier analysis (EFA) and image processing tools for the investigation of the early flame details from its shape features. An endoscopic ICCD camera was used to capture the flame images, at an interval of 2° CA starting from ignition onset for a period of 30° CAs (about 3 ms), from a CNG DI single cylinder SI engine operation in stratified and homogeneous charge conditions. The intake configuration was adjusted to acquire tumble or swirl induction, and engine speed was made to vary between 1500 and 2100 rpm. The sequences of collected images were processed to investigate wrinkles, distortion and growth rate of the early flame within the 3 ms combustion duration. Some tools of image processing, such as intensity enhancement, filtering, thresholding and boundary tracing, were applied. Once the flame boundary identified, it was chain coded, and elliptic Fourier function was utilised to characterise the contour. For this purpose, a computer programming code was proposed by the authors for automatic processing of the flame image data. The application of the elliptic Fourier analysis was found useful in the investigation of the early flame characteristics from its shape features; led to the portrayal of wrinkles and distortion levels quantitatively in a simpler way.

Keywords: Chain code; elliptic Fourier analysis; image processing; wrinkles; early flame.

INTRODUCTION

The study of early flames in SI engine is important to investigate the interrelation of flame propagation with combustion performance and exhaust emissions. A better flame development improves combustion, which results in better fuel efficiency and reduced unburned hydrocarbon emissions [1].

Flame development period in an SI engine can be defined as the period in which up to 10 % of the fuel mass burned. The flame kernel growth is mainly dominated by the ignition system property when the flame is below 1 mm radius. The kernel expansion rate is more controlled by the balance between laminar flame speed and strain rate up to the size of 2 mm radius. Then after the flame kernel starts to interact with the surrounding in-cylinder turbulent flow field. The fully developed flame structure property is acquired when the size reaches about 10 mm and in this period, the fuel fraction burned may reach up to 10% of the total mass [2].

Flame visualisation and experimental study of flame characteristics may require recording of the flame data directly or indirectly by imaging devices [3]. The light source for the illumination purpose can be the natural luminosity of the flame itself or an external light source such as a high-power laser [4]. The direct imaging can be done by flame region identification using the Planar Laser-Induced Fluorescence (PLIF) method by imaging exited radicals of combustion gas products. The imaging is at an appropriate laser wavelength, such as OH at 266 nm, or application of two-dimensional Mie scattering method to image seed particles in the flow outside the flame region because of the burning up of the seed particles in the flame region. The application of these methods for early flame imaging in which the small flame is wandering around by the flow in the cylinder is very difficult. The laser sheet must intersect the flame to get the flame boundary. Having a laser sheet at a specific location and small flame wandering here and there depending on the nature of the flow, it is very difficult to implement laser tomography for this specific study. Besides, applying laser tomography method for initial flame kernels could be impractical due to the nature of flame orientation In an actual engine combustion scenario [5]. Since the flame in the early stage of development is very small in size, it can be easily taken away from the spark centre by the surrounding airflow. This random position of the flame kernel attempts capturing it with a laser sheet very challenging [6].

Fibre-optic instrumented spark plug (FOSP) is one of the available techniques used to study flame kernel growth rate, as has been used by Ancimer et al. [7, 8]. This technique works with the recording of flame arrival time by the eight fibre-optics implemented at the periphery of the spark plug tip. Mathematical models are essential to construct 2-D flame kernel boundary from the arrival time signals. The most adopted models in this area are; an elliptic fit model that was developed by Kerstein and Witze [9], and the cubic-spline model by Lord et al. [10]. Since the model prediction lacks boundary details, this technique is not capable of identifying flame wrinkles and distortion correctly.

Chemiluminescence and Schlieren imaging are still other possible techniques to apply for flame visualisation. Chemiluminescence technique depends on the imaging of electromagnetic radiation signal from combustion radicals because of the chemical reaction. In the investigation of the early flame kernel, this signal is too weak to identify clear flame boundaries as discussed in [11]. On the other hand, the Schlieren method has limited application in quantitative analysis of flame characteristics [12]; besides, it demands a large visualisation window on the engine cylinder.

The choice of the techniques especially in SI engine applications boiled down to direct visualisation method. Direct visualisation method is the imaging of the early flame using its luminosity by CCD or high-speed camera. With the increase in technical capability of CCD cameras, image intensifiers and high frame rate video cameras, direct imaging of weak flames for quantitative analysis become more apparent. The high dynamic ranges of modern CCD cameras incorporated with the advancement of image

processing technology maximise the capability of the direct visualisation technique for flame kernel study [13]. With the presence of too much noise in the engine and the weak signal of the early flame kernel growth, interpretation of the flame behaviour and characteristics is the major challenge. The basic morphological parameters to be considered in the visualisation of the flame kernel description are the wrinkles level of the flame front and the global flame distortion. These physical parameters mainly influence the flame growth rate. The aim of this study is, therefore, to utilise chain code and elliptic Fourier analysis (EFA) tools to investigate the characteristics of the early flame development from its shape features.

METHODS AND TECHNIQUES

Image Acquisition

Experimental work was performed to investigate wrinkles and distortion effects on the flame kernel caused by a change in engine speed and induction flow structures using the technique discussed earlier. A chain code and elliptic Fourier analysis (EFA) was used to analyses the flame wrinkles and distortion. A single cylinder direct injection engine was made to operate at partial load using CNG fuel injected at 18 bars. The fuel injection was set at 90° before the top dead centre (BTDC) for the stratified charge and 180° BTDC for the homogeneous charge cases. The air-fuel ratio was controlled at the lean condition in both stratified and homogeneous charge combustion model [14]. The engine speed considered in the current study is from 1500-2100 rpm. Early flame development visualisation is challenging at lower end performance with the engine speed lower than 3000 rpm as the luminosity of the flame is low [15]. The imaging system used was a HiSence 12 bit CCD camera equipped with Hamamatsu CA2098 image intensifier and AVL KARL STORZ M00060 30° endoscope to capture the flame image from the combustion chamber through a 10 mm hole on the cylinder head, as the installation shown in Figure 1 and the arrangement schematics in Figure 2.

Figure 1. The imaging device fixed on the engine at an installation angle of 30°.
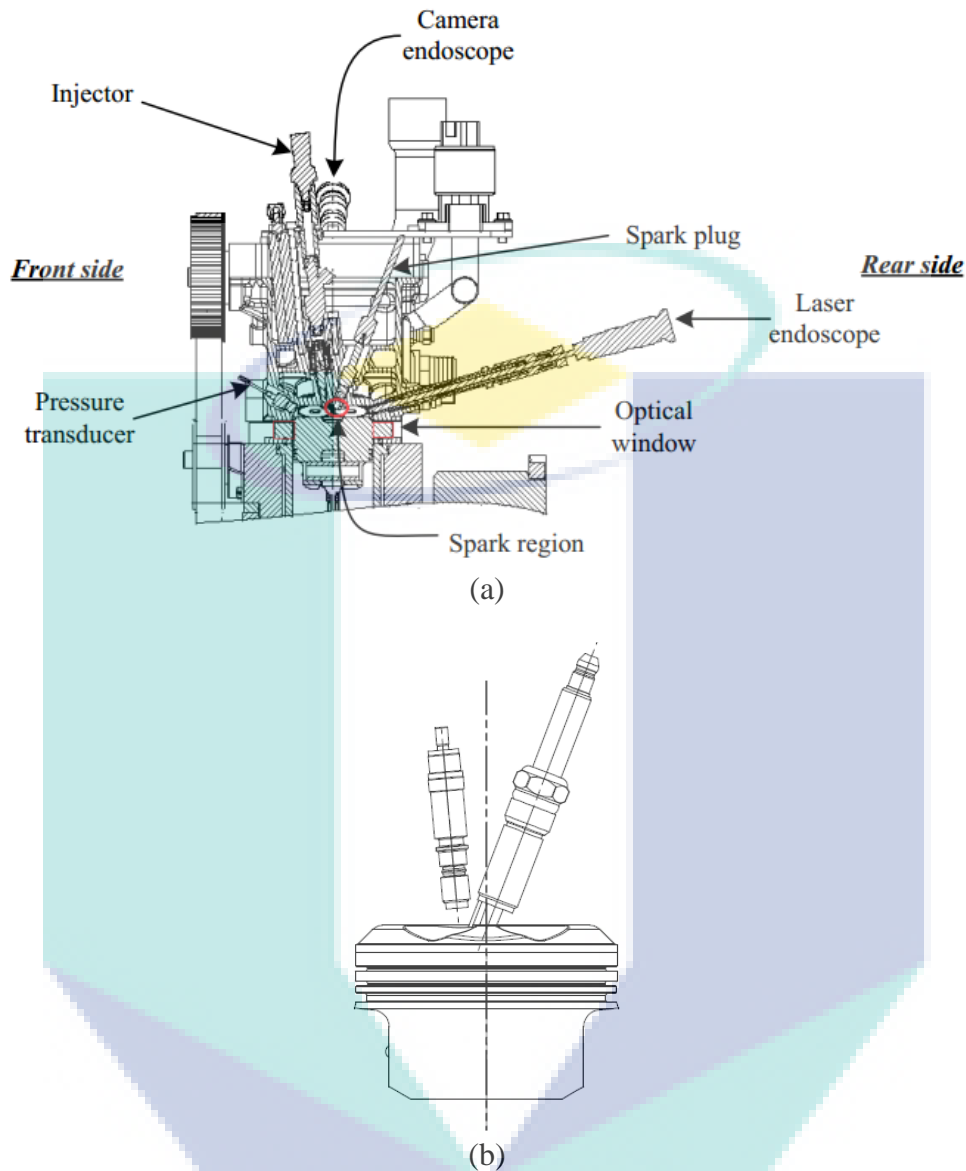
Figure 2. The CNG DI engine with the endoscopic optical access (a) complete and (b) clear cross-section of the piston along with injector and spark plug arrangement.

The main consideration in the image acquisition system was the synchronisation of the imaging system with that of the engine operating speed and top dead centre (TDC) position sensors. The synchronisation of the external camera trigger signal by using the cam position as in input with the crank angle and TDC signal by the use of LabVIEW control program [16]. Figure 3 shows the schematics of all the sensors, the camera and the data acquisition system used in the current experiment.
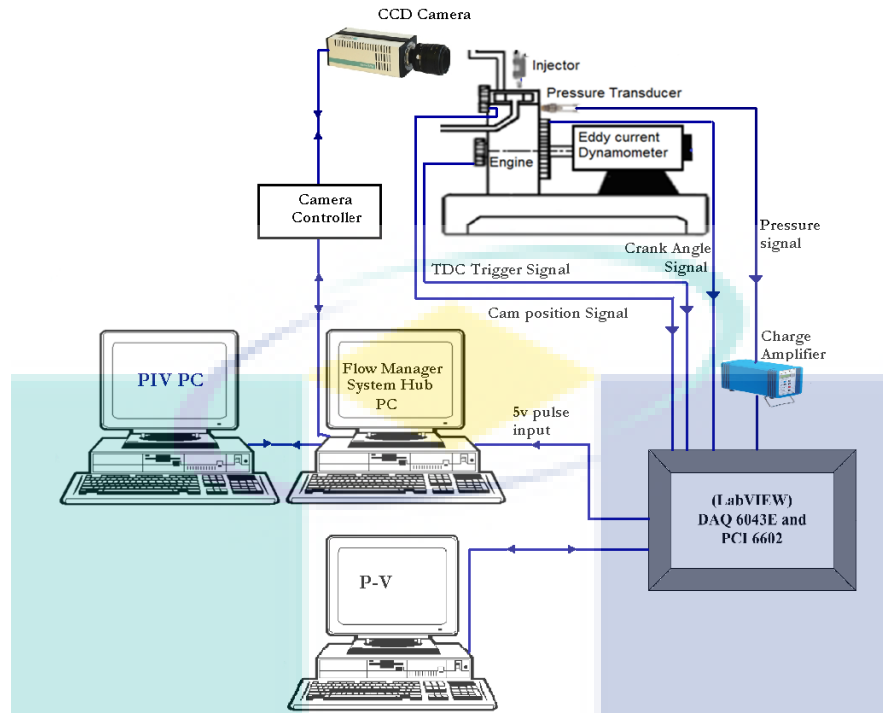
Figure 3. Flame imaging setup [16].

The crank angle sensor generated a signal tick for every 0.5° rotation of the crank producing a total of 1440 ticks for every complete cycle (two revolutions). Out of this, another signal tick (TDC trigger) was generated by the crank angle sensor for every revolution. However, this signal could not match with the exact position of TDC due to the difficulty encountered during engine assembly. Therefore, there was an offset of 126.5° CA between the TDC trigger signal and the exact TDC position, which was taken to be an initial delay in the calculation of the TDC position [17].

The TDC trigger signal was generated twice every complete cycle, one at the end of the exhaust stroke and the other at the end of compression stroke. Identification of the TDC at the end of the compression stroke was very important to define the exact position of the external camera triggering signal. The camshaft sensor with the help of the crank angle sensor was used to define the TDC position. This sensor was attached to camshaft wheel, and its signal was generated in every complete cycle. This signal was positioned at 31.5° after the compression stroke TDC. These all three signals were calibrated and synchronised with the help of a four-channel oscilloscope. Figure 4 shows the signal synchronisation of different sensors used for flame imaging.

LabVIEW program was used to control the external camera triggering position taking the crank angle and cam position signals as an input from NI-DAQ system. Flame image was then captured starting from the onset of ignition for 20° CA at an interval of 2° CA. A total of 30 flame images were captured at every required crank angle in order to get the average properties of the developing flame for that specific crank angle [16].
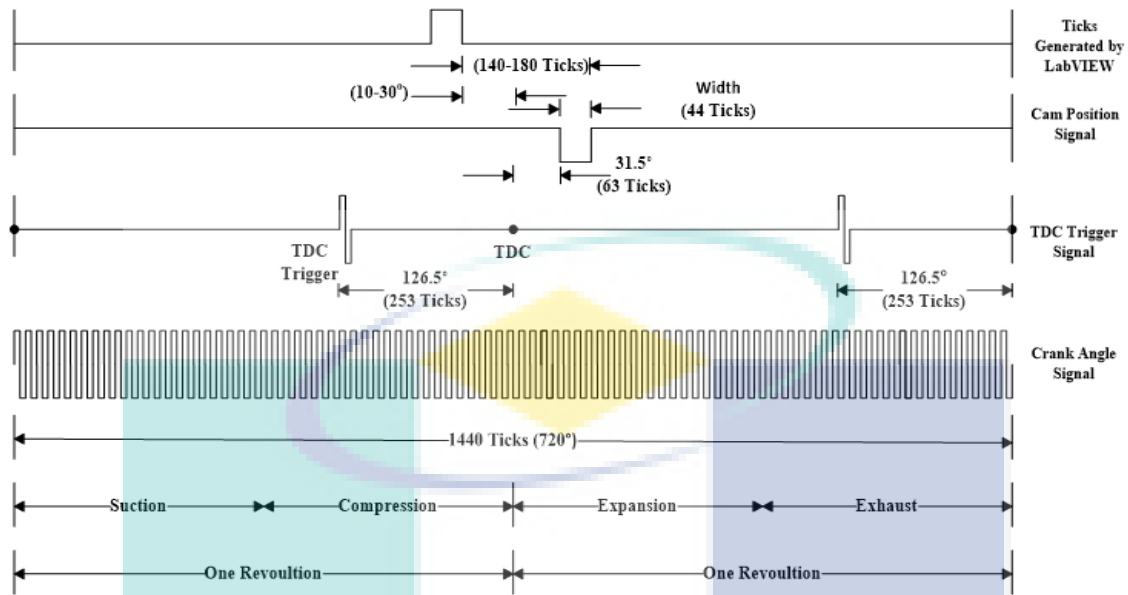
Figure 4. Signal synchronisation of different sensors for flame imaging.

Image Filtering

Early flame kernels are flames of small sizes, about 5 mm radius, with intensity too weak to be visualised. In such case, digital imaging using CCD cameras have immense contribution to get the weak intensity flame visualized due to their high dynamic ranges. From these images, meaningful physical information can be derived through image processing and Fourier transform applications.

Noise in digital imaging is unavoidable occurrences. Noise can occur during image capturing, transmission or processing. The thermoelectric cooling system in modern CCD cameras minimises thermal noises due to rise in temperature. Therefore, the first task to be considered in the flame image analysis can be the removal of noises from the images using digital filters. This leads to the implementation of a 2-D convolution of a filter function directly on the image in the spatial domain. For a square filter kernel size M×M with input image f(m,n) and filter function G(x,y), the output image is given by:

$$g(m,n)= \sum_{x=-\frac{M}{2}}^{\frac{M}{2}} \sum_{y=-\frac{M}{2}}^{\frac{M}{2}} G(x,y)\, f(m-x,n-y) \tag{1}$$

The filter function used in this work was the 2-D Gaussian weighted average given by,

$$G(x,y;\sigma)=\frac{1}{2\pi\sigma^2}\, e^{-\frac{x^2+y^2}{2\sigma^2}} \tag{2}$$

where, σ is the standard deviation of the Gaussian function.

Image Binarisation

Binarisation is a process of segmenting an image into an object and a background according to the gray level of image pixels using a specific threshold value. Pixels of the binary image categorised as black or white, or a logical value of '1' or '0'.

The important step in binarisation is to find the appropriate marginal value that can separate the foreground (or the object) from the background effectively. Sezgin and Sakur [18] made a comprehensive evaluation of around 40 thresholding techniques by categorising them into six groups according to their thresholding performance. The criteria they considered for every thresholding method were classification error, edge mismatch, relative foreground area error, modified Hausdorff distance, and region non-uniformity. Out of the evaluated techniques, the histogram based Ostu thresholding method showed better performance, and due to its simplicity, it has been the most applied in the image segmentation process.

Ostu thresholding technique was first introduced by N. Otsu in late 1970's [19], and has been used for decades for image segmentation process in many areas; such as weld defect identification of radiographic images [20], and plant leaf classification [21]. It uses the statistics of the pixel intensity to identify threshold value in generating the binary images. Its simplicity to implement in an efficient algorithm for multiple images in an automatic segmentation process makes Ostu thresholding the most preferred method.

The Ostu thresholding technique depends on the statistical distribution of gray-level values of the image pixels. Assume a total of L gray levels represents the pixels intensity, and the number of pixels in the ith gray level is denoted by h_i. With N to be the total number of image pixels, the probability of a pixel to be in the ith gray level is given by,

$$P_i = \frac{h_i}{N} \tag{3}$$

Now, let us classify pixels of the image into two classes; background and foreground. The background class contains pixels with gray level values range 0 to k, and the foreground class contains pixels of gray level range k to (L-1), in which k is the threshold value. Thus, the probability of class occurrence (ω), class mean (μ) and class variance (σ^2) is given by:

$$\omega_0 = \sum_{i=0}^{k} P_i \; ; \qquad \omega_1 = \sum_{i=k+1}^{L-1} P_i = 1 - \omega_0 \tag{4}$$

$$\mu_0 = \sum_{i=0}^{k} \frac{iP_i}{\omega_0} \; ; \qquad \mu_1 = \sum_{i=k+1}^{L-1} \frac{iP_i}{\omega_1} \tag{5}$$

$$\sigma_0^2 = \sum_{i=0}^{k} (i-\mu_0)^2 P_i \; ; \quad \sigma_1^2 = \sum_{i=k+1}^{L-1} (i-\mu_1)^2 P_i \tag{6}$$

$$\mu_T = \sum_{i=0}^{L-1} iP_i \; ; \quad \sigma_T^2 = \sum_{i=0}^{L-1} \left(i - \mu_T\right)^2 P_i \tag{7}$$

where subscripts 0, 1 and T represent background, foreground and total classes, respectively. To identify the optimum threshold, it is important to look at the between-class variance;

$$\sigma_B^2 = \omega_0 \left(\mu_0 - \mu_T\right)^2 + \omega_1 \left(\mu_1 - \mu_T\right)^2 \tag{8}$$

A threshold value that maximises the between-class variance (σ_B^2) is considered as the optimum threshold value for the formation of binary images, as discussed in [19]. Therefore, the optimum threshold value k is the one that gives maximum σ_B^2 for $1 \le k \le L$.

Flame Boundary Tracing

The pixels of the binary flame images identified by the Ostu thresholding method have a logical expression that can be black for object and white for the background or can be quantified as '1' for the object (foreground) and '0' for the background. For further flame image analysis, the boundary pixels of the flame images had to be identified using Moore-neighbor tracing method. The algorithm is simple and can be implemented on the Matlab platform. It works by scanning the binary image along the columns starting from bottom left until the first object pixel (or '1') is found. Then, returning to the immediate previous background pixel and trace clockwise around the neighbourhood of the object pixel identified earlier until another object pixel found. The algorithm terminates tracing when the first object pixel is met for the second time. Finally, the coordinates of all the pixels that constitute the closed boundary of the flame are identified.

Elliptic Fourier Analysis and Chain Codes

Elliptic Fourier analysis was first introduced by Kuhl and Giardina in the '80s [22]. Since then it has been used in many identification and classification applications in plant and animal species studies [23, 24], and human anatomy studies [25]. The coefficients of EFA are functions of the shape of the flame boundary under consideration. The coefficients can be size invariant so that they define shape character in spite of size variations of an object. This code is very effective for data reduction process by minimising the boundary points used for reconstruction without affecting the ultimate shape, and also able to avoid details of the boundary by changing the harmonic levels.

Chain coding is widely used as a standard input format for image shape description algorithms, such as EFA. It describes a 2-D image boundary via 1-D directional codes by forming a series of connected straight-line segments. H. Freeman [26] was the first to create this code, and his principle was based on the idea that any continuous curve can be represented by many small straight line segments and angles describing their directions. Any desired precision of curve prediction by the chain code can be obtained with a coarse angle representation and arbitrarily small distances of line segments.

The Freeman chain-code, which is named after the inventor, can be constructed using 4-directional or 8-directional codes. The 8-directional code considers all the neighbouring pixels, and it is the most preferred to code any closed boundary. The codes

that represent the segmented lines are given by 0 1 2 3 4 5 6 7, and each code represents a specific direction of traversing to the next pixel throughout the boundary of the binary image until it returns to the starting pixel as illustrated in Figure 5. The segment size can be taken to be the step to the next pixel on the image boundary, which is equal to either 1 or $\sqrt{2}$ pix. The outputs of the chain code are used as standard inputs for the EFA algorithm.
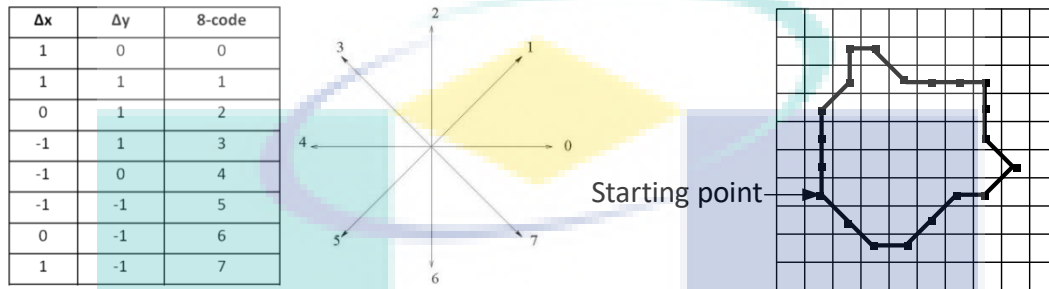
Figure 5. Eight-directional Freeman chain code and depiction of the typical boundary of an image expressed by the code 22212070006675455433 [27].

Elliptic Fourier coefficients maintain a description of object boundary in a two-dimensional space of the complex plane in which real and imaginary components represent each pixel in the image space. Thus, a curve in the closed boundary can be defined as:

$$c(t)=X(t)+jY(t) \tag{9}$$

where *t* is the arc length. Based on the general complex plane representation of curves by Eq. (9), it is possible to identify the Elliptic Fourier coefficients through Fourier series expansion. After some analysis, as detailed in the work presented by Nixon and Aguado (2008) [28], the x and y coordinates of the boundary points at t can be represented by the sum of the elliptic Fourier series:

$$x_N(t)=A_0+\sum_{n=1}^{N} a_n\cos\left(\frac{2n\pi t}{T}\right)+b_n\sin\left(\frac{2n\pi t}{T}\right) \tag{10}$$

$$y_N(t)=C_0+\sum_{n=1}^{N} c_n\cos\left(\frac{2n\pi t}{T}\right)+d_n\sin\left(\frac{2n\pi t}{T}\right) \tag{11}$$

where the arc-length *t* is the step required to traverse one pixel along the closed contour; $t_{p-1}<t<t_p$ for $1\leq p\leq k$; k is the total number of codes describing the boundary contour; n is the number of Fourier series or the level of harmonics; T is the basic period of the chain-code, that is $T=t_k$; A_0 and C_0 are the bias coefficients. Setting A_0 and C_0 to be zero makes the center of the region under the closed boundary to be at the center of coordinate axis.

The use of higher harmonic levels increases the description of details of the flame boundary in the reconstruction process. Lower frequencies, which contain the general feature of the boundary shape, are described by the lower harmonics; as a result, the total number of Fourier coefficients used to define the boundary is reduced. This technique

was found to be efficient in the approximation of the mean flame contour to quantify the level of the contour wrinkles. On the other hand, the high frequency details of the flame contour structure are revealed by the higher harmonic level reconstruction. The Fourier coefficients appeared in Eq. (10) and (11), at the nth harmonic level are obtained from;

$$a_n = \frac{T}{2n^2\pi^2} \sum_{p=1}^{k} \frac{\Delta x_p}{\Delta t_p} \left[\cos\left(\frac{2n\pi t_p}{T}\right) - \cos\left(\frac{2n\pi t_{p-1}}{T}\right) \right] \tag{12}$$

$$b_n = \frac{T}{2n^2\pi^2} \sum_{p=1}^{k} \frac{\Delta x_p}{\Delta t_p} \left[\sin\left(\frac{2n\pi t_p}{T}\right) - \sin\left(\frac{2n\pi t_{p-1}}{T}\right) \right] \tag{13}$$

$$c_n = \frac{T}{2n^2\pi^2} \sum_{p=1}^{k} \frac{\Delta y_p}{\Delta t_p} \left[\cos\left(\frac{2n\pi t_p}{T}\right) - \cos\left(\frac{2n\pi t_{p-1}}{T}\right) \right] \tag{14}$$

$$d_n = \frac{T}{2n^2\pi^2} \sum_{p=1}^{k} \frac{\Delta y_p}{\Delta t_p} \left[\sin\left(\frac{2n\pi t_p}{T}\right) - \sin\left(\frac{2n\pi t_{p-1}}{T}\right) \right] \tag{15}$$

where, $\Delta t_p = \sqrt{\Delta x_p^2 + \Delta y_p^2}$ and $t_p = \sum_{i=1}^{p} \Delta t_i$ in which Δx_p and Δy_p are the spatial changes in the respective axis that can be identified from the chain code at point *p* of the flame contour. Δt_p is the step change that is required to travel from point (p-1) to p in the chain code. t_p is the total number of steps required to travel up to point p in the chain code.

The elliptic Fourier coefficients contain non-redundant information. They can uniquely describe shapes of closed contours by representing dimensions of the ellipse at each harmonic level, as illustrated in Figure 6.
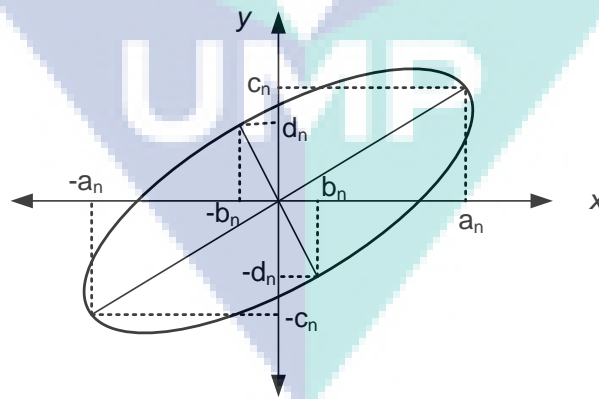
Figure 6. Representation of the Fourier coefficients in the harmonic ellipses.

The x- and y-coordinates are computed separately using Eq. (10) to (15), and the shape of the object can be recreated by combining these coordinates for identical value of t, as shown in Figure 7. As discussed earlier, the elliptic Fourier coefficients represent an ellipse at any level of harmonic. The ellipses at lower harmonic levels are bigger to

describe the general shape of the boundary. As the harmonic level increases the size of the harmonic ellipse drops, and thus the details of the flame contour will be revealed. The sum of the series of harmonic ellipses at the different levels converges into a polygon that represents the given contour, as portrayed in Figure 8 for a typical flame. The level of harmonics defines the features of the reconstructed flame contour. The higher the harmonic levels, the higher the chance of revealing contour details. Figure 9 shows the reconstructed flame contour of the typical flame image shown in Figure 8(a) at different harmonic levels; the exact reconstruction of the flame contour was found at the 120th harmonic level. Table 1 shows the Fourier descriptors of the first ten harmonic levels.
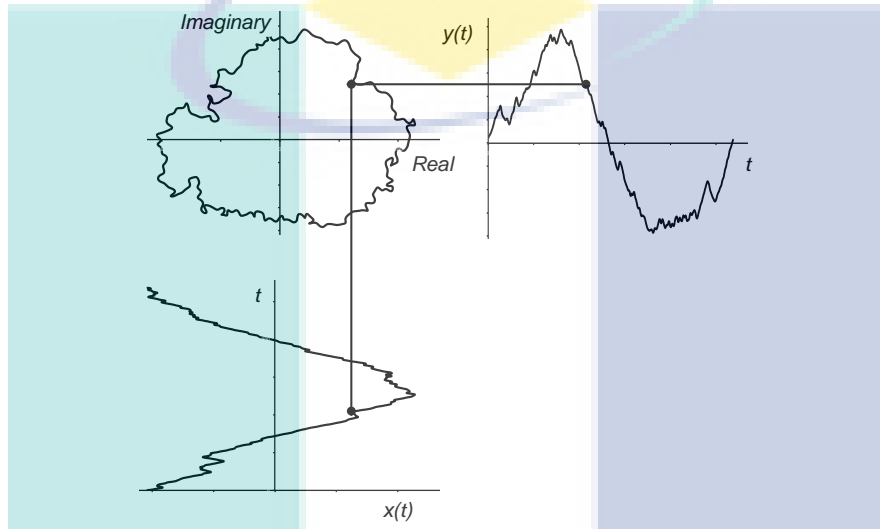
Figure 7. The complex curve representation from the two coordinates.

(a)

(b)
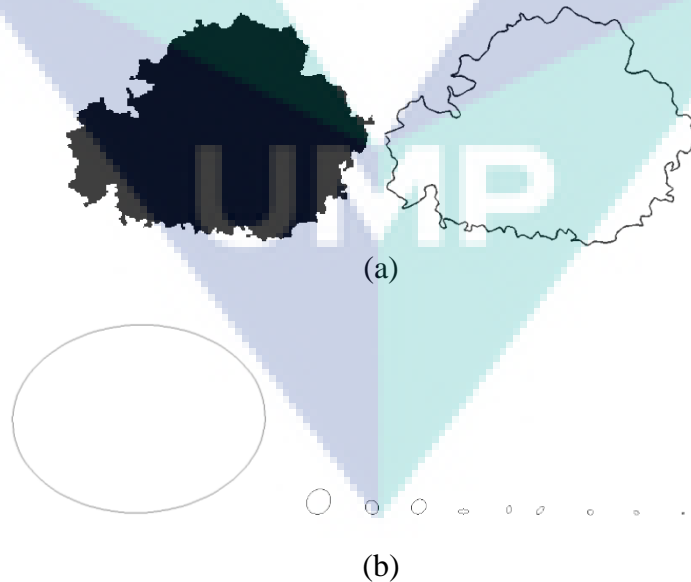
Figure 8. (a) Binary image of a typical flame and its contour (b) Harmonic ellipses for the first 10 harmonic levels of the flame boundary shown in (a).
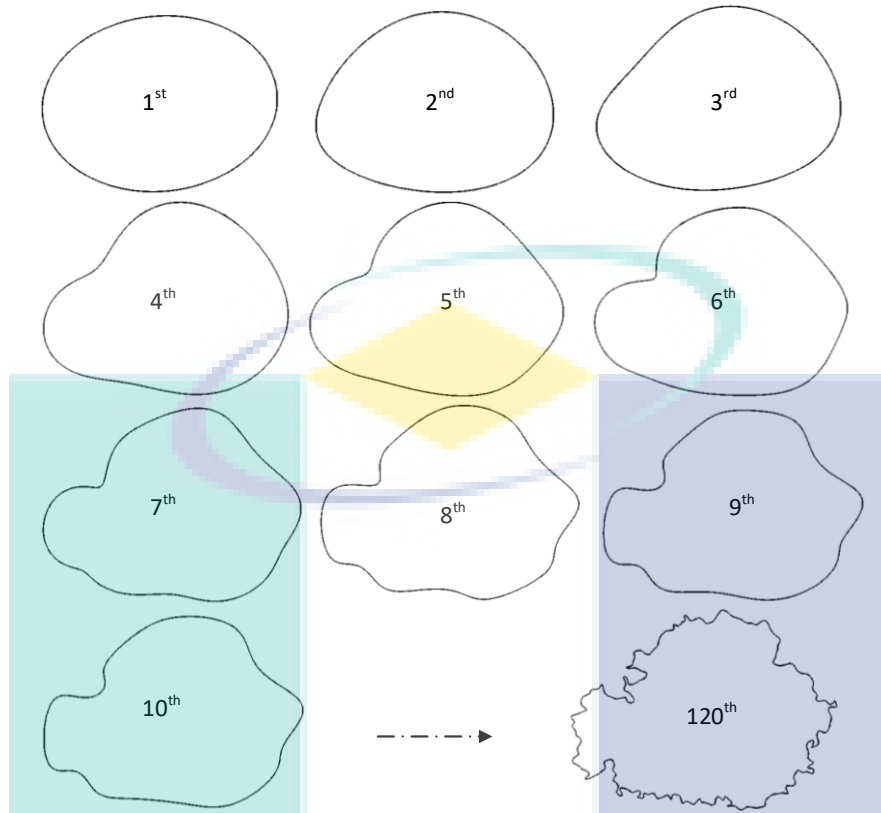
Figure 9. Reconstructed flame contour at different harmonic levels.

Table 1. Fourier descriptors of the first ten harmonic levels.

Harmonic level	a_n	b_n	c_n	d_n
1	-96.9337	-0.4725	-4.7904	76.2928
2	7.4116	4.2382	-4.2777	-9.0534
3	-2.0552	4.6294	4.9356	-0.0781
4	-3.8106	2.0718	3.4938	5.6907
5	-3.9951	0.6284	0.1699	1.579
6	-1.4266	2.0469	1.1297	2.9539
7	-1.4179	-1.924	0.1514	2.1478
8	1.2555	-2.0859	1.3608	0.8021
9	0.8262	1.2002	0.9225	1.514
10	-0.2626	-0.1611	0.5201	0.4741

Reconstruction of flame contours using EFA is performed by summing up a series of harmonic ellipses, like the one shown in Figure 8(b). The extent to which the wrinkles detail of the contour to be included in the reconstruction depends on the number of harmonic levels considered. Such details of the flame boundary are achieved by the inclusion of the small-sized harmonic ellipses whose major radius is less than 1% of the equivalent flame radius, as observed from the analysis of few flame images. Therefore, the 1% threshold was set to be the cut-off harmonic level to identify the mean contour. Figure 10 shows the mean contour of a typical flame identified by the 1% threshold value superimposed on the wrinkled flame contour. Once the mean flame is identified the

wrinkles level can be approximated from the standard deviation (STD) of the displacements of the boundary points from the mean to the wrinkled flame contour.
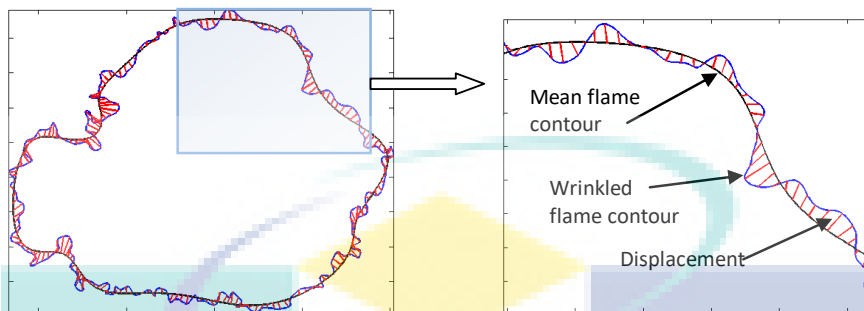
Figure 10. Mean flame contour superimposed on the wrinkled one.

ANALYSIS AND DISCUSSION

A total of 30 flame images were collected at every set crank angle with a 2° CA interval starting from 0.5° CA after ignition onset (38° CA BTDC) up to 10° CA BTDC. The series of collected images portrayed the development stage of the flame kernel within 3 ms after ignition onset. The authors developed a computer code to examine a large number of collected flame images quantitatively in an automatic manner. The flame wrinkles level, distortion and growth rate in the early development stage were the parameters investigated by the technique discussed earlier in this work.

Flame Wrinkles

Figure 11 shows the degree of wrinkles obtained for the tumble and swirl induction for both stratified and homogeneous charge combustions at different engine operating speeds ranging from 1500 to 2100 rpm. The wrinkling level was identified from the standard deviation of the Euclidean distances between similar boundary points of mean flame and turbulent flame contours. The fundamental wrinkles formation behaviour was shown differently in stratified and homogeneous charge combustion cases. In the stratified charge combustion, both tumble and swirl inductions exhibited the occurrence of a direct relation between wrinkles formation and engine speed; whereas, homogeneous charge combustion showed the opposite.

The level of small-scale turbulence and the air-fuel ratio at the surrounding of the spark electrode play a major role in the formation of wrinkles on the early flames [2]. A higher degree of wrinkles could be exhibited with lean fuel-air due to the relatively lower burn rate as compared to the wrinkling rate caused by turbulence. Then again, increasing of the engine speed could increase the turbulence intensity inside the cylinder [29, 30], which facilitates the flame wrinkles formation [31]. Therefore, it can be affirmed that the trade-off between the fuel-air mixture leanness and the degree of turbulence caused as a result of variation of engine operating speed at the time of ignition is the determinant factors of the level of the early flames shown in Figure 11. The maximum degree of wrinkles is observed in the early flames in the homogeneous charge combustion with an engine speed of 1500 rpm. The fact that the local fuel-air ratio of the mixture is richer or close to stoichiometric near the spark electrode region with a stratified charge, the degree of wrinkles tends to increase with an increase in engine speed [27].

(a)

(b)

(c)

(d)
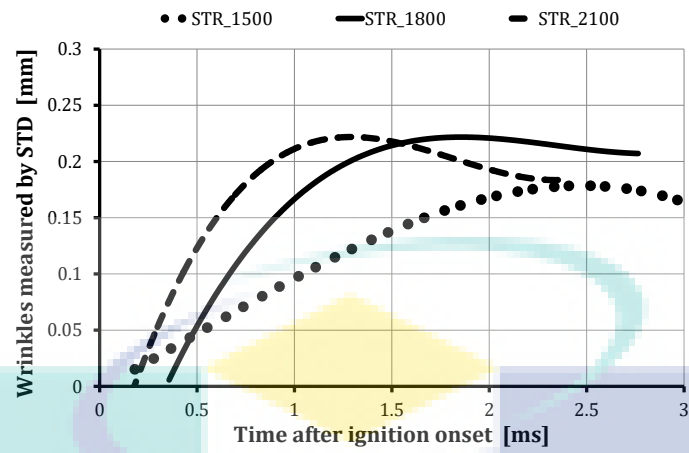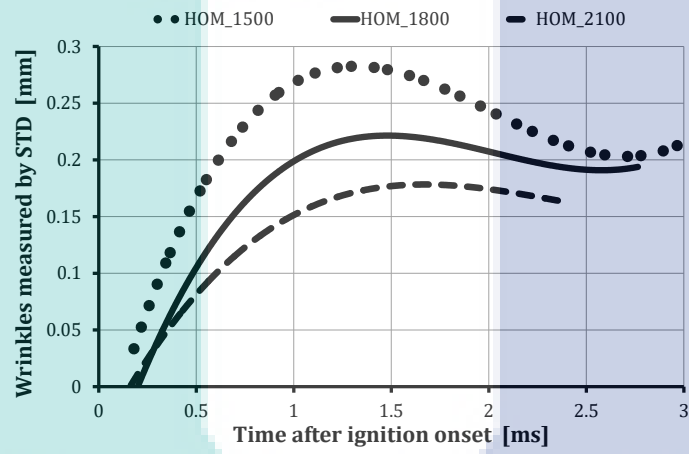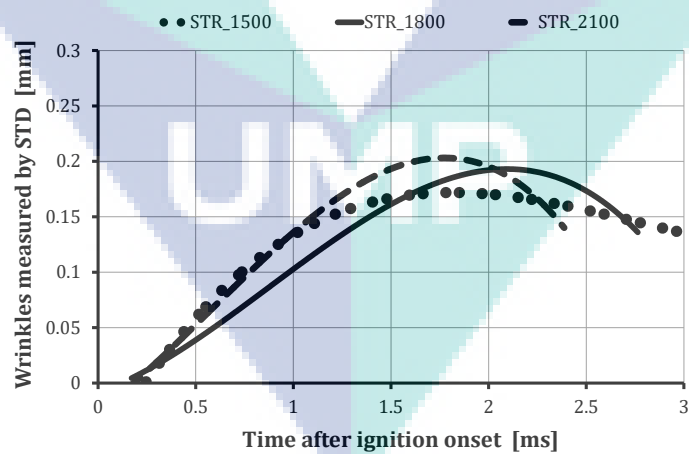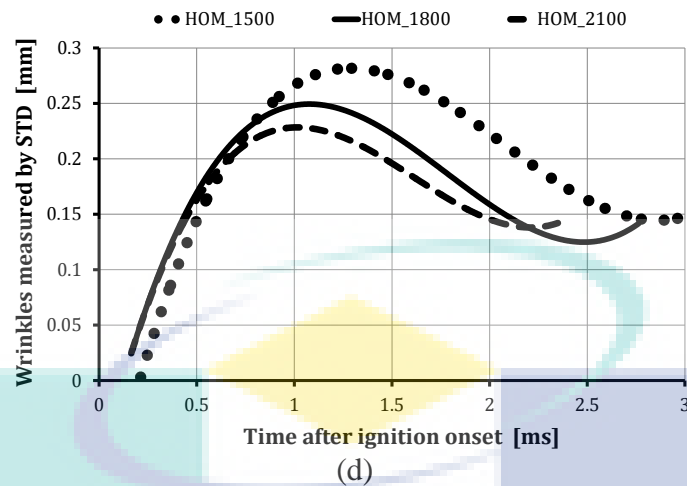
Figure 11. Flame wrinkles measurement in (a), (b) tumble induction and; (c), (d) swirl induction.

Flame Distortion

The measure of global change in the flame structure is called flame distortion [27, 32]. The computer programming code is developed to evaluate the flame distortion degree of the early flame by processing of the successive images taken in the region of ignition onset. The factors affecting the flame distortion of the early flame are the interaction with large-scale flow structures, the local quenching of the flame having contact with cold surfaces such as spark electrodes and the hydrodynamic strain effects of the in-cylinder bulk flow [33].

The flame distortion level was measured by the ratio of the flame perimeter to the perimeter of a circle whose radius is the equivalent radius of the flame. Similar techniques were used in the works of [6], [7], and [34]. To eliminate the influence of the small-scale local curvatures created by the wrinkles, a mean flame boundary was used for the calculation of flame distortion degree in the current work. Figure 12 shows early flame distortion measured by the techniques discussed earlier at the different engine operating speeds and induction flows for both stratified and homogeneous charge combustions. It was observed that the degree of flame distortion increased with an increase in engine operation speed in all engine operating conditions. This increase in the degree of flame distortion is as the result of the mean bulk velocity. Within the first 1.5 ms duration after the start of ignition, there was no significant global change in the shape of the flame observed especially in the tumble induction. Though insignificant, swirl intake showed higher flame distortion than the tumble intake. This might be due to the presence of large-scale eddies near compression TDC in swirl intake configuration, because of its lower turbulence decaying rate compared to tumble induction. On the other hand, flame distortion behaviour did not show significant changes between the stratified and homogeneous charge combustion cases.
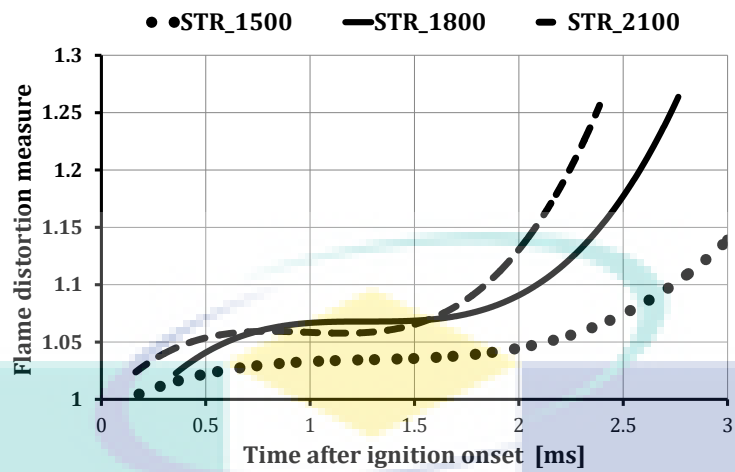
(a)
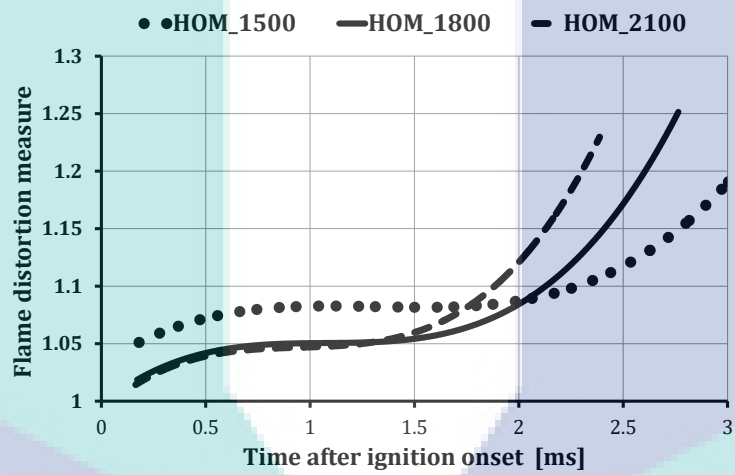
(b)
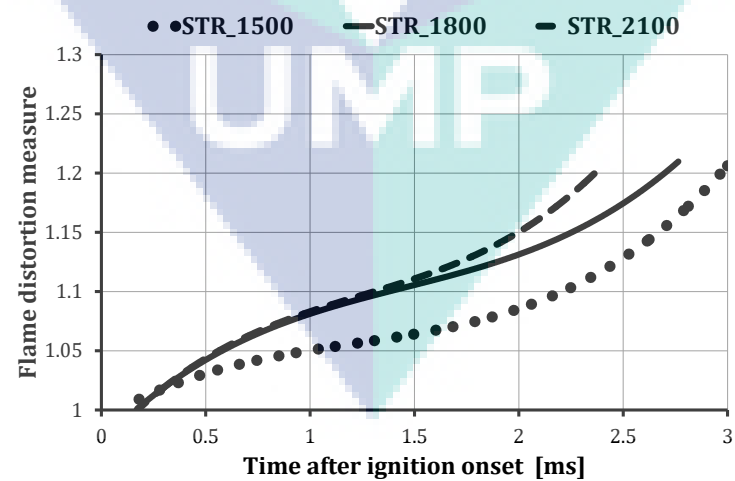
(c)
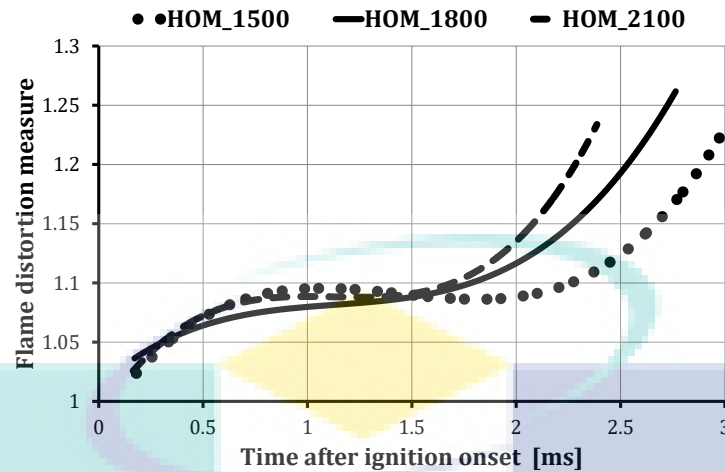
(d)

Figure 12. Flame distortion measurement in (a), (b) tumble induction and; (c), (d) swirl induction.

Flame Growth Rate

The rate of flame growth was measured by the rate of change of equivalent radius of the mean flame. The flame kernel growth rate varies with the wrinkles and distortion conditions of the flame. Wrinkles can increase flame surface area. As a result, burning rate increases. The flame growth rate can also be affected by the position of the small flame at the early stages of combustion. Contact of the flame kernel with the relatively cold surfaces, such as spark electrodes, quenches the small flame globally or locally. This might affect the growth rate of the early flame.

Figure 13 shows the average flame growth rate during the development period for stratified and homogeneous combustion cases. It can be observed in Figure 13 (a) that in the stratified charge combustion, tumble induction showed a better growth rate than the swirl induction especially with the rise in engine speeds. This report is supported by Gunasekaran and Ganesan [35] findings that showed tumble intake with the late injection would provide better mixture formation and combustion characteristics. The sequence of flame images within 2.4 ms after ignition onset for the tumble induction, stratified combustion at the highest engine speed of 2100 rpm.
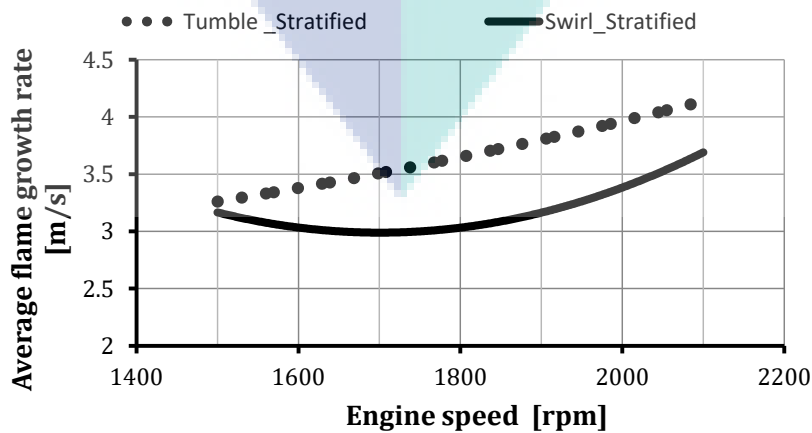
(a)
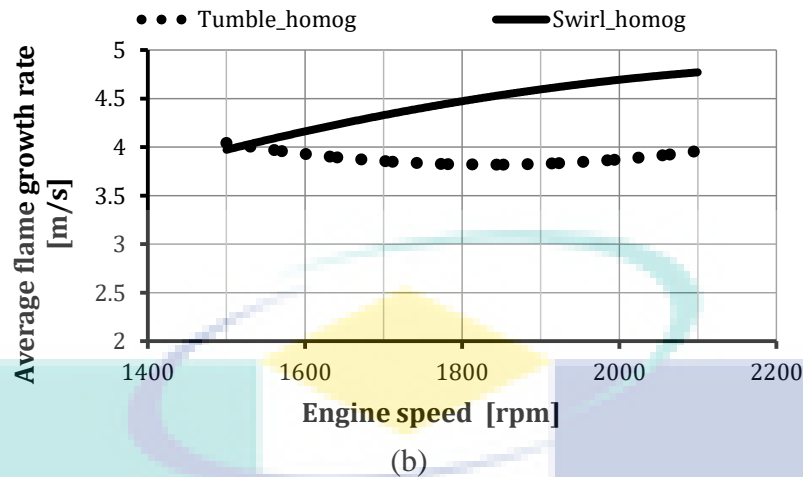
Figure 13. Average flame growth rate at the different engine parameters of (a) stratified charge combustion, (b) homogeneous charge combustion.

On the other hand, inhomogeneous charge combustion, swirl induction caused for the highest flame growth rate performance, whereas tumble induction showed almost no variation with change in engine speed as shown in Figure 13 (b). It was also observed that homogeneous swirl combustion had the fastest growing flame in the early combustion period, and the rate was increasing much more with engine speed.

CONCLUSION

Early flame characteristics of a CNG DI SI combustion was investigated using image processing and elliptic Fourier analysis methods. This technique was used to overcome the drawback of the conventional Fourier analysis method for the flame contour characterisation such as divisions being equal on the construction of contours, the method being dependent on coordinate and requirement of multi-valued function for defining of complex contours. The technique chosen was effective in the description of flame shape features for the approximation of wrinkled and mean flame boundaries; from which level of wrinkles, distortion and growth rate of the early flame obtained. This study summarises that the early flame growth rate depended not only on the intake configurations (tumble or swirl) but also on mixture level of stratification or homogeneity. The technique used in this work is found effective because of its simplistic algorithm to process multiple flame data automatically. It has overcome the limitations of the conventional Fourier analysis method to provide a quantitative flame description from the qualitative flame image.

ACKNOWLEDGEMENT

REFERENCE

[1]   Lawal M, Abolarin M, Nasir A, Musa A. Differential air/fresh charge demand, supply and utilisation in two-stroke spark ignition engines. International Journal of Automotive and Mechanical Engineering. 2017;14:4769-.

[2]   Arcoumanis C, Kamimoto T. Flow and combustion in reciprocating engines. Berlin: Springer; 2009.

[3]   Lu G, Stasiak A, Shao J, Yan Y. Digital imaging based measurement of combustion flame characteristics. Imaging Systems and Techniques, 2007 IST'07 IEEE International Workshop on: IEEE; 2007. p. 1-4.

[4]   He C, Kuenne G, Yildar E, van Oijen J, di Mare F, Sadiki A, et al. Evaluation of the flame propagation within an SI engine using flame imaging and LES. Combustion Theory and Modelling. 2017;21:1080-113.

[5]   Winklhofer E, Philipp H, Fraidl G, Fuchs H. Fuel and flame imaging in SI engines. SAE Transactions. 1993:1263-72.

[6]   Aleiferis PG, Taylor AMKP, Ishii K, Urata Y. The nature of early flame development in a lean-burn stratified-charge spark-ignition engine. Combustion and Flame. 2004;136:283–302.

[7]   Ancimer R, Jaaskelainen H, Wallace J. Experiments into the Flame Kernel Development in High Swirl Production Spark Ignition Engine. SAE. 1999.

[8]   Ancimer RJ. The influence of in-cylinder flows on the flame kernal growth in natural gas fuelled spark ignition engines: University of Toronto; 2000.

[9]   Kerstein AR, Witze PO. Flame-Kernel Model for Analysis of Fiber-Optic Instrumented Spark Plug Data. SAE. 1990.

[10]   Lord DL, Anderson RW, Brehob DD, Kim Y. The Effects of Charge Motion on Early Flame Kernel Development. SAE. 1993.

[11]   Ikeda Y, Nakajima T, Ohira T. Flame propagation characteristics by planar OH Measurment. SAE Paper. 1999.

[12]   Wang J, Huang Z, Tang C, Zheng J. Effect of hydrogen addition on early flame growth of lean burn natural gas–air mixtures. International Journal of Hydrogen Energy. 2010;35:7246-52.

[13]   Aleiferis PG, Taylor AMKP, Whitelaw JH. Cyclic Variations of Initial Flame Kernel Growth in a Honda VTEC-E Lean-Burn Spark-Ignition Engine. SAE. 2000.

[14]   Chala G, Aziz A, Hagos F. Combined effect of boost pressure and injection timing on the performance and combustion of CNG in a DI spark ignition engine. International Journal of Automotive Technology. 2017;18:85-96.

[15]   Chala G, Abd Aziz A, Hagos F. Natural Gas Engine Technologies: Challenges and Energy Sustainability Issue. Energies. 2018;11:2934.

[16]   Hagos FY, Aziz ARA, Sulaiman SA. Early flame development image comparison of low calorific value syngas and CNG in DI SI gas engine. IOP Conference Series: Earth and Environmental Science: IOP Publishing; 2013. p. 012070.

[17]   Aziz ARA, Shahzad R. Combustion analysis of a CNG direct injection spark ignition engine. International Journal of Automotive and Mechanical Engineering. 2010;2:157-70.

[18]   Sezgin M, Sankur B. Survey over image thresholding techniques and quantitative performance evaluation. Journal od Electronic Imaging. 2004;13:146-65.

[19]   Otsu N. A threshold selection method from Gray level Histogram. IEEE transactions. 1979;9:62-5

[20]   Nacereddin N, Hamami L, Tridi M, Oucief N. Non-parametric Histogram-based thresholding methods for weld defect detection in radiography. Worl Academy of Science, Engineering and Technology. 2005;9.

[21]   Neto JC. A combined statistical-soft computing approach for classification and mapping weed species in minimum-tillage system. Lincoln: University of Nebraska; 2004.

[22]   Kuhl FP, Giardina CR. Elliptic Fourier features of a closed contour. Computer Graphics and Image Processing. 1982;18:236-58.

[23]   Neto JC, Meyer GE, Jones DD, Samal AK. Plant species identification using elliptic Fourier leaf shape analysis. Computers and electronics in agriculture. 2006;50:121-34.

[24]   Tort A. Elliptic Fourier functions as a morphological descriptor of the genus Stenosarina (Brachiopoda, Terebratulida, New Caledonia. International Association for Mathematical Geology. 2003;35:873-85.

[25]   Le Minor JM, Schmittbuhl M. Importance of elliptic Fourier methods for morphometry of complex outlines: application to the distal human femur. Surgical and Radiologic Anatomy. 1999;21:387-91.

[26]   Freeman H. On the encoding of arbitrary geometric configurations. IRE Transactions on Electronic Computers. 1961;2:260-8.

[27]   Aziz ARA, Anbese YT, Hagos FY, Heikal MR. Characteristics of Early Flame Development in a Direct-Injection Spark-Ignition CNG Engine Fitted with a Variable Swirl Control Valve. Energies. 2017;10:964.

[28]   Nixon MS, Aguado AS. Feature extraction and image processing. 2nd ed. Oxford: Academic Press; 2008.

[29]   Heim D, Ghandhi J. A detailed study of in-cylinder flow and turbulence using PIV. SAE Paper. 2011.

[30]   Andwari AM, Aziz AA, Said MFM, Esfahanian V, Latiff ZA, Said SNM. Effect of internal and external EGR on cyclic variability and emissions of a spark ignition two-stroke cycle gasoline engine. Journal of Mechanical Engineering and Sciences. 2017;11:3004-14.

[31]   Ting D, Checkel M, Johansson B. The importance of high frequency, small eddy turbulence in spark ignited, premixed engine combustion. SAE. 1995.

[32]   Merola SS, Tornatore C, Irimescu A, Marchitto L, Valentino G. Optical diagnostics of early flame development in a DISI (direct injection spark ignition) engine fueled with n-butanol and gasoline. Energy. 2016;108:50-62.

[33]   Samaniego JM, Mantel T. Fundamental Mechanisms in Premixed Turbulent Flame Propagation via Flame–Vortex Interactions. Combustion and Flame 1999;118:537–56

[34]   Gillespie L. Imaging and analysis of turbulent flame development in spark ignition engines. Leeds: University of Leeds; 1998.

[35]   Gunasekaran J, Ganesan V. Effect Of Swirl and Tumble on the Stratified Combustion of a DISI Engine - A CFD Study. SAE Paper. 2011.

CHAPTER 4
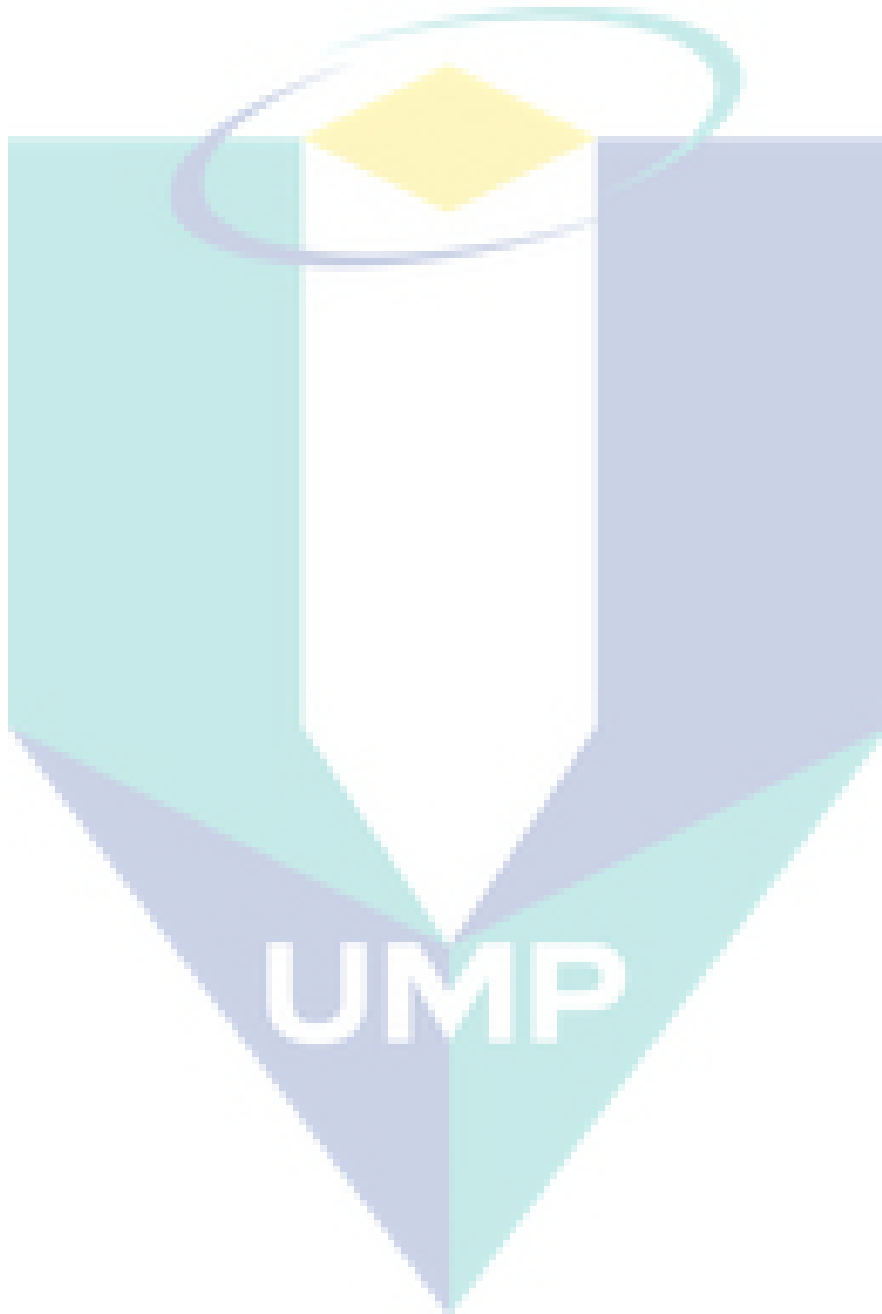
DESIGN OF AN INLINE REFORMER FOR SYNGAS PRODCUTION IN A NATURAL GAS VEHICLE
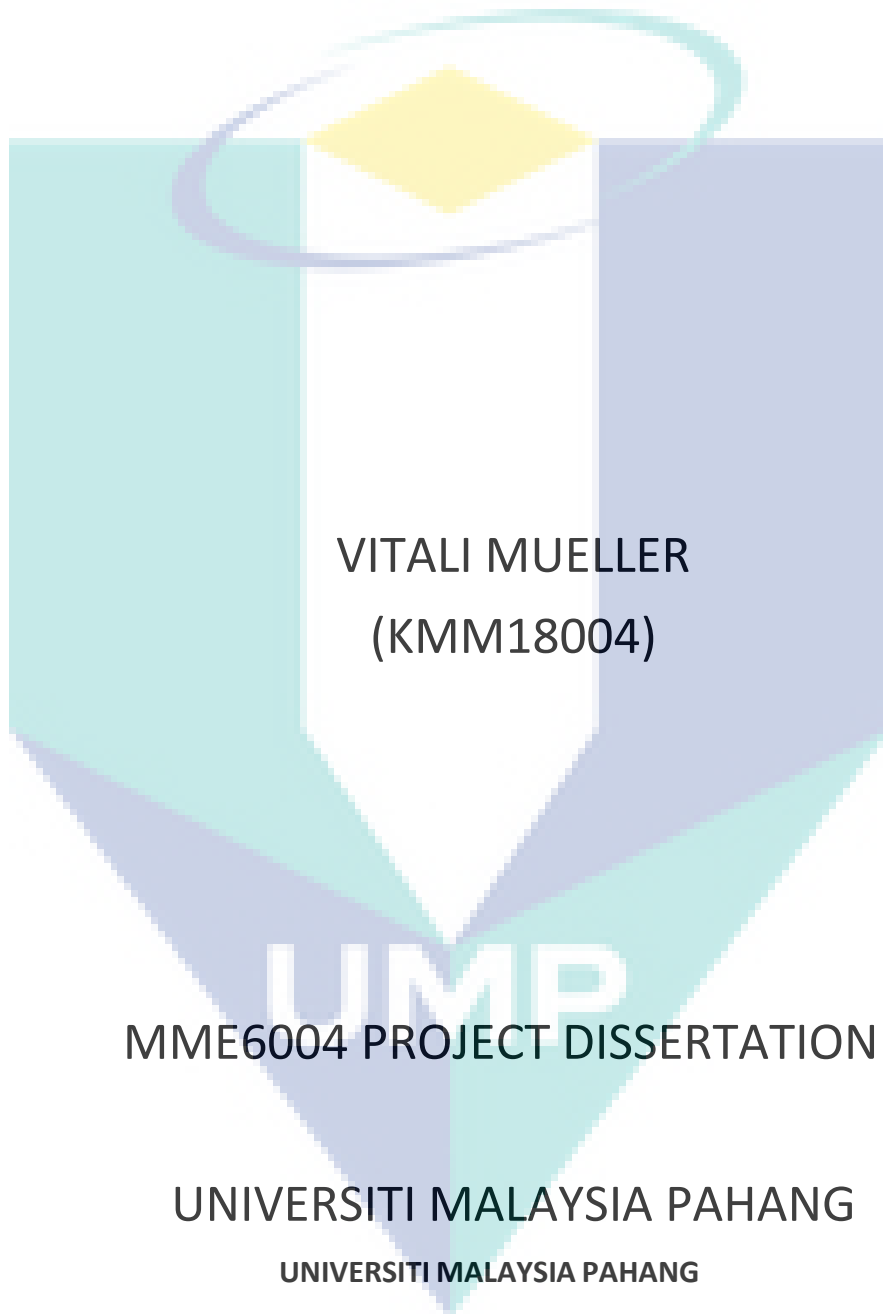
VITALI MUELLER

(KMM18004)

MME6004 PROJECT DISSERTATION I

UNIVERSITI MALAYSIA PAHANG

DECLARATION OF THESIS AND COPYRIGHT

Author's Full Name :

_____

Date of Birth :

_____
_

Title :

_____
_

_____
_

_____
_

Academic Session :

_____

I declare that this thesis is classified as:

I acknowledge that Universiti Malaysia Pahang reserves the following rights:

1. The Thesis is the Property of Universiti Malaysia Pahang
2. The Library of Universiti Malaysia Pahang has the right to make copies of the thesis for the purpose of research only.
3. The Library has the right to make copies of the thesis for academic exchange.

NOTE : * If the thesis is CONFIDENTIAL or RESTRICTED, please attach a thesis declaration letter.

THESIS DECLARATION LETTER (OPTIONAL)

Librarian,
Perpustakaan Universiti Malaysia Pahang,
Universiti Malaysia Pahang,
Lebuhraya Tun Razak,
26300, Gambang, Kuantan.

Dear Sir,

CLASSIFICATION OF THESIS AS RESTRICTED

Please be informed that the following thesis is classified as RESTRICTED for a period of three (3) years from the date of this letter. The reasons for this classification are as listed below.

Author's Name

Thesis Title

Reasons   (i)

                 (ii)

                 (iii)

Thank you.

Yours faithfully,

_____
    (Supervisor's Signature)

Date:

Stamp:

Note: This letter should be written by the supervisor, addressed to the Librarian, *Perpustakaan Universiti Malaysia Pahang* with its copy attached to the thesis.
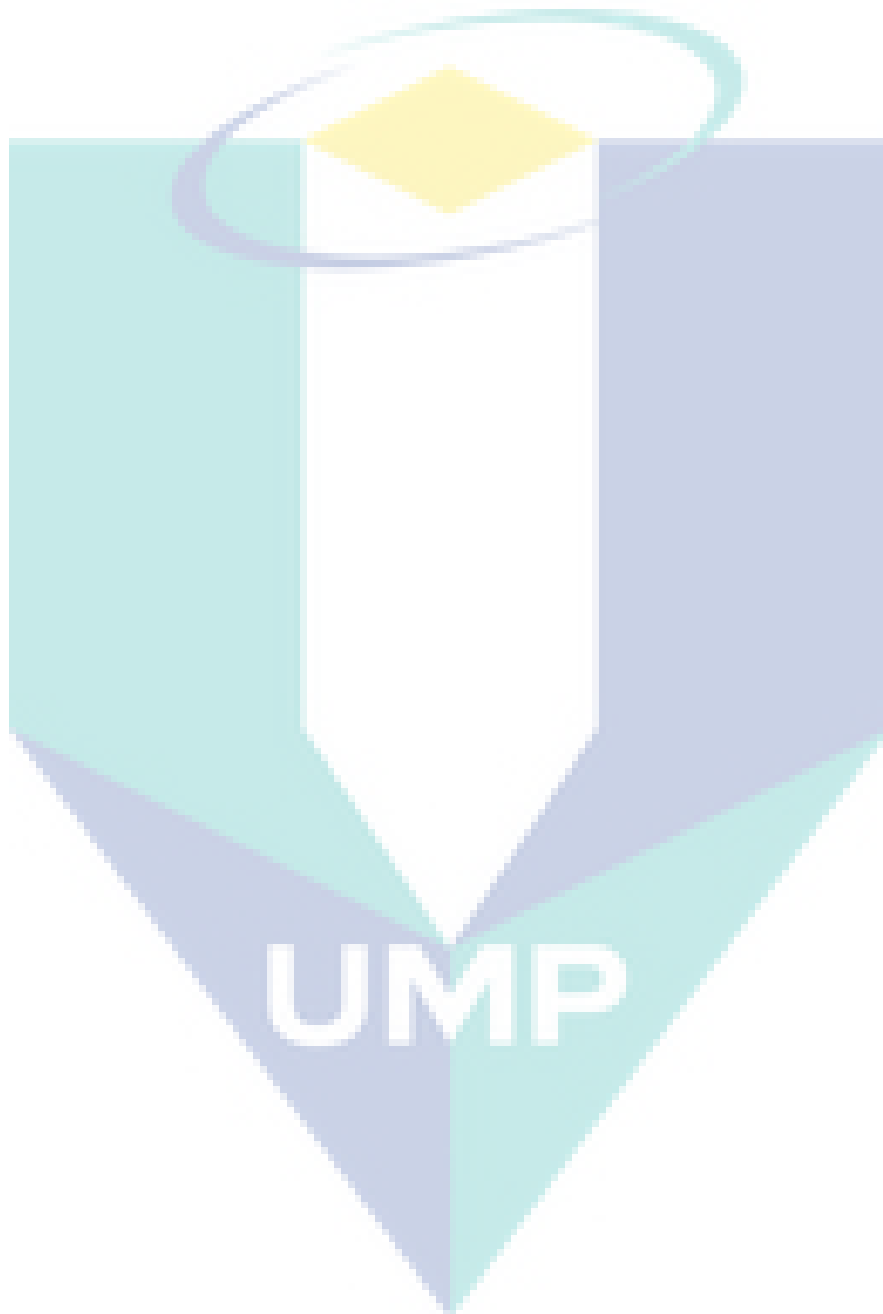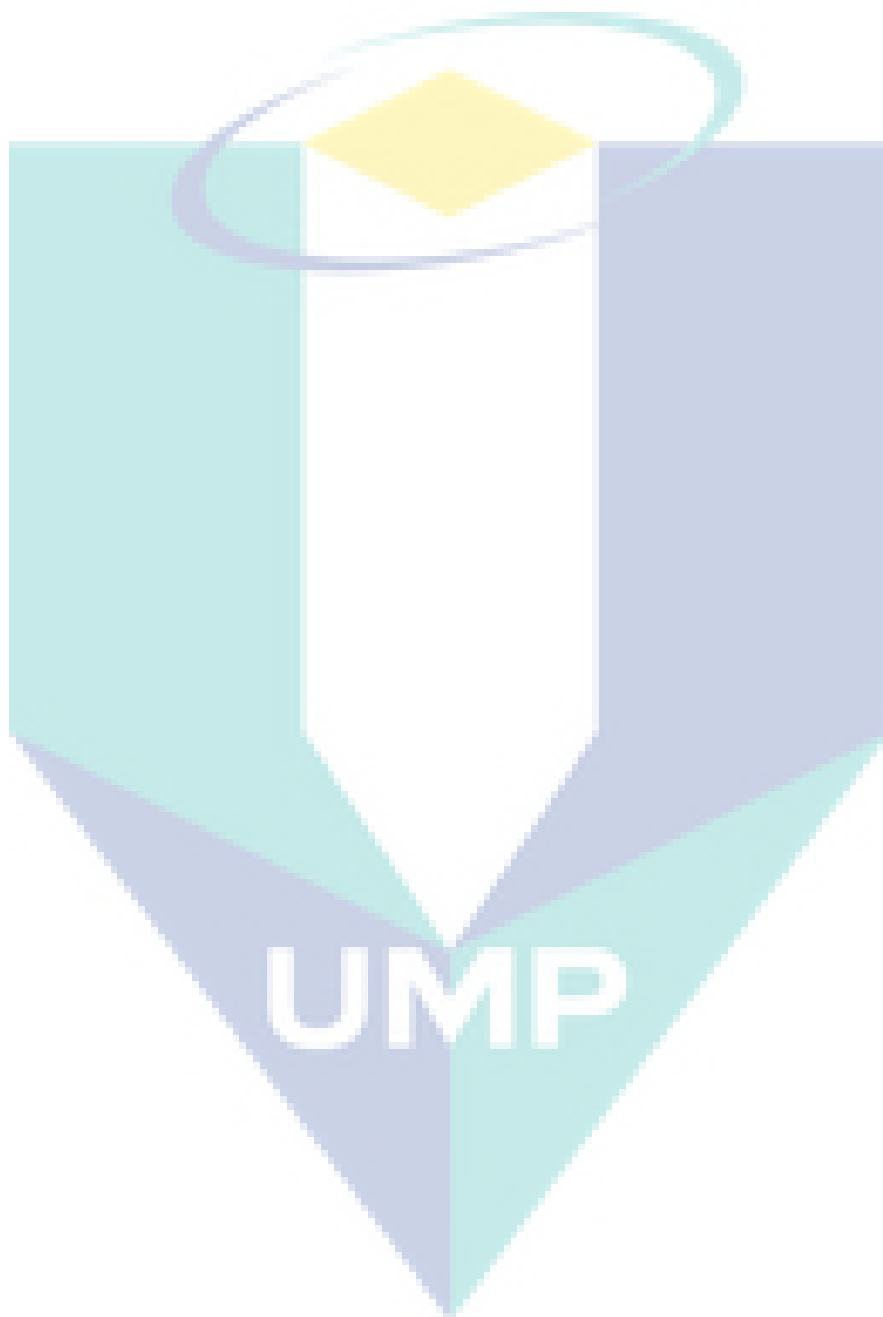
SUPERVISOR's DECLARATION

I/We* hereby declare that I/We* have checked this thesis/project* and in my/our* opinion, this thesis/project* is adequate in terms of scope and quality for the award of the degree of *Doctor of Philosophy/ Master of Engineering/ Master of Science in ……………………………..

_____
(Supervisor's Signature)

Full Name   :

Position   :

Date   :

_____
(Co-supervisor's Signature)

Full Name   :

Position   :

Date   :
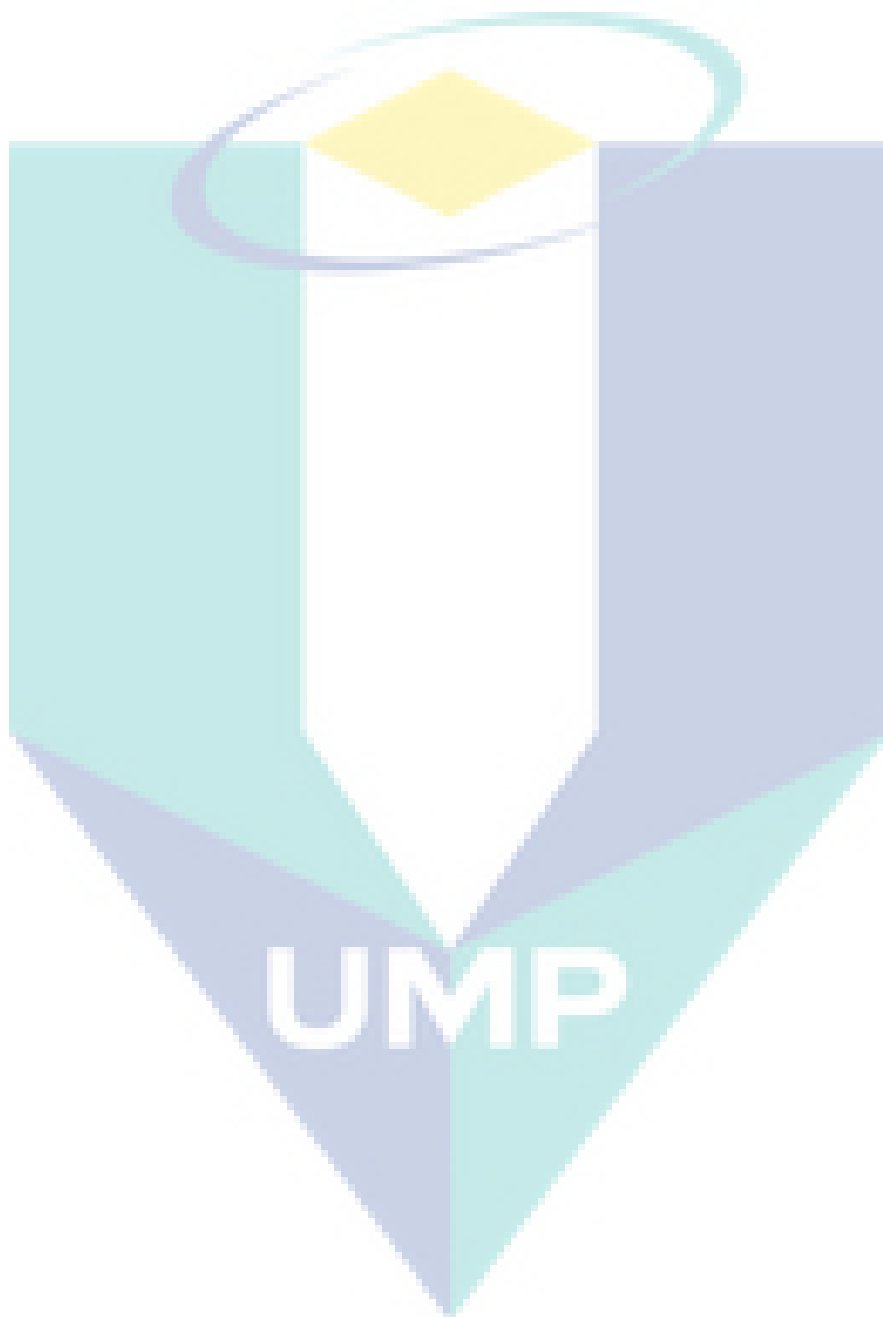
STUDENT'S DECLARATION

I hereby declare that the work in this project dissertation is based on my original work except for quotations and citations which have been duly acknowledged. I also declare that it has not been previously or concurrently submitted for any other degree at Universiti Malaysia Pahang or any other institutions.

_____

(Student's Signature)

Full Name   : Vitali Mueller

ID Number   : KMM18004

Date   : 03 January 2019
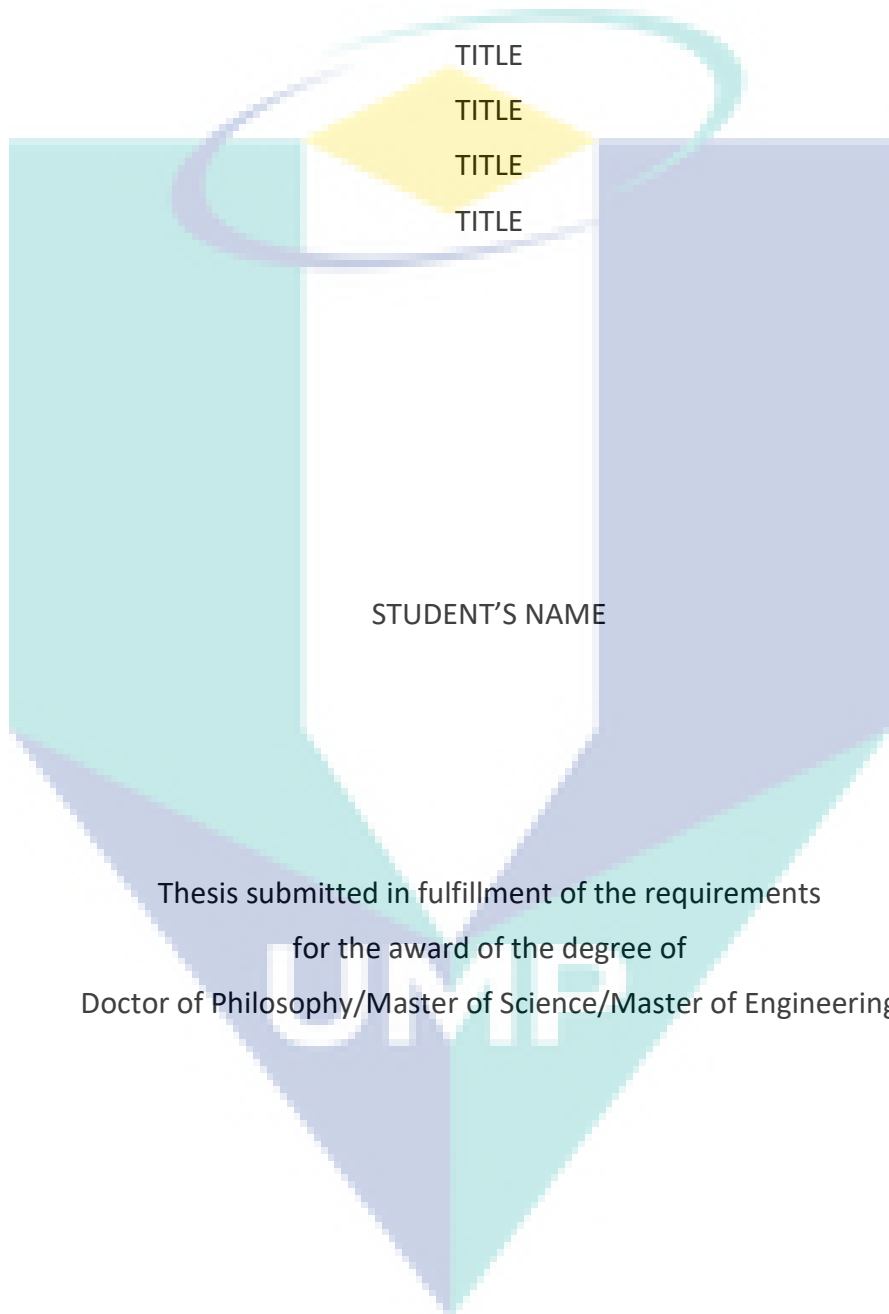
TITLE
TITLE
TITLE
TITLE

STUDENT'S NAME

Thesis submitted in fulfillment of the requirements

for the award of the degree of

Doctor of Philosophy/Master of Science/Master of Engineering

Faculty of Electrical & Electronics Engineering

UNIVERSITI MALAYSIA PAHANG

ABSTRACT

The growth of the world population as well as the ever-advancing development of the developing countries into industrialized countries leads to an increasing demand for energy and raw materials. As energy production increases, the emissions emitted increase as well. To counteract this pollution, the states adopt measures to reduce air pollution. The car industry is also affected. Lowering both, CO and NO_X is the challenge. One possibility for the internal combustion engine is the use of alternative fuels to achieve this goal. These can reduce the emissions incurred. One alternative fuel is synthetic gas which consist primarily of hydrogen, carbon monoxide and often carbon dioxide. Using this gas the unburned hydrocarbons will decrease and an increase in thermal efficiency is to observe. To produce syngas, there are many reforming processes, each with its own benefits and disadvantages. This project has the task of designing an inline reformer for producing syngas in a retrofitted Otto internal combustion engine with natural gas. The fuel supply of the internal combustion engine has to be completely converted to a natural gas - syngas mixture. The engines demand for fuel should inherit a maximum amount of 15% syngas which will be mixed to the prime source, natural gas, after conversion.

TABLE OF CONTENT

DECLARATION

TITLE PAGE

LIST OF TABLES

LIST OF FIGURES

LIST OF SYMBOLS

K	Kelvin
°C	Degree Celsius
kW	Kilowatt
Nm	Newton meter
rpm	Revolutions per minute
V	Volume
m	Mass
$\dot{m}$	Mass flow
$\dot{m}_{NG}$	Natural gas mass flow
ρ	Density
c	Amount of cylinders
n	Revolutions in min-1
i	Work cycle per revolution
$\dot{V}$	Volume flow
$\dot{V}_n$	Volume flow in norm cubic meter
$\dot{Q}$	Heat flow
h	Specific enthalpy

LIST OF ABBREVIATIONS

SR   Steam reforming

POX   Partial oxidation

ATR   Autothermal reforming

HE   Heat exchanger
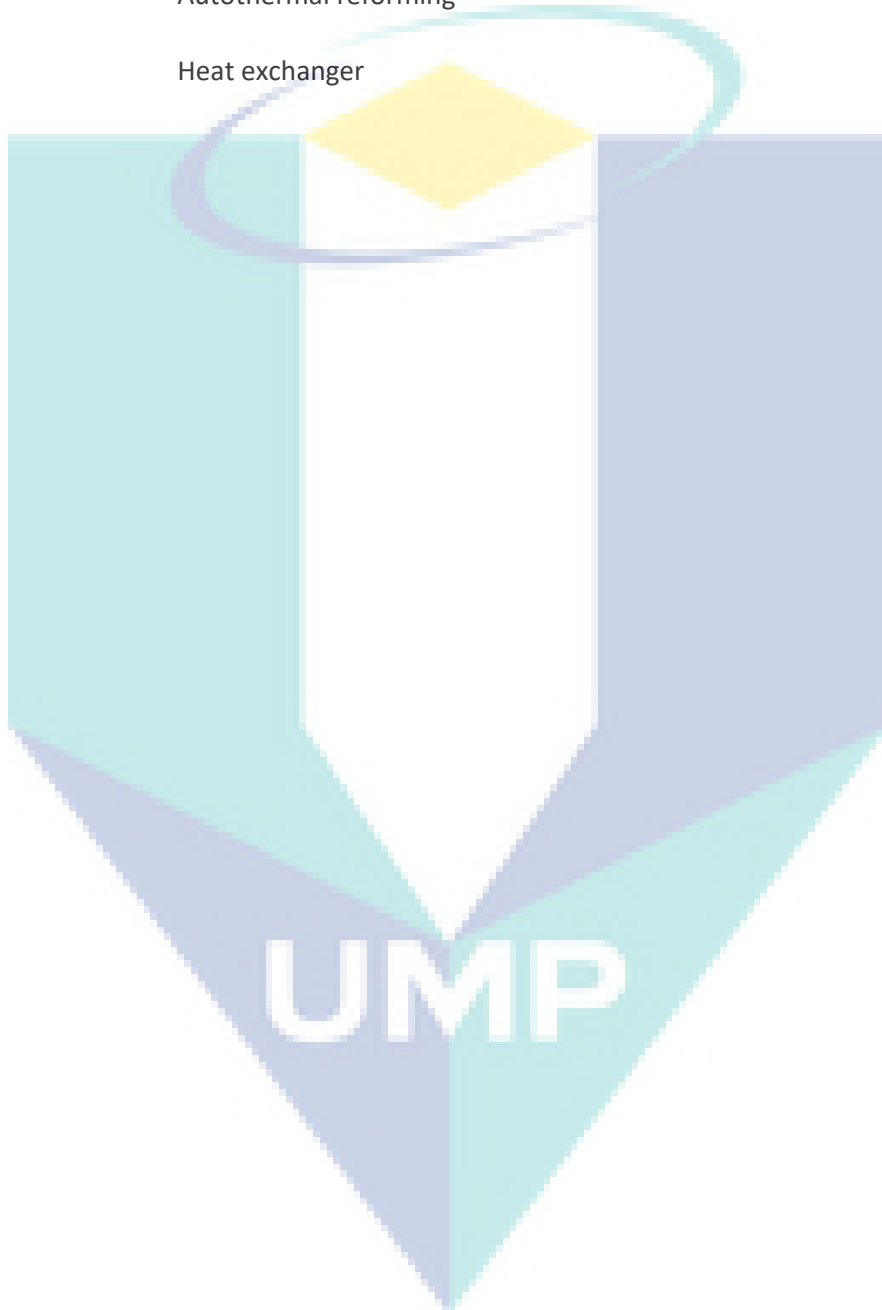
FINAL YEAR PROJECT

SIMULATION OF ONE-STEP DIMETHYL ETHER PRODUCTION
FROM GASIFICATION OF PALM OIL WASTE

CHAN SOON YIN

MH 11141

FACULTY OF MECHANICAL ENGINEERING

UNIVERSITI MALAYSIA PAHANG

JUNE 2015

SUPERVISOR'S DECLARATION

I/We* hereby declare that I/We* have checked this thesis/project* and in my opinion, this thesis/project* is adequate in terms of scope and quality for the award of the degree of Bachelor of Mechanical Engineering.

Signature

Name of Supervisor   :   DR. FTWI YOHANESS HAGOS

Position   :   SENIOR LECTURER

Date   :

Signature

*Name of Co-supervisor :

Position   :

Date   :

STUDENT'S DECLARATION

I hereby declare that that the work in this thesis/project* is my own except for quotation and summaries which have been duly acknowledged. The thesis/project* has not been accepted for any degree and is not concurrently submitted for award of other degree.

Signature   :

Name   :   CHAN SOON YIN

ID Number   :   MA11141

Date   :   /6/2015

ACKNOWLEDGEMENT

I would like to express my deepest gratitude to my supervisor, Dr. Ftwi Yohanes Hagos who come up with the great idea of this title for me to show my hard work. I also wish to thanks him for his patient guidance, encouragement and support along the way until the end of this project. He always had concerned about our problem and has spent much time in helping me clearing my doubt and always able to make a clear path for me whenever I feel doubt about my decision. I would not have able to complete this project solely without his helping. Secondly, I wish to thanks, Prof. Yusoff Bin Ali. Prof. has provided much knowledge and correct me whenever he found out my mistake, and at the same time giving me suggestion and ways to improve on my work. I would also wish to express my thanks to Dr. Samson from Faculty of Engineering Technology that provide technical help in the way of using the Aspen Plus software. Without him, it is not possible for me to pick up the pace and learn the software in such a short duration. I would also like to thanks to my chemical friends who give much help in solving my problem and would like to apologize as I cannot listed out every one of them individually.

I wish to thanks to all the lectures and staff of University Malaysia Pahang, whoever that provides help and guidance and different method. I would like to thank also University Malaysia Pahang that allow me to take my degree for mechanical engineering course here. I also wish to thanks to my coursemate in University Malaysia Pahang as we fight together to strive for the target, sharing of idea and support each other to improve and grow mutually.

I want to thanks to my parents and all my friends for their gradually support, love, caring, and understanding. The word alone is not enough to describe the energy the provided. Without them help in building my character in my life, I would be lost long ago.

ABSTRACT

Dimethyl Ether (DME) is a renewable fuel produced by the gasification of biomass substances. The first gasification process is carried out at years 1659. It is a potential fuel for replacing old generation diesel fuel. DME is also being concerned as new burning resources as it has low pollution and is less greenhouse emitting fuel as compared to crude oil. However, there is a limitation in achieving this target as the fuel is not available in large scale or mass production. This project aims to achieve the objective of producing 50 kg of DME per days by using a simple one-step dimethyl ether synthesis plant. Oil Palm Trunk (OPT) was selected as the main biomass material as this material is easily obtainable in Malaysia with large quantities. The simulation of this practice was done using Aspen Plus software. By supplying the feed OPT up to 30 kg/hr, the simulation was able to obtain a DME production of 0.0882 kmol/hr. The analysis result shows that lower temperature favors the formation of DME. At higher temperature, the reactions of DME synthesis counter back and turn into Carbon monoxide and hydrogen gas. The maximum mole of DME produced at a temperature of $280^{\circ}C$ in this simulation with the total amount of 0.0882 kmol/hr. The DME also have higher yield percentage at a moderate pressure range of 1 Mpa to 2 Mpa compare to lower pressure.

ABSTRAK

Dimetil Eter (DME) adalah bahan api yang boleh diperbaharui dihasilkan daripada pengegasan bahan biomass. Proses pengegasan yang pertama diperjalankan pada tahun 1659. Ia adalah bahan api yang berpotensi untuk mengantikan minyak diesel generasi lama. DME juga dikhuatirkan sebagai sumber bahan api yang baru disebabkan kadar pencemarannya rendah dan ia adalah bahan api yang menyebabkan 0 kesan rumah hijau apabila dibandingkan dengan minyak mentah. Walau bagaimanapun, minyak ini terdapat batasinya disebabkan ia tidak didapati dalam hasilan skala besar dan pengeluaran besar-besaran. Matlamat projek ini adalah untuk mencapai objektif untuk menghasilkan 50kg dimetil eter sehari dengan menggunakan kilang sintesis satu langkah dimetil ether. Batang pokok kelapa sawit (OPT) dipilih sebagai bahan biomass yang utama dalam simulasi ini disebabkan ia mudah diperolehi dalam kuantiti yang besar di Malaysia. Praktis simulasi ini dijalankan dengan mempergunakan teknologi Aspen Plus. Dengan bekalan OPT 30kg sejam, simulasi ini dapat memperolehi produksi dimetil eter sebanyak 0.882 kmol sejam. Hasil analisis menunjukkan suhu rendah memihak kepada formasi dimetil eter. Pada suhu yang lebih tinggi, reaksi sintesis DME and dikaunter balik dan bertukar menjadi karbon monoxida dan gas hidrogen. Mole produksi DME adalah tertinggi pada suhu 280ºC dalam simulasi ini dengan jumlah produksi sebanyak 0.882 kmol sejam. Produksi DME juga adalah tinggi pada tekanan sederhana iaitu sekitar 1 MPa ke 2 MPa berbanding dengan tekanan yang rendah.

<center>**TABLE OF CONTENT**</center>

LIST OF TABLES

LIST OF FIGURES

LIST OF ABBREVIATIONS

CI   Compression ignition
NOx   Nitrogen Oxide
CO   Carbon Monoxide
DME   Dimethyl Ether
C   Carbon
H_2 Hydrogen
CH3OH   Methanol
CH_3OCHC_3 Dimethyl Ether
H_2O Water
LPG   Liquid Petroleum Gas
O_2 Oxygen
S   Sulphur
Cu   Cupper
Zn   Zinc
Al   Aluminium

CHAPTER 5

CONCLUSIONS AND RECOMMENDATIONS

5.1 INTRODUCTION

In the current study, an equilibrium model of downdraft gasification of OPF was developed in order to facilitate prediction of syngas composition for a range of operating conditions. Experimental data from the current study was used to validate the model results. The results from the model of the gasification process are used for optimization of the process in terms of three independent operating parameters of the gasification process (temperature, equivalence ratio, and moisture content). The resulting syngas heating value, gasification efficiency as well as suitability as automotive fuel in terms of cleanliness are investigated. The following concluding remarks and future recommendation are provided.

5.2 CONCLUSIONS

In a nutshell, the objective to produce 50 kg of DME per days for the purpose of mass production is achieved. In further, this volume of production can further be enhanced by improving current technologies on gasification process and also DME synthesis processes. OPT is chosen in this simulation as OPT is large in scale and available in a large amount when the Oil Palm the value of the tree is used up. Although other material also can be used for this purpose, Oil Palm Trunk is easier to achieve as Malaysia is one of the main production places for oil palm making more possible for large production. The process intensification can be used, in addition, to produce useful side substances.

By using Aspen Plus simulation, a plant model for the large production of DME is simulated. The total DME produced from the simulation result are 0.093 kmol per hours; this amount sums up to 2.236 kmol of DME for one day or equivalent to 103 kg of DME production.   Although the objective of this project is achieved, there are many improvements can be done to this simulation. One of the main improvements that

should be made is to improve the cycle efficiency. As stated in the discussion earlier, the rate of DME conversion is quite low although the hydrogen and carbon monoxide gas convert fully into carbon monoxide and methanol solution. This means the etherification process in this simulation has to be enhanced.

5.3 RECOMMENDATIONS

In this project, the energy analysis for all chemical equation that occur is not considered. For future study, energy analysis of all processes should be considered in making a decision and to determine the accuracy of the simulation flow. Economic analysis of the simulation should also be done to predict on the profit of this simulation to consider the suitability of this design to be executed. The efficiency of the cycle should also be increased to increase the productivity of the DME to achieve an even higher level of production. The simulation can also be improved by adding processes such as process intensification and recycle process into the flow sheet.

REFERENCES

AZNAR, M. P., M. A. CABALLERO, J. A. SANCHO, AND E. FRANCÉS, "Plastic waste elimination by co-gasification with coal and biomass in fluidized bed with air in pilot plant," *Fuel Processing Technology*, vol. 87, pp. 409-420, 2006.

BASU, Biomass gasification and pyrolysis: practical design and theory. Burlington, MA: Academic press, 2010.

BOZGA, G., APAN, I. T. & BOZGA, R. E. 2013. Dimethyl Ether Synthesis Catalysts, Processes and Reactors. *Recent Patents on Catalysis,* 2**,** 68-81.

CHANG, J., FU, Y. & LUO, Z. 2012. Experimental study for dimethyl ether production from biomass gasification and simulation on dimethyl ether production. *Biomass and Bioenergy,* 39**,** 67-72.

CHEN, H.-J., FAN, C.-W. & YU, C.-S. 2013. Analysis, synthesis, and design of a one-step dimethyl ether production via a thermodynamic approach. *Applied Energy,* 101**,** 449-456.

CHEN, Z., ZHANG, H., YING, W. & FANG, D. 2010. Global Kinetics of Direct Dimethyl Ether Synthesis Process from Syngas in Slurry Reactor over a Novel Cu-Zn-Al-Zr Slurry Catalyst. *World Academy of Science, Engineering and Technology,* 68**,** 1426-1432.

DONATELLI, A., P. IOVANE, AND A. MOLINO, "High energy syngas production by waste tyres steam gasification in a rotary kiln pilot plant. Experimental and numerical investigations," *Fuel*, vol. 89, pp. 2721-2728, 2012.

HAMEED, B. H. & EL-KHAIARY, M. I. 2008. Batch removal of malachite green from aqueous solutions by adsorption on oil palm trunk fibre: Equilibrium isotherms and kinetic studies. *Journal of Hazardous Materials,* 154**,** 237-244.

HAN, Y., ZHANG, H., YING, W. & FANG, D. 2009. Modeling and simulation of production process on dimethyl ether synthesized from coal-based syngas by one-step method. *Chinese Journal of Chemical Engineering,* 17**,** 108-112.

HANAOKA, T., S. INOUE, S. UNO, T. OGI, AND T. MINOWA, "Effect of woody biomass components on air-steam gasification," *Biomass and Bioenergy*, vol. 28, pp. 69-76, 2005.

HIGMAN C. AND M. VAN DER BURGT, Gasification: Gulf Professional Publishing, 2008.

JALIL, R., MIYAZAWA, T., SAKANISHI, K., YUSOFF, M. N. M. & ASMA, W. 2010. Synthesis of Dimethyl Ether (DME) from Woody Biomass Syngas via One Step Synthesis Process over Bi-functional Catalysts.

JU, F., CHEN, H., DING, X., YANG, H., WANG, X., ZHANG, S. & DAI, Z. 2009. Process simulation of single-step dimethyl ether production via biomass gasification. *Biotechnology Advances,* 27**,** 599-605.

LARSEN, M. B., L. SCHULTZ, P. GLARBORG, L. SKAARUP-JENSEN, K. DAM-JOHANSEN, F. FRANDSEN, AND U. HENRIKSEN, "Devolatilization characteristics of large particles of tyre rubber under combustion conditions," *Fuel,* vol. 85, pp. 1335-1345, 2006.

LEE, S., Alternative Fuels. Washington, D.C.: Taylor & Francis, 1996.

MASTELLONE, M. L., L. ZACCARIELLO, AND U. ARENA, "Co-gasification of coal, plastic waste and wood in a bubbling fluidized bed reactor," *Fuel*, vol. 89, pp. 2991-3000, 2010.

MITTA, N. R., S. FERRER-NADAL, A. M. LAZOVIC, J. F. PERALES, E. VELO, AND L. PUIGJANER, "Modelling and Simulation of a Tyre Gasification Plant

for Synthesis Gas Production," *Computer Aided Chemical Engineering*, vol. 21, p. 1771, 2006.

NIPATTUMMAKUL, N., AHMED, I. I., GUPTA, A. K. & KERDSUWAN, S. 2011. Hydrogen and syngas yield from residual branches of oil palm tree using steam gasification. *International Journal of Hydrogen Energy,* 36**,** 3835-3843.

NIPATTUMMAKUL, N., AHMED, I. I., KERDSUWAN, S. & GUPTA, A. K. 2012. Steam gasification of oil palm trunk waste for clean syngas production. *Applied Energy,* 92**,** 778-782.

PONZIO, A., S. KALISZ, AND W. BLASIAK, "Effect of operating conditions on tar and gas composition in high temperature air/steam gasification (HTAG) of plastic containing waste," *Fuel Processing Technology*, vol. 87, pp. 223-233, 2006.

RAHIMPOUR, M. R., VAKILI, R., POURAZADI, E., BAHMANPOUR, A. M. & IRANSHAHI, D. 2011. Enhancement of hydrogen production via coupling of MCH dehydrogenation reaction and methanol synthesis process by using thermally coupled heat exchanger reactor. *International Journal of Hydrogen Energy,* 36**,** 3371-3383.

SAIT, H. H., HUSSAIN, A., SALEMA, A. A. & ANI, F. N. 2012. Pyrolysis and combustion kinetics of date palm biomass using thermogravimetric analysis. *Bioresource Technology,* 118**,** 382-389.

SHUIT, S. H., TAN, K. T., LEE, K. T. & KAMARUDDIN, A. H. 2009. Oil palm biomass as a sustainable energy source: A Malaysian case study. *Energy,* 34**,** 1225-1235.

SUMATHI, S., CHAI, S. P. & MOHAMED, A. R. 2008. Utilization of oil palm as a source of renewable energy in Malaysia. *Renewable and Sustainable Energy Reviews,* 12**,** 2404-2421.

VAKILI, R. & ESLAMLOUEYAN, R. 2012. Optimal design of an industrial scale dual-type reactor for direct dimethyl ether (DME) production from syngas. *Chemical Engineering and Processing: Process Intensification,* 62**,** 78-88.

VAKILI, R., POURAZADI, E., SETOODEH, P., ESLAMLOUEYAN, R. & RAHIMPOUR, M. R. 2011a. Direct dimethyl ether (DME) synthesis through a thermally coupled heat exchanger reactor. *Applied Energy,* 88**,** 1211-1223.

VAKILI, R., SETOODEH, P., POURAZADI, E., IRANSHAHI, D. & RAHIMPOUR, M. R. 2011b. Utilizing differential evolution (DE) technique to optimize operating conditions of an integrated thermally coupled direct DME synthesis reactor. *Chemical Engineering Journal,* 168**,** 321-332.

XIAODONG, Z., X. MIN, AND S. RONGFENG, "Study on biomass pyrolysis kinetics," *Journal of Engineering for Gas Turbines and Power*, vol. 128, pp. 493-496, 2006.

YAMADA, H., TANAKA, R., SULAIMAN, O., HASHIM, R., HAMID, Z. A. A., YAHYA, M. K. A., KOSUGI, A., ARAI, T., MURATA, Y., NIRASAWA, S., YAMAMOTO, K., OHARA, S., MOHD YUSOF, M. N., IBRAHIM, W. A. & MORI, Y. 2010. Old oil palm trunk: A promising source of sugars for bioethanol production. *Biomass and Bioenergy,* 34**,** 1608-1613.

YANG, H., YAN, R., LIANG, D. T., CHEN, H. & ZHENG, C. 2006. Pyrolysis of palm oil wastes for biofuel production. *As J Energy Env,* 7**,** 315-323.

ZAINAL, Z. A., R. ALI, C. H. LEAN, AND K. N. SEETHARAMU, "Prediction of performance of a downdraft gasifier using equilibrium modeling for different biomass materials," *Energy conversion and management*, vol. 42, pp. 1499-1515, 2001.